DOCTORAATSPROEFSCHRIFT

2009 | Faculteit Wetenschappen

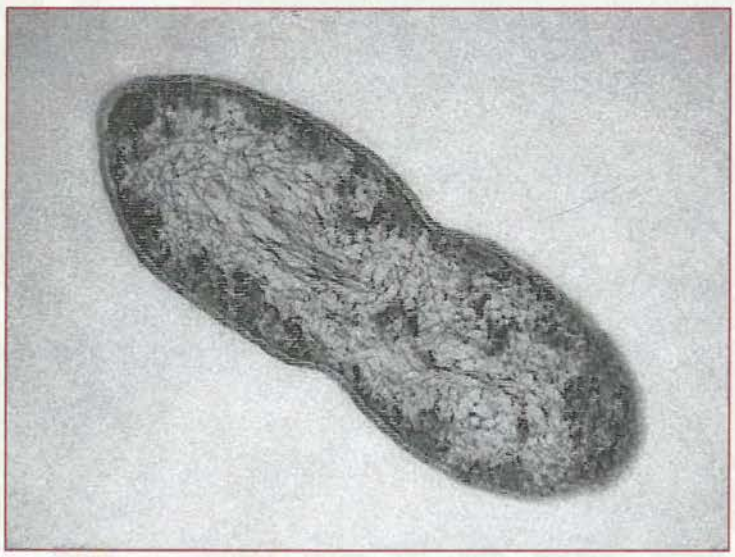

Endophytic propagation of *Erwinia amylovora* in *Rosaceae*: a proteomic and microscopic approach

Proefschrift voorgelegd tot het behalen van de graad van
Doctor in de Wetenschappen, richting biologie, te verdedigen door:

Mieke THOELEN

Promotor: prof. dr. R. Valcke
Copromotor: prof. dr. ir. W. Keulemans

universiteit hasselt
CENTRUM
VOOR MILIEUKUNDE

DOCTORAATSPROEFSCHRIFT

2009 | Faculteit Wetenschappen

Endophytic propagation of *Erwinia amylovora* in *Rosaceae*: a proteomic and microscopic approach

Proefschrift voorgelegd tot het behalen van de graad van
Doctor in de Wetenschappen, richting biologie, te verdedigen door:

Mieke THOELEN

Promotor: prof. dr. R. Valcke
Copromotor: prof. dr. ir. W. Keulemans

universiteit hasselt
CENTRUM
VOOR MILIEUKUNDE

D/2009/2451/6

Members of the jury

Prof. dr. J. Manca, Universiteit Hasselt, Belgium, Chairman
Prof. dr. R. Valcke, Universiteit Hasselt, Belgium, Promotor
Prof. dr. ir. W. Keulemans, K.U. Leuven, Belgium, Co-promotor
Dr. ir. M.M. López, Instituto Valenciano de Investigaciones Agrárias, Valencia, Spain
Prof. dr. M. Höfte, Universiteit Gent, Gent, Belgium
Dr. M. Maes, ILVO, Merelbeke, Belgium
Dr. J.-P. Noben, Universiteit Hasselt, Belgium
Dr. M. vandeVen, Universiteit Hasselt, Belgium
Ir. T. Deckers, PC Fruit, Sint-Truiden, Belgium

Learn from yesterday, live for today, hope for tomorrow.
The important thing is not to stop questioning.

Albert Einstein

Table of contents

List of abbreviations

2D-GE	two -dimensional gel electrophoresis
ABC	ATP-binding cassette
ACN	acetonitrile
Acn	aconitase
AFLP	amplified fragment length polymorphism
AhpC	Putative alkyl hydroperoxide reductase subunit C
AI	autoinducer
ams	amylovoran synthesis
ATP	adenosine-5'-triphosphate
AVR	avirulence
cfu	colony-forming units
CHAPS	(3-[(3-cholamidopropyl)-dimethylammonio]-1-propane sulfonate)
CHCA	α-Cyano-4-hydroxycinnamic acid
cps	capsule synthesis
CRP	camp receptor protein
DabE	N-succinyl-diaminopimelate deacylase
DFO	desferroxamine
DIGE	differential in-gel electrophoresis
DNA	deoxyribonucleic acid
Dps	DNA protecting during starvation protein
dsp	disease specific
DTT	dithiothreitol
Ef-Tu	elongation factor Tu
Eop	Erwinia outer protein
EPS	exopolysaccharide
ESI	electrospray ionization
ETI	effector-triggered immunity
ETS	effector-triggered susceptibility
FliC	flagellin
GalU	glucose-1-phosphate uridylyltransferase
GapA	glyceraldehyde 3-phosphate dehydrogenase A
GFP	green fluorescent protein
GLV	green-leaf volatiles
Gnd	gluconate-6-phosphate dehydrogenase

Gst	glutathione S-transferase
H2O2	hydrogen peroxide
HAc	acetic acid
HAE	Hrp-associated enzymes
HEE	Hrp effectors and elicitors
HGT	horizontal gene transfer
Hns	heat-stable necleoid-structuring protein
HP	hydroperoxidase
HR	hypersensitive response
hrc	hypersensitive response and conserved
hrp	hypersensitive response and pathogenicity
ID	internal diameter
IEF	iso-electric focusing
IPG	immobilized pH gradient
ISH	in situ hybridization
IT	island transfer
JA	jasmonic acid
kb	kilo base
LB	Luria-Bertani
LCQ	liquid chromatography quadrupole
Lipid-OOH	lipid peroxides
LPS	lipopolysaccharide
LRR	leucine rich repeat domain
m/z	mass over charge
MALDI	matrix-assisted laser desorption/ionization
MAMP	microbial associated molecular pattern
MeJA	methyl jasmonate
MeSA	methyl salicylate
MM	minimal medium
mRNA	messenger ribonucleic acid
MS/MS	tandem mass spectrometry
MW	molecular weight
N-AHL	N-acyl homoserine lactone
NB	nucleotide binding
NCBI	National Center for Biotechnology Information
O2-	superoxide
Ohr	organic hydroperoxide resistance protein
Orn	oligoribonuclease

ORF	Open Reading Frame
OsmY	osmotically inducible protein Y
PAI	pathogenicity island
PAMP	pathogen associated molecular pattern
PBS	phosphate buffered saline
PCR	polymerase chain reaction
Pgk	phosphoglycerate kinase
pI	isoelectric point
Ppiase	peptidyl-prolyl isomerase
PR	pathogen related
PRR	pattern recognition receptor
PRX	peroxiredoxin
PTI	PAMP-triggered immunity
QS	quorum sensing
R-(genes)	resistance (genes)
RecA	Recombinase A
RH	relative humidity
RNA	ribonucleic acid
ROI	region of interest
ROOH	alkyl hydroperoxide
ROS	reactive oxygen species
SA	salicylic acid
SAR	systemic acquired resistance
Sbp	periplasmic sulphate binding protein
SDS	sodium dodecyl sulphate
SDS-PAGE	sodium dodecyl sulphate polyacrylamide gel electrophoresis
sHsp	small heat shock protein
SOD	superoxide dismutase
TEM	transmission electron microscopy
TFA	trifluoracetic acid
ThrC	threonine synthase
TOF	time-of flight
TpiA	triose-phosphate isomerase
TTSS	type III secretion system
UTR	untranslated region
UQ	ubiquininone
UQH2	ubiquinol

XenA	Xenobiotic reductase A
ZnuA	ABC superfamily high Zn transport protein

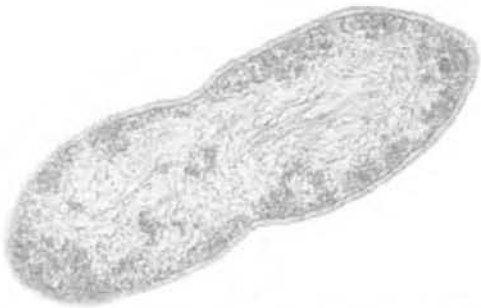

Chapter 1

General introduction

1.1 *Erwinia amylovora*: general features

E. amylovora was the first bacterium identified as a plant pathogenic bacterium and was shown to be the causative agent of the necrotic disease fire blight (Burrill, 1883)

E. amylovora is a Gram-negative bacterium belonging to the family of *Enterobacteriaceae,* which includes *Escherichia coli*, *Yersinia* spp., *Shigella* spp. and *Salmonella* spp., which are human and animal pathogens.
Cells of *E. amylovora* are rod-shaped and have a size of about 0,3 µm x 1-3 µm. *E. amylovora* is motile in culture media by means of two to seven peritrichous flagella per cell. On the plant surface, the motility of *E. amylovora* is easily expressed (Paulin, 2002), but no motile bacterial cells could be observed in the intercellular spaces of infected plant tissues.

E. amylovora is facultative anaerobe and is quoted as being weekly fermentative (Holt et al., 1994). *E. amylovora* does not reduce nitrate to nitrite, which is the general rule in *Enterobacteriaceae.* The optimal temperature for *E. amylovora* is between 25 and 27°C. *E. amylovora* is capable of growth between 3-5°C and 37°C (Billing et al., 1961).

1.2 *Erwinia amylovora* and fire blight

Fire blight, caused by the bacterium *Erwinia amylovora*, is a common and very serious bacterial plant disease. The necrotic disease is also referred to as blossom blight, spur blight, fruit blight, twig blight or rootstock blight, depending on the plant part that is attacked.

E. amylovora infects approximately 75 plant species, all in the family of the *Rosaceae*. The most important and most susceptible hosts are members of the sub-family *Malaceae* (Heimans et al.; 1998). From the economic point of view, apple and pear are very important hosts. Fire blight can, however, damage other *Maloideae* fruit crops such as quince (*Cydonia*) and loquat (*Eriobotrya japonica*). Also many ornamental plants in the *Maloideae* are hosts of *E. amylovora*, such as mountain ash (*Sorbus*), hawthorn (*Crataegus*), firethorn (*Pyracantha*) and *Cotoneaster*. *E. amylovora* infects also members of the *Rosoideae* subfamily. Examples of these are blackberry (*Rubus fruticosus)* and raspberry (*Rubus idaeus*). Several species of the *Amygdaloideae* (*Prunoideae*) are suspected hosts for *E. amylovora* as well. A full list of genuine and doubtful hosts is found in Van der Zwet & Keil (1979) and Bradbury (1986).

The term "fire blight" describes the appearance of the disease, which can make affected plant tissues appear blackened, shrunken and cracked, as though scorched by fire.
Blossom and twig blight symptoms appear in the spring. Diseased blossoms become water-soaked and turn brown. The bacteria may then grow down into the blossom bearing twigs (spurs and extension shoots). Leaves on the shoots become blighted, turning brown on apple and black on pear. Droplets of milky tan-coloured bacterial ooze may be visible on the surface of diseased tissue. These droplets contain millions of bacteria, which can cause new infections.
Twig blight starts at the growing tips of shoots and moves down into older parts of the twig. Blighted twigs first appear water-soaked and then turn dark brown or black. Blighted leaves remain attached to the dead shoots through the summer. The end of the shoot may bend over, resembling a shepherd's crook or an upside down "J". As the fire blight bacteria move through blighted twigs into main branches, the bark sometimes cracks along the margin of the infected area on the main branch causing a distinct canker.
Both apple and pear fruit may be blighted. Rotted areas turn brown to black and become covered with droplets of ooze. The fruit remains firm but later dries out and shrivels into mummies (van der Zwet & Keil, 1979).

1.2.1 Distribution

E. amylovora is native to North America. The first observations go back to the end of the 18th century from the Hudson Valley in New York. Later on observations were made throughout Northern America including the Gulf of Mexico. The spread of the disease is probably promoted by the first colonists, who planted fruit orchards and moved further over the continent. From America, the bacterium was introduced in the Far East (Japan, 1903; New Zealand, 1919; Australia, 1997) and Europe. However, there is an uncertainty about the presence of *E. amylovora* in Japan and Australia today. The first report of fire blight in Europe dates from 1958 in Great Britain, probably due to the import of infected plants. At present the disease has been found in almost all European countries. In Belgium, the disease was first discovered in 1972 near the coast of the North Sea. It took fire blight about five years to spread from the coastal province of West Flanders to the eastern province of Limburg (Deckers, 1996). Nowadays fire blight is reported in more than 40 countries that are shown in the figure below (fig 1.1).
Long distance dispersal of the pathogen is thought to result from

transport of infected plant material, that can be non-symptomatic (Thomson, 2000). Once the inoculum is present in an orchard, the disease spreads rapidly over short distances under favourable conditions of temperature and humidity.

1.2.2 Infection cycle and migration of *Erwinia amylovora* in host plant tissues

Fire blight bacteria hibernate in the bark at the edge of cankers formed during previous growing seasons. As weather becomes warm in the spring, the bacteria multiply and ooze to the surface in sticky droplets. This ooze, composed of viable bacteria in an hygroscopic polysaccharide matrix, may appear as a very sticky and viscous liquid or it may dry to a hard, shiny, amber-coloured glaze. Under low relative humidity the bacteria can survive in the dry exudate for over a year (Rosen, 1938). Relatively few cankers survive winter, become active and produce bacteria in the spring. However, a single active canker will produce millions of bacteria, enough to infect an entire orchard. The cankers most likely to produce bacteria in the spring are those with smooth margins between healthy and infected tissue, and those formed in older wood. The cankers with no sharp border between healthy and diseased tissue develop frequently when the infections take place late in the season or on young plants or on certain sensitive cultivars. Cankers produce bacteria in droplets of ooze that are transferred to flowers by splashing rain or by insects, mostly bees, flies and ants (fig 1.2). Once on the flower stigmas, the bacteria can grow epiphytically under favourable circumstances and reaching 10^6-10^7 colony-forming units (cfu) per healthy flower. The presence of high densities of epiphytic bacteria on healthy flowers guarantees for efficient movement of the bacteria from flower to flower by rain or by any insects that visit the flowers. Blossom infection occurs when the bacteria are washed by rain to natural openings at the flower base. These openings located in the hypanthium are specialized stomata, termed nectar glands. Blossoms wilt and die about 1-2 weeks after infection, and the bacteria that ooze from them provide inoculum for secondary spread to other flowers and to young succulent shoots. The bacteria are moved to shoots by insects and rain. Bacteria may enter the leaves through stomata and water pores (hydathodes) but usually they enter through wounds made by insects, hailstorms and other mechanical damage. Additional bacterial ooze is produced from these new infection sites, providing inoculum for further spread as long as shoots keep growing and wounds are produced.

As the season advances, shoots become progressively less susceptible to new infections as their growth slows and stops. Bacterial progression through woody tissues also slows and cankers are formed, where some bacteria winter and renew the disease cycle the next spring.

In addition to producing surface ooze in the spring, hibernating bacteria occasionally move internally from canker margins to nearby shoots, which they infect systemically. Such "canker blight" infections produce a characteristic yellow-orange colour in the wilting shoot tips during the early post bloom period. These infection sites can provide an alternative source of inoculum for initiating summer shoot blight epidemics in years when blossom blight is scarce.

Rootstock infections can occur as a specialized form of shoot blight and canker formation, when succulent rootstock suckers become blighted and infection progresses into the rootstock portion of the trunk. However, most rootstock infections are not associated with suckers, and it appears that many develop when bacteria move systemically from scion infections down into the rootstock. The factors that influence this systemic movement are unknown. Rootstocks can be infected by direct infections through the young roots that are present on the burr knots.

Once the bacteria entered the plant, they move intercellularly. Nearby cortical or xylem parenchyma cells collapse and break down, forming large cavities. If bacteria reach the phloem, they are carried upward to the tip of the twig and to the leaves. Invasion of large twigs and branches is restricted primarily to the cortex. Infection of succulent tissues is rapid under warm, humid conditions. Under cool, dry conditions the host forms cork layers around the infected area and limits the expansion of the canker. In susceptible varieties and during warm, humid weather, bacteria may progress from bourse shoots or long shoots into the second-year, third-year and older growth, killing the bark all along the way.

E. amylovora can be described as inducing a dynamic necrosis. It can migrate inside the plant tissues from the top of the tree down to the rootstock, leaving behind tissues that will rapidly necrose. The ability to rapidly invade the host plant has been the subject of a number of studies. However, today there is no consensus on how *E. amylovora* migrates and invades the tissues of a host plant. *E. amylovora* does not produce cell wall-degrading enzymes and does not progress in the plant by dissolving the tissues (Vanneste & Eden-Green, 2000).

1.2.3 *Economic* impact and control treatments

A number of bacterial diseases are of major economic importance, with direct financial loss due to decreased agricultural production and indirect loss due to the implementation of expensive control measures. The financial loss in agricultural production typically arises both due to a direct effect on the quality and quantity of the agricultural product as well as an overall deleterious effect on the plant itself.

Erwinia amylovora has proved extremely destructive to the apple and pear industries in a number of countries and also to the cultivation of various ornamentals. With apple and pears, the disease not only destroys the current season's crops but may also lead to loss of branches and whole trees, leading to long-term devastation of orchards and fruit tree nurseries. After favourable weather conditions during blooming, yield is considerably reduced and in some cases nullified. The next year's productivity is also significantly affected because of the destruction of fruiting spurs. In susceptible hosts the infection spreads so rapidly through the tree that, once infected, trees cannot be saved, even by drastic and immediate surgery, and die in a short time after the first visual sign of infection. (Van der Zwet & Keil, 1979). Originating in the New York area of the USA, fire blight caused destructive epidemics in its westward spread across the USA and major economic losses after its appearance in New Zealand and Europe.

Belgium lost about 50% of the areal of the pear variety Durondeau in the period between 1981 and 1991. This reduction is due to the presence of fire blight in the country. Nowadays the areal of Durondeau in Belgium is about 310 hectares.
For apple there are less problems for the classic variations such as Golden Delicious and Jonagold. However, some new apple varieties are very sensitive for fire blight. The new apple variety Kanzi is sensitive for flower infections, especially when trees are planted in summer and come to bloom. Also the new variety Belgica is sensitive and has to face with massive flower infections when temperature rises in spring. The most sensitive apple varieties like James Grieves and Gloster are even almost gone from the assortment. In Belgian nurseries is the apple variety Breaburn very sensitive for fire blight and also two-year-old trees, which were pruned back at 70 cm, has higher chance for flower infections.

In general, effective management of fire blight requires an integrated approach of several practices. These practices are aimed at reducing the

amount of inoculum that is available to initiate new infections, impose barriers to successful establishment of the pathogen on the host and reduce host susceptibility to infection (Aldewinckle & Beer, 1979 and Van der Zwet & Beer, 1995).

Today's fire blight management strategies lead to a reduced amount of inoculum in the orchard and the use of spray treatments to prevent infection, especially blossom infections.
Nearly all recommendations for fire blight management start with the thorough removal of all infected branches during the dormant pruning

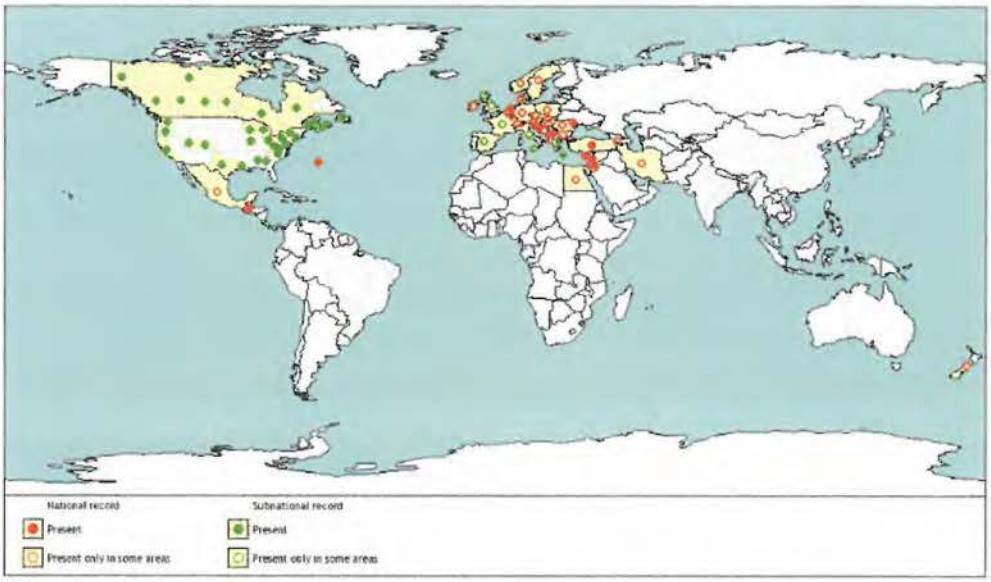

Figure 1.1:
Global distribution map of *E. amylovora* of 2006. The figure shows if *E. amylovora* is present in the entire country or only in some areas. For a subnational record, data are derived from a country division. Data originating from EPPO (European and Mediterranean Plant Protection Organization).

operation. This is followed by an early-season, full-coverage spray with either Bordeaux mixture or several fixed copper formulations to reduce the efficacy of any remaining inoculum. Major emphasis is given to the use of a series of sprays to prevent blossom infections. These could be copper sprays (e.g. copper hydroxide, copper oxychloride, copper sulphate), antibiotics (e.g. streptomycin, oxytetracycline). After bloom, about the only effective treatment for limiting the damage caused by fire blight is to prevent late blossom formation and to cut out new infections when symptoms appear (Covey and Fisher, 1990).
Several models that predict the occurrence of fire blight during bloom are available and help the farmers to choose the best moment to use preventive control treatments. These models are based on climatic and phenological data to predict the occurrence of fire blight infection periods during bloom. The most known models for fire blight disease management are the MARYBLYT system (Steiner, 1990) and the COUGARBLIGHT model (Smith, 1996) in the USA. In Europe they mainly use Billing's revised system and PAREFEU, which is a French prediction model.

Managing fire blight is difficult because options are limited largely to cutting out infected branches and applying copper-containing formulations or antibiotics. Unfortunately, copper formulations are often phytotoxic, antibiotics are really only effective against blossom infections and wound infections on shoots and fruits, and cutting can be inefficient when the amount of diseased trees is high. The use of antibiotics is also limited in some areas because resistant strains of the pathogen are present or because government regulations in some countries prohibit this practice. (Steiner, 2000). Also the models sometimes fail to accurately predict infection periods due to either the use of inaccurate weather information or the occurrence of unusual conditions which are not described by the prediction parameters of the models. Models are made to predict infections during primary bloom, but secondary bloom, later on the season, is not incorporated into the prediction models.

Due to these difficulties, new strategies of fire blight management are increasingly being used. One of these strategies is the use of biological control agents (Wilson and Lindow, 1993; Johnson and Stockwell, 2000; Stockwell et al., 2002).
Because the organs most susceptible to infection by *E. amylovora* are flowers, biological control of fire blight is based on the establishment of antagonist bacteria on blossoms prior to the arrival of the pathogen (Wilson et al., 1992; Johnson et al., 1993; Wilson & Lindow, 1993). Several

biological control agents have been developed and are authorized or in the process of registration, such as *Pseudomonas fluorescens* A506 (Wilson & Lindow, 1993), *Pantoea agglomerans* C9-1 (Ishimaru et al., 1988), *Pa. agglomerans* D325 (Pusey, 1997), *Pa. agglomerans* Pc10 (Vanneste et al., 2002), *Bacillus subtilis* QST713 (Aldwinckle et al., 2002), and *B. subtilis* BD170 (Broggini et al., 2005). Beside bacteria, also epiphytic yeasts are potential antagonists to fire blight in apple blossoms (Seibolt et al., 2006). Despite the promising result with the use of antagonists, there is much discussion on the possible human hazards. For instance it is known that the antagonist *Pantoea agglomerans* causes human infections (Cruz at al., 2007). The strains isolated from human infections were not showing the same characteristics than those utilized as biological control agent, however care has to be offered. The subject is also currently under investigation by B. Duffy (Switzerland) and other teams.

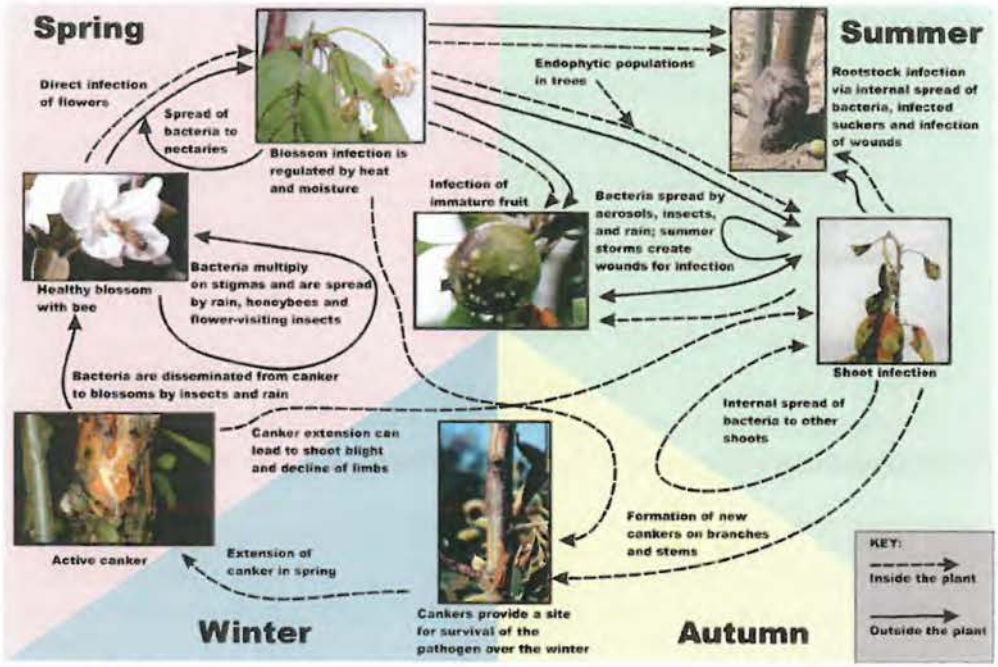

Figure 1.2:
Disease cycle of fire blight caused by *Erwinia amylovora.* Dashed lines represent movement of bacteria and spread of disease within the plant and solid lines represent movement of bacteria outside the plant. Modified from disease cycle of Sherman Thomson (2000) by Norelli et al. (2003).

Another approach is the development of new fire blight control technologies that enhance host resistance by chemical or genetic means. Prohexadione-calcium (Apogee or Regalis) for instance, is a plant growth regulator that reduces shoot growth by inhibiting gibberellin biosynthesis (Rademacker, 2000). On apple, control of vegetative growth with prohexadione-calcium also reduces the incidence and severity of fire blight shoot infection (Yoder et al., 1999). Prohexadione-calcium does not exhibit antibacterial activity against *Erwinia amylovora* but increases host resistance by reducing plant vigour. In addition, treatment of apple with prohexadione-calcium results in alteration of phenylpropanoid biosynthesis pathways that may also enhance resistance (Evans et al., 1999). Its use is most appropriate in established orchards where it reduces tree growth; therefore it may not be of value in young orchards where tree growth is important for developing productive trees. However, tree losses from fire blight are usually most devastating in young orchards (Norelli et al., 2003). Also genetic engineering is a promising approach. Genes with direct antimicrobial activity, constructs altering the expression of native apple genes involved in host resistance or silencing genes involved in pathogenesis, appear to have great potential for commercial use (Norelli et al., 2003).

1.3 *Erwinia amylovora*: pathogenicity factors

During the past quarter century, many genes and gene products involved in the ability of *Erwinia amylovora* to cause fire blight in host plants, have been identified and characterized. The following topics will give an overview of the known pathogenicity factors.

1.3.1 *Ex*opolysaccharides

One of the main pathogenicity factors of *Erwinia amylovora* are the exopolysaccharides (EPS) of its capsule.

EPS are very hygroscopic and promote tissue invasion as a result of the swelling pressure of hydrated EPS. Such pressure being exerted on all sides of the intercellular space pushes the bacteria to move according to the path of lowest resistance. This path might sometimes lead masses of bacteria to the outside of the plant, which could explain the presence of exudate or ooze (Vanneste and Eden-Green, 2000). The ooze droplets produced by *E. amylovora* on plant surfaces consist of EPS and bacteria. The hygroscopic feature of the EPS capsules prevent cells from losing water, which might be beneficial in increasing ion concentration in

neighbouring plant cells. In addition it causes water soaking and tissue collapse. Further, EPS is barely immunogenic and masks cell surface components. This property allows pathogens to elude host recognition and escape host defences (Geider, 2000).

Plant-associated bacteria produce complex EPS, whose composition and sugar linkages are characteristic for a bacterial species. The polymerization of a repeated unit results in high-molecular-weight EPS. Amylovoran, the main EPS of *Erwinia amylovora* contains about 1000 repeats per molecule. The structure of the repeating unit is displayed in figure 1.3. The size of an amylovoran molecule depends on the growth conditions and to a lesser extends on individual strains (Langlotz et al., 1999). The structure of the repeat of amylovoran consists of a backbone of three galactose residues and a side-chain of glucoronic acid and another galactose residue, which is substituted by acetyl groups and pyruvate (Geider, 2000). Because of its complex sugar linkages, biosynthesis of amylovoran requires a large number of genes. Most of the structural genes are located in an approximately 17 kb region on the chromosome called *ams* (Bugert and Geider, 1995). The *ams* region comprises 12 open reading frames (ORFs).

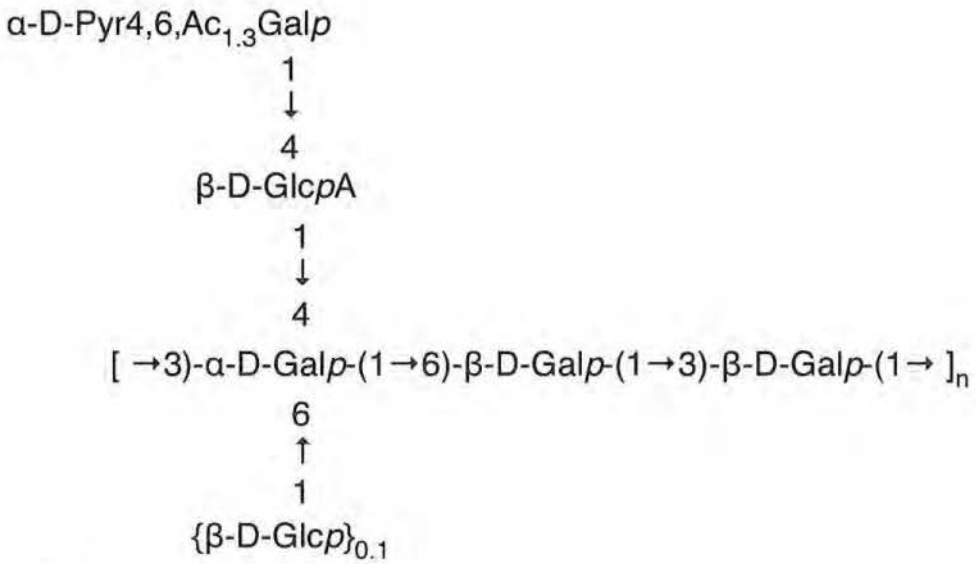

Figure 1.3:
Structure of the repeating unit of amylovoran (Nimtz et al., 1996).
Gal, galactose; GlcA, glucuronic acid; Pyr, pyruval residue with keto linkage; α, β, sugar linkage at C1; D, sugar configuration; *p*: pyranoside; *n*, degree of polymerization (at least 1000).

The products of all 12 genes are involved in individual steps of amylovoran synthesis. These genes encode sugartransferase activities (*amsB, amsD, amsE*), a lipid-carrier transferase homologe (*amsG*) indicative that amylovoran synthesis may be membrane linked, components of a postulated ABC transporter (*amsA, amsL*), a protein thought to be involved in amylovoran translocation across the outer membrane (*amsH*) and a polysaccharide polymerase (*amsF*) (Bugert and Geider, 1995). Beside the *ams* operon, on the right adjacent, two genes are located which are involved in the synthesis of precursors: *amsM* (analogous to *galF*) and *galE* (UDP-galactose epimerase). The *ams* operon is controlled by a two-component system, first identified in *E. coli* as regulator of capsule synthesis (cps). An environmental sensor, RcsC, phosphorylates RcsB. Phosphorylated RcsB binds an enhancer protein RcsA and the resulting heterodimer binds to the *ams* promoter region and stimulates transcription (Wehland et al., 1999).

Beside amylovoran, there is a second EPS: levan. Although levan is involved in virulence (Gross et al., 1992), it is not essential for pathogenicity (Belleman and Geider, 1992). Levan is an EPS composed of a single sugar, a homopolymer of fructose residues. The *lsc* gene, which encodes levansucrase, controls the biosynthesis of levan (Geier and Geider, 1993). Levan synthesis is positively regulated by RlsA (Zhang and Geider, 1999)

1.3.2 The Hrp pathogenicity island of *E. amylovora*

The process, in which an organism incorporates genetic material from another organism without being the offspring of that organism, is called horizontal gene transfer (HGT). Pathogenicity islands (PAIs) are a distinct class of genomic islands, which are acquired by HGT. They are present in the genome of pathogenic microorganisms but are usually absent in non-pathogenic organisms of the same or closely related species. They usually occupy relatively large genomic regions ranging from 10-200 kb and encode genes which contribute to the virulence of the respective pathogen. Typical examples are adherence factors, toxins, iron uptake systems, invasion factors and secretion systems. Pathogenicity islands are discrete genetic units flanked by direct repeats, insertion sequences or tRNA genes, which are sites for recombination into the DNA. Cryptic mobility genes may also be present, indicating the provenance as transduction (Hacker and Kaper, 2000).

Plant-pathogenic bacteria in the genera *Erwinia, Pseudomonas, Ralstonia* and Xanthomonas contain clustered genes called *hrp* (hypersensitive

response and pathogenicity) (Alfano and Collmer, 1997). They constitute important components of PAIs. Initially, they were named *hrp* genes because mutations in them led to loss of the ability to elicit the hypersensitive response (HR) in resistant plants and because the ability of the wild types of these genes to cause disease (pathogenicity) in susceptible plants. *Hrp* genes are components of a protein secretion system called the Hrp type III secretion system (TTSS) or are secreted through this pathway. Some *hrp* genes encode proteins that control gene expression.

The type III secretion system (TTSS) is a specialized protein-secretion pathway and it is encoded by many bacteria that are pathogenic for eukaryotic organisms (Cornelis and Van Gijsegem, 2000; Galán and Collmer, 1999). A remarkable feature of this pathway is that it not only directs the secretion of proteins through the bacterial envelope but also mediates the translocation of these proteins into eukaryotic host cells. The translocated virulence factors, which vary widely among the different bacterial pathogens, have the capacity to modulate or interfere with various host-cell functions. The main component of this system is a supramolecular structure – the 'needle complex' – which spans the bacterial envelope. (Stebbins and Galán, 2003). The structure of the TTSS is presented in figure 1.4.

The *hrp* PAI of *Erwinia amylovora* contains ca. 60 genes in ca. 62-kb of genomic DNA, which can be divided into four distinct DNA regions as shown

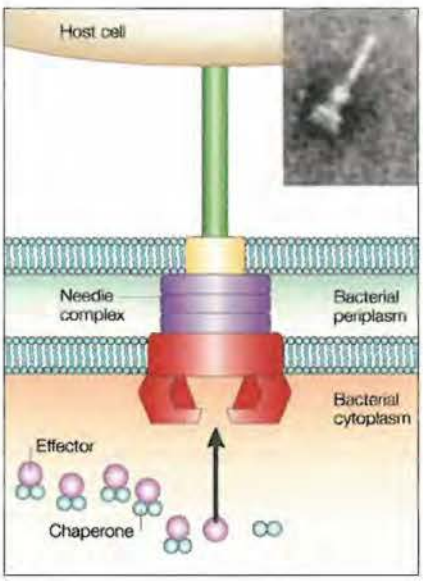

Figure 1.4:
The type III secretion system of gram-negative bacterial pathogens, injecting virulence factors into host cells (Stebbins and Galán, 2003).
The needle complex is drawn on the basis of its appearance in electron-microscopy images (see inset), with several ring structures that span the inner and outer membranes. The green protrusion is the 'needle' filament, which is thought to engage a bacterial pore-forming complex that becomes lodged in the host cell membrane. The virulence factors/effectors are bound to chaperones when they are waiting to be transported through the export machinery.

in figure 1.5, the *hrp/hrc* region, the Hrp effectors and elicitors (HEE) region, the Hrp-associated enzymes (HAE) region and the island transfer (IT) region (Oh and Beer, 2005). Each of these regions will be discussed in the following parts.

Hrp/hrc region

The *hrp/hrc* region contains 25 genes. The *hrc* genes were renamed because they are highly conserved among pathogenic bacteria (Bogdanove et al., 1996).

The most important role of the genes in this region is to form a protein secretion/translocation pathway, called the "Hrp TTSS", to secrete and deliver proteins from bacteria to plant apoplasts or cytoplasm.

Four regulatory genes *hrpL, hrpS, hrpX* and *hrpY* control the expression of other *hrp/hrc* genes. In *Erwinia amylovora*, HrpL controls expression of all known *hrp* and *hrc* genes, as it does in *P. syringae* (Wei and Beer, 1995). HrpL recognizes promoters with a *hrp* box, which consists of specific DNA sequences. Expression of the *hrpL* gene is controlled by HrpS, a member of the NtrC family of sigma 54 enhancer-binding proteins and sigma 54 (Wei et al., 2000). In addition, HrpX, a putative sensor protein and HrpY, a

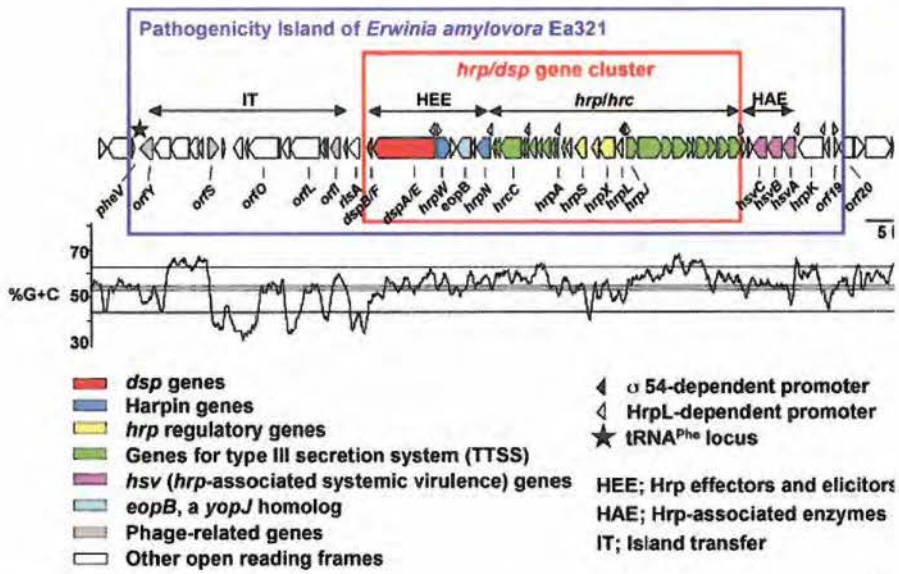

Figure 1.5:
The Hrp pathogenicity island of E. amylovora strain Ea321. It consists of four DNA regions: the hrp/hrc region, the HEE region, the HAE region, and the IT region. The hrp/dsp gene cluster includes the hrp/hrc region and the HEE region. The genes having significant functions or homology with other significant genes are color-coded as indicated. The % G + C graph is the result of a sliding window of 500 nucleotides (Oh and Beer, 2005).

potential response regulator, which together constitute a two-component regulatory system, are involved in expression of the *hrpL* gene (Wei et al., 2000). The identity of the molecules that actually are responsible for stimulating expression of *hrp* and *hrc* genes *in planta* remains to be determined.

HEE region

The HEE region contains seven genes; two (*hrpN* and *hrpW)* encode harpins, two are *dsp* genes (*dspA/E* and *dspB/F*), one is a *yopJ* homolog (*eopB)* and two encode putative chaperones (*orfA* and *orfC)* (Oh et al., 2005).

Harpins elicit the HR in plants and were the first proteins demonstrated to be secreted via the *hrp* TTSS (Kim ad Beer, 2000). Harpins have been considered as "helper proteins" (Collmer et al., 2002) that may facilitate the translocation of effector proteins into plant cells. Unlike effector proteins, which are translocated to the plant cytoplasm, harpins are secreted and targeted to the intercellular spaces of plant tissues through the *hrp* TTSS. However, the exact function of harpins in disease development remains to be determined.
To date, two harpins, HrpN and HrpW, have been found in *Erwinia amylovora*. HrpW has a putative pectate lyase domain in its C-terminal; no virulence function for HrpW has been detected (Kim and Beer, 1998). HrpN on the other side, was considered to be involved in disease development based on mutational analysis and it was described as the first cell-free elicitor of a HR in the early 1990s (Wei et al., 1992). HrpN not only induces HR, but it has other pleiotropic effects in plants. First, it induces the salicylic acid (SA)-dependent and the jasmonate (JA)-dependent pathways in *Arabidopsis*. Moreover, HrpN-treated plants have increased resistance against pathogens (Peng et al., 2003; Dong et al., 1999) and aphids (Dong et al., 2004). Furthermore, treating plants with HrpN results in enhanced growth and increased productivity in Arabidopsis, tomato and cotton (Dong et al., 2004). How HrpN induces these pleiotropic effects *in planta* remains to be determined.

The "disease-specific" (*dsp*) genes are required for pathogenesis in host plants but are not required for elicitation of defence responses in non-host plants. Two genes in the HEE region are considered as *dsp* genes, namely *dspA/E* and *dspB/F.*
DspA/E, a homolog of AvrE of *P. syringae*, is known as a pathogenic-

ity factor in *Erwinia amylovora*, *dspA/E* mutants are not pathogenic to apple shoots, immature pear fruit slices (Bogdanove et al., 1998) or pear seedlings (Gaudriault et al., 1997).
DspA/E is secreted through the Hrp TTSS (Boganove et al., 1998) and its secretion is dependent on DspB/F, which seems to be a DspA/E-specific chaperone (Gaudriault et al., 2002)

Whether EopB (*Erwinia* outer protein B) is involved in virulence remains to be determined in apple. However, EopB probably does not play a role in virulence or pathogenicity of *Erwinia amylovora* in immature pear fruit and in HR elicitation because its mutant's responses did not differ from those of the wild-type strain in pear fruit and *N. tabacum* cv. Xanthi, respectively (Kim, 1997).

HAE region

The HAE region, which stands for Hrp-associated enzymes, includes five genes. These genes are homologous to genes encoding enzymes involved in peptide synthesis (Oh and Beer, 2005).
The *hrpK* gene is positioned beside the HAE region. The function of HrpK in the fire blight pathogen remains to be determined.

IT region

The Island Transfer region includes 17 genes; three are homologous to phage genes (Oh et al., 2005). Because a mutant in which the complete IT region was deleted still caused disease symptoms in immature pear fruit slices and induced an HR in tobacco leaves, it is unlikely that the IT region contributes to pathogenicity in immature pear and to elicitation of the HR in tobacco.

The IT region starts with a tRNAPhe gene. This probably served as the port, from which the Hrp PAI of Erwinia amylovora begins. Also the nucleotide similarity of the *E. amylovora* Hrp PAI with the conjugative transposon CTn*scr*94 seems to extend beyond the tRNA gene, suggesting that the *E. amylovora* Hrp PAI once was a conjugative transposon. *orfY* could have encoded the recombinase responsible for integration of the island (Oh et al., 2005). Moreover the fact that the left border of the PAI of *E. amylovora*, located in the IT region, is highly conserved with a PAI of *Y.*

pseudotuberculosis, suggests that this region which is present in both animal and plant pathogens, may have been mobile through horizontal gene transfer (Oh and Beer, 2005).

1.3.3 Sorbitol metabolism

Sorbitol is the most important transport and storage carbohydrate compound of numerous plant species of the Rosaceae family (Lewis and Smith, 1967; Loescher, 1987; Nosarszewski et al., 2004), rather than sucrose, which is used in many other plants.

For *E. amylovora*, sorbitol is a good carbon source to synthesize amylovoran (Bennett and Billing, 1978) and increases EPS synthesis (Bellemann et al., 1994). Sorbitol could also be essential for *E. amylovora* to colonize plants, restricting fire blight to members of the *Rosaceae* (Geider, 2000). The *srl* operon, which is necessary for sorbitol metabolism consists of six genes. The genes *srlA, srlB* and *srlE* are needed for sorbitol uptake. The gene product of *srlD* converts sorbitol to fructose. The two other genes, *srlM* and *srlR* are regulatory genes. (Aldridge et al., 1997)

1.3.4 Desferrioxamine (siderophore)

Siderophores allow *E. amylovora* to overcome conditions of iron limitation encountered in host tissues but act also as protective agents against iron toxicity. To optimize iron acquisition, *E. amylovora* produces and secretes cyclic desferroxamines (DFOs), hydroxamate-type siderophores and a ferrioxamine receptor required for iron uptake (Dellagi et al., 1998).

Siderophores are low-molecular-weight compounds (<1500 Da) possessing a high affinity for Fe(III), which is the predominant form of iron in aerobic and microaerobic environments (Expert et al., 2000). Of the DFO family, DFOE appeared to be the predominant produced siderophore. The receptor FoxR is responsible for recognition and uptake of the DFE-Fe(III) complexes.

1.4 The plant defence system

The first step of the defence system of a plant against pathogens is its surface, which the pathogen must adhere to and penetrate to cause infection. Some structural defences are present in the plant even before the pathogen comes in contact with the plant tissues. Such structures include the amount and quality of wax and cuticle that cover the epidermal cells, the structure of the epidermal lenticels and the presence of tissues made of thick-walled cells that prevents the penetration of the pathogen in the plant.
Although structural characteristics may provide a plant with various degrees of defence it is clear that the resistance of a plant against pathogen attacks depends not so much on its structural barriers as on the substances produced in its cells before or after infection. (Agrios, 2005)

Once pathogens invade, plants respond to infection by activating its active defence system. In a first phase, plants use transmembrane pattern recognition receptors (PRRs) that respond to slowly evolving microbial- or pathogen-associated molecular patterns (MAMPs or PAMPs), such as flagellin (Zipfel and Felix, 2005), lipopolysaccharides (LPS), bacterial cold shock proteins and elongation factor Tu (Ef-Tu) (Felix and Boller, 2003; Kunze et al., 2004). PAMPs (or MAMPs) are recognized by PRRs, resulting in PAMP-triggered immunity (PTI) that can halt further colonization. Recognition of PAMPs or MAMPs leads to the activation of the plant basal defence (or resistance), which is the first response and triggers a generic mechanism consisting of plant cell wall thickening, papilla deposition, apoplast acidification and signal transduction and transcription of defence genes, such as the corresponding genes of the pathogen related (PR) proteins (Alfano and Collmer, 2004). This generic basal defence mechanism has been observed in several incompatible plant-microorganism interactions and is believed to corroborate the observation that most plants are resistant to invasion by the majority of pathogens.

To be effective, pathogens must evolve mechanisms to interfere with or suppress basal defence to colonize the host and develop disease. Successful pathogens deploy effectors that contribute to pathogen virulence. Effectors can interfere with PTI. This results in effector-triggered susceptibility (ETS). Plant pathogenic bacteria, for instance, deliver 15-30 effectors per strain into host cells using Type III secretion systems (TTSS). These bacterial effectors contribute to pathogen virulence often by mimicking or inhibiting eukaryotic cellular functions (Abramovitch et

al., 2006). Pathogens could also produce small molecule effectors that mimic plant hormones. However, the influence of pathogen mimics on PTI and normal hormone signalling is only just beginning to be unravelled (Jones and Dangl, 2006).

A bacterial effector, however, could be 'specifically recognized' by one of the plants 'nucleotide binding – leucine rich repeat' (NB-LRR) proteins, resulting in effector-triggered immunity (ETI). This recognition acts largely inside the cell, using the polymorphic NB-LRR protein products encoded by most *R* (resistance) genes (Dangl and Jones, 2001). They are named after their characteristic NB and LRR domains. The recognized effector is termed an avirulence (AVR) protein.

ETI is an accelerated and amplified PTI response, resulting in disease resistance (Truman et al., 2006) and usually a hypersensitive cell death response (HR) at the infection site (Greenberg and Yao, 2004).
The function of the hypersensitive response (HR) is to 'isolate' the pathogen. It puts an end to pathogen invasion and prevents further disease development (Alfano and Collmer, 2004).
The hypersensitive response is typified by activating a cascade of biochemical reactions in the attacked and surrounding plant cells which leads to new or altered cell functions and to new or greatly activated defence-related compounds. The most common new cell functions and compounds include a rapid burst of reactive oxygen species, leading to a dramatic increase of oxidative reactions; increase in ion movement, especially of K^+ and H^+ through the cell membrane; disruption of membranes and loss of cellular compartmentalization; cross-linking of phenolics with cell wall components and strengthening of the plant cell wall; transient activation of protein kinases (wounding-induced and salicylic acid-induced kinases); production of antimicrobial substances such as phenolics (phytoalexins) and synthesis of anti-microbial so-called pathogenesis-related proteins such as chitinases (Agrios, 2005).
During bacterial infections of leaves, the hypersensitive response results in the destruction of all cellular membranes of cells in contact with bacteria, which is followed by desiccation and necrosis of the leaf tissues invaded by the bacteria. The necrotic tissue isolates the parasite from the living substance on which it depends for its nutrition and, thereby, results in its starvation and death. Also the amount of numerous biochemical cell responses and anti-microbial substances that neutralize the pathogen will be important. The faster the host cell dies after invasion, the more resistant to infection the plant seems to be (Agrios, 2005).

In a next phase, natural selection selects pathogens that avoid ETI either by shedding or diversifying the recognized effector gene or by acquiring additional effectors that suppress ETI. Natural selection results in new *R* specificities so that ETI can be triggered again (Jones and Dangl, 2006).

Most plants resist infection by most pathogens; they are said to be 'non-hosts'. This non-host resistance could be mediated by at least two mechanisms. First, a pathogen's effectors could be ineffective on a potential new, but evolutionarily divergent, host, resulting in little or no suppression of PTI and failure of pathogen growth. This could be possible because some plants do not produce one of the substances essential for the survival of an obligate parasite or for development of infection. Alternatively, one or more of the effector complements of the would-be pathogen could be recognized by the NB-LRR repertoire of plants other than its adapted host, resulting in ETI. Non-host resistance can also be mediated by parallel ETI responses (Jones and Dangl, 2006).

Once the plant immune system is activated, plants develop a generalized resistance. Induced resistance is at first localized around the point of plant necrosis caused by infection by the pathogen and is called local acquired resistance. Subsequently, resistance spreads systemically and develops in distal, uninfected parts of the plant and is called systemic acquired resistance (SAR). Systemic acquired resistance acts non-specifically throughout the plant and reduces the severity of disease caused by many classes of pathogens, including normally virulent ones (Agrios, 2005).
SAR induction starts once the host recognizes the pathogen-derived elicitors. A series of alarm signals is sent out to host cell proteins and to nuclear genes. These signals cause these genes and host cell proteins to become activated, to produce substances inhibitory to the pathogen and to mobilize themselves or their products toward the point of cell attack by the pathogen. Some of the alarm substances and signal transductions are only intracellular, but in many cases the signal is also transmitted to several adjacent cells and, apparently, the alarm signal is often transmitted systemically to most or all of the plant tissues. Systemic signal transduction, which leads to SAR, is thought to be carried out by salicylic acid (SA), oligogalacturonides released from plant cell walls, jasmonic acid (JA), systemin, fatty acids, ethylene and others (Agrios, 2005). Recently, Park and co-workers (2007) provided evidence that methyl salicylate (MeSA), rather than SA functions as a critical mobile signal to induce SAR. Methylated JA and SA, namely MeJA and MeSA, can become volatile. Together with ethylene and green-leaf volatiles (GLV) MeJA and MeSA are likely

candidates in airborne long-distance signalling to mediate long-distance induction of resistance (Heil and Ton, 2008).

Figure 1.6 is a schematic overview of the functioning of the plant immune system as described in the previous text.

The hypersensitive response and oxidative burst are generally associated with incompatible plant/pathogen interactions. However, Venisse et al. (2001) showed that *Erwinia amylovora* induces in its susceptible host also such a stress response as well as related consequences (lipid peroxidation, electrolyte leakage, modulation in the antioxidant status) with intensity and kinetics similar to those induced by an incompatible bacterium. This ability is linked to a functional TTSS in the bacterium. This suggest tat *E. amylovora* is first recognized as an incompatible pathogen by its susceptible host, this bacterium copes with the lethal action of ROS on plant cells for a successful pathogenesis and Hrp effectors are responsible for the triggering of the oxidative burst (Venisse et al. 2003).

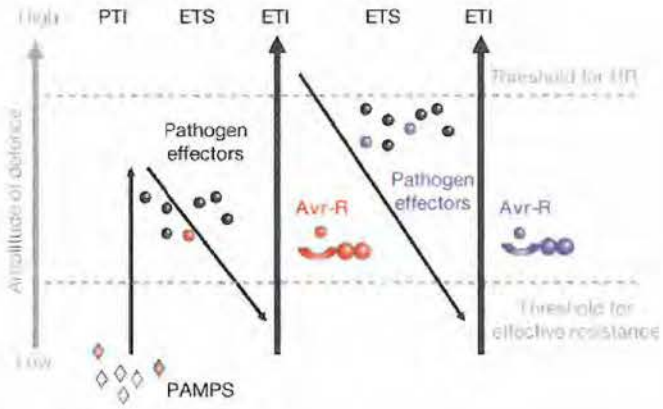

Figure 1.6:
A zigzag model illustrates the quantitative output of the plant immune system. In this scheme, the ultimate amplitude of disease resistance or susceptibility is proportional to [PTI – ETS1ETI]. In phase 1, plants detect microbial/pathogen-associated molecular patterns (MAMPs/PAMPs, red diamonds) via PRRs to trigger PAMP-triggered immunity (PTI). In phase 2, successful pathogens deliver effectors that interfere with PTI, or otherwise enable pathogen nutrition and dispersal, resulting in effector-triggered susceptibility (ETS). In phase 3, one effector (indicated in red) is recognized by an NB-LRR protein, activating effector-triggered immunity (ETI), an amplified version of PTI that often passes a threshold for induction of hypersensitive cell death (HR). In phase 4, pathogen isolates are selected that have lost the red effector, and perhaps gained new effectors through horizontal gene flow (in blue)—these can help pathogens to suppress ETI. Selection favours new plant NB-LRR alleles that can recognize one of the newly acquired effectors, resulting again in ETI (Jones and Dangl, 2006).

1.5 Aims of the present work

Fire blight, caused by the bacterium *Erwinia amylovora*, affects most species of the *Malaceae* and some species in other families of the *Rosales*. Apple and pear are economically the most important host species. Fire blight is a devastating disease as it can decimate apple and pear orchards in a single season. The severity of the disease results from its destructive character on the one hand and the lack of effective control methods on the other hand. The main objective of this work was to gain a better insight into the infection process in order to develop more accurate and environmental friendly control strategies. To achieve this, three aims were formulated:

- to gain a better insight in the way E. amylovora colonizes and infects host plant flowers and in the propagation of the bacteria throughout flower tissues. To obtain this, the expansion of the bacteria inside the host plant tissue was studied using microscopic techniques, such as transmission electron microscopy (TEM), light microscopy (LM) and confocal microscopy. Braeburn, Conference and Crataegus flowers were used as experimental material. Braeburn and Conference are respectively sensitive cultivars of apple and pear. Crataegus is an important ornamental host plant of E. amylovora. The results are presented in chapter 2.

- to gain a better insight in the bacterial proteome and in those bacterial proteins, which could play an important role during fire blight infection. This study focussed on the mechanisms how the bacteria cope with the lethal action of ROS, released during the compatible plant/pathogen interaction. To achieve this, we studied the protein expression profile (proteome) of E. amylovora. We compared the bacterial proteome during infection (in planta) with the proteome of E. amylovora grown in vitro, by two-dimensional gel electrophoresis (2D-GE). Shoots of the sensitive M9 rootstock were used as experimental material. Shoots were available year round and provided sufficient material for infection. The results of this study are described in chapter 3.

- to gain a better insight in the possible relation between the virulence and the occurrence of specific proteins. To reach this goal four wild type *E. amylovora* strains, differing in pathogenicity, were analysed *in vitro* and *in planta*. Using a DIGE-approach, the proteome of these four different strains was compared and correlated with the degree of virulence. The results of this study are presented in chapter 4

Chapter 2

Blossom infections by *Erwinia amylovora*

2.1 Introduction

During early spring, in response to warmer temperatures and rapid bud development, the bacteria at canker margins begin to multiply rapidly and produce a thick yellowish to white ooze that is produced onto the bark surface up to several weeks before the bloom period. Many insect species (mainly flies) are attracted to the ooze and subsequently disperse the bacteria throughout the orchard, including open flowers. Once the first few open blossoms are colonized by the bacteria, pollinating insects rapidly move the pathogen to other flowers, initiating more blossom blight.

E. amylovora is not generally considered to be a very good epiphyte and populations usually decline rapidly on most flower parts or leaves within a few hours or days (Miler, 1984), however epiphytic growth is supported on some flower parts. The epiphytic build-up and entry of *E. amylovora* during blossom infection has been investigated particularly in flowers of apple, hawthorn and pear and involves three major sites: the stigma, anthers and nectary (Thomson, 2000). A schematic overview of a typical *Rosaceae* flower is given in figure 2.1.

The stigmatic surface is important as a site of major epiphytic inoculum, but is generally a region of limited tissue penetration. In arid environments, the permanently moist stigmatic surface is the only part of the flower supporting an epiphytic population of the pathogen, which may reach levels of 10^7 colony-forming units (cfu) per stigma. At low humid-

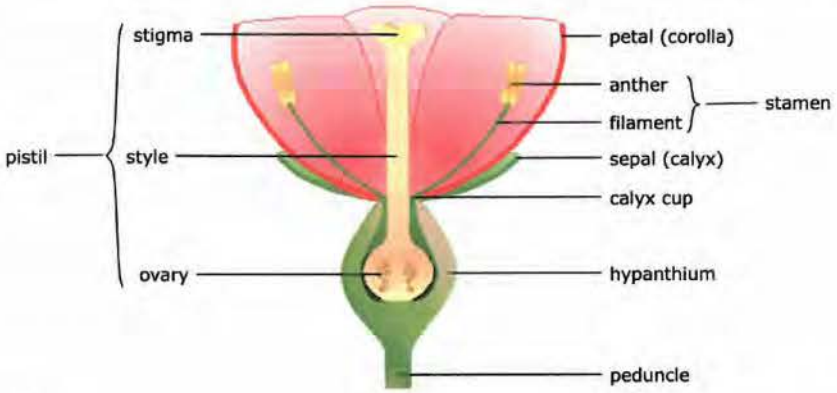

Figure 2.1:
Cross-section of a typical *Rosaceae* flower, which is an epigynous flower with inferior ovary. The hypanthium is an enlargement of the receptacle, loosely surrounding the ovary. The calyx cup contains the nectarthodes in the nectarial region and is surrounded by the sepals and petals. Figure reworked from http://biology.clc.uc.edu/Courses/bioall/plant%20families.htm

ity, high stigmatic populations can appear in apparently healthy blossoms, which suggests that there is no resulting infection under these conditions (Thomson, 1986). In contrast to this, epiphytic build-up on the stigmatic surface in wet environments almost always leads to floral infection, since the bacteria are washed off by rain or dew and enter the flower via the nectary surface.

Epiphytic growth of *E. amylovora* is also supported by anthers. Just as infection through the stigma infection through the anthers is also rarely seen. The population sizes on anthers are smaller than on stigmas, but play an important role in pathogen spread dispersal throughout the orchard. Bacteria can enter and multiply in the locule, with as a result the contamination of pollen. Infection in this part of the flower occurs mainly via the dehiscence zone, but some entry may also occur via stomata (Wilson et al., 1989). Contaminated pollen may serve as a means of disease spreading.

The presence of high populations of epiphytic bacteria on healthy flowers accounts for efficient movement of the bacteria from flower to flower by rain or by any insects that visit the flowers. From flower visiting insects it is known that pollen collecting bees mainly affect the anthers and stigma. They transfer the bacteria or contaminated pollen to the stigma. Nectar

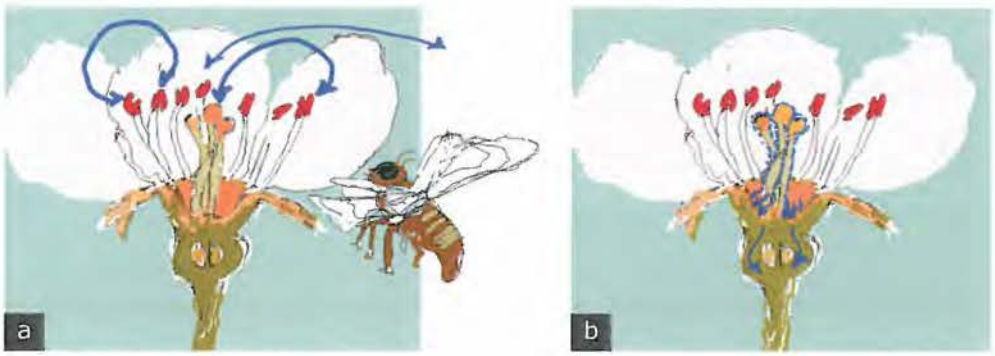

Figure 2.2:
Infection of apple flower by *Erwinia amylovora*. The figure shows the flower in half-section and illustrates potential sites of bacterial multiplication, dissemination and tissue penetration. The blue thin lines (--->) and arrows symbolize the bacteria and their distribution path. Figure based on Sigee (1993) and modified by N. Festjens.

a Flower visiting insects transfer bacteria from the stigma to the anthers and vice versa. They spread the bacteria also from flower to flower.

b After colonizing stigmatic surfaces, in humid circumstances, bacteria flush into the calyx cup, where bacteria enter the hypanthium tissue and spread throughout the entire hypanthium and the tissues below.

collecting bees stand on the petals and affect with their mouth parts the receptacle. Moreover they brush with their back the anthers and probably spread bacteria from anthers to other flower parts. Other insects such as bumblebees, wild bees and flies are less goal-oriented and affect all flower parts. Within a tree, bacteria can also be transported from top to bottom by raindrops (Thomson et al., 1999).

After colonizing stigmatic surfaces, bacteria can flush into the hypanthium where infection occurs (fig. 2.2). In contrast to the stigma, the hypanthium appears to be the major site of bacterial entry, but with limited epiphytic populations. The transfer from stigma to hypanthium requires a continuous film of free water (Bubán et al., 2003). *E. amylovora* also exhibits positive chemotaxis to apple nectar, to the organic acid fraction of apple nectar and to one amino acid (aspartate) in it, but not to any of the sugars (sucrose, glucose and fructose) tested. The main sugar components of the nectar are glucose and fructose. Only a few pear cultivars produce nectar containing a small amount of sucrose. Total concentration of sugar in nectar may be as high as 60%, although rain may dilute the sugars to <2%. Infection occurs freely when sugar concentrations are low but not at medium or high concentrations. A concentration of sugar higher than approximately 30% in the nectar of pear and apple flowers was proposed as the mechanism restricting development of fire blight (Thomson, 1986).

The nectarial region or nectary consists of tree tissue types: epidermis, glandular tissue and nectary parenchyma. Nectarthode is the term for the nectar excreting structure in the calyx cup of pear and apple blossoms. As shown on figure 2.3, these nectarthodes consist in surface view, of

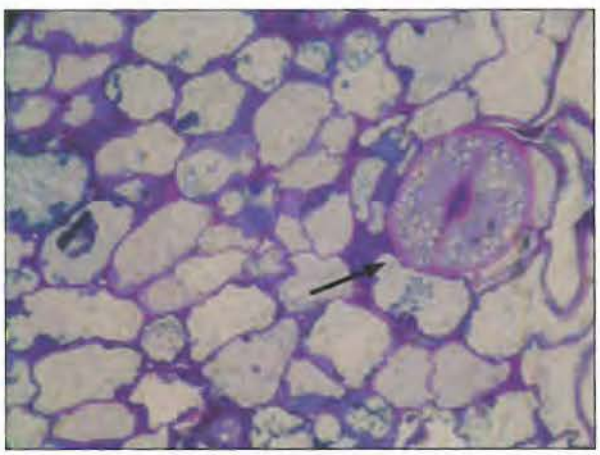

Figure 2.3:
Nectarthode (indicated by the arrow), present in the calyx cup of a *Crataegus* flower. A nectarthode consists of two curved, sausage shaped guard cells. Between the guard cells a stomata-like opening can be seen.

two curved, sausage shaped guard cells, each of which is usually several times as large as the surrounding epidermal cells. Between the guard cells a stoma-like opening can be seen. Immediately below the guard cells of nectarthodes are some open areas, varying considerably in size, and corresponding to sub-stomatal chambers of the nectary (Rosen, 1936).

Once *Erwinia amylovora* is present at the calyx cup and the conditions are favourable, bacteria can penetrate through the natural openings of the nectary, the nectarthodes, and from this point they can migrate and invade the tissues of the host plant.
First, blossoms appear water soaked, then wilt, shrivel and turn brownish to black. The blight progresses into the peduncle, which also appears water soaked, becomes dark green and finally turns dark. During warm humid weather, drops of bacterial ooze exude from the peduncle. The dead flowers do not fall down, but remain attached to the tree for weeks. On a sensitive host the bacteria move rapidly from the flower to the pedicel and then to the shoots, twigs, reaching the main branches and potentially causing the death of the entire tree (Vanneste and Eden-Green, 2000).

The nectarthodes are the most common sites for bacterial invasion in pear and apple flowers. In blossom blight, an invasion other than through nectarthodes is rarely reported. Nevertheless, infection on flowers can also occur through stigmas and anthers and numerous natural openings, including stomata on the styles, fruit surfaces and sepals and hydathodes (Rosen, 1935; Hildebrand, 1937).

The flowers colonized by *Erwinia amylovora* are subject to infection when the flowers are open and with intact petals. Infection can occur after a wetting event such as rain (≥ 2.5 mm), dew or rain on the previous day (≥2.5 mm). Temperature also plays an important role in infection. There must be an average daily temperature of ≥15.6°C and an accumulation of at least 110 degree hours >18.3°C (Steiner, 1990).
Pear flowers were shown susceptible for 2 days after opening, but susceptibility declined rapidly with flowers older than 2 days (Hildebrand, 1937). The basis for this decline might be explained by the work of Gouk et al (1996), who showed that *E. amylovora* was unable to grow on the stigmas of 'Royal Gala' apple flowers older than 4-5 days. This may be related to the normal degeneration of the papillae on the stigma of most apple cultivars, which occurs within 2-3 days after flowers open (Braun and Stösser, 1985). The degradation of the papillae should also explain why pear flowers older than 2 days show a decreased susceptibility. There may also be

inhibitory compounds produced on the stigma that prevent colonization by microbes as the flowers age (Thomson, 2000).

2.2 Objective

The aim of this chapter was to obtain a better insight in the colinization, infection and propagation of *E. amylovora* on apple (Braeburn), pear (Conference) and hawthorn (*Crataegus*) blossom. To achieve this goal a combination of confocal, light and transmission electron microscopic techniques has been used. Earlier studies on this topic were mainly based on electron and light microscopic techniques. The use of confocal microscopic techniques supplements the current vision on the infection process. In combining these techniques we want to verify and refine the present understanding of blossom infections by *Erwinia amylovora*.

2.3 Material and Methods

2.3.1 Bacteria

The bacterial strain used, BCCM-LMG2024, was isolated from pear, *Pyrus communis*, in the UK. The *E. amylovora* LMG2024 cells were transformed with the pfdC1Z'-gfp plasmid. This plasmid was made by the group of Prof. Dr. Klaus Geider (University of Heidelberg, Germany, (Bogs et al., 1998; Geider et al., 1995). pfdC1Z' is a high copy number plasmid with a replication function of the phage fd. A DNA fragment with the optimized *gfp* (green fluorescent protein) gene is transferred from pGFPm1 into plasmid pfdC1Z', yielding pfdC1Z-gfp. This plasmid also carries a kanamycin resistance gene. The bacteria were kindly provided to us by Dr. Martine Maes (ILVO, Institute for Agricultural and Fisheries Research, Ghent).

The bacteria were inoculated on Luria-Bertani (LB) broth that was supplemented with 1% w/v sorbitol and 20 µg/ml kanamycin. They were grown overnight at 24°C in an incubator.

2.3.2 Plant material

Flowering branches from the following trees were used for the experiments: common hawthorn (*Crataegus monogyna*), apple (*Malus* x *domestica* – Braeburn) and pear (*Pyrus communis* – Conference). For *Crataegus* and Conference, flower clusters on two-year-old wood were used. For Braeburn, we used flower clusters on one-year-old wood from two-year-

old trees, which were pruned back at 70 cm in the nurseries. For Braeburn we didn't distinguish between flower clusters in lateral or terminal position. For all studied trees, we didn't distinguish between the different flowers of a cluster.
The flowering branches were cut before bloom and placed in water containing cut flower nutrition (Chrysal CLEAR, Pokon & Chrysal-Naarden, The Netherlands). The blossoming is early induced in a growth chamber (Weis Technik, Liedekerke, Belgium, 205503/8/0001) at 24°C, 95% relative humidity (RH), 12 hours of light (with an average intensity of 200 µmol/m²s).

2.3.3 Treatment

One-day-old flowers were inoculated with a bacterial suspension of 10^8 cfu in PBS. Bacteria were obtained from an overnight culture of the *E. amylovora* strain BCCM-LMG2024, containing the pfdC1Z'-gfp plasmid. Inoculation was performed with a brush on the anthers or the stigma or near the calyx cup. Using this method, 10^4 to 10^5 CFU were applied per flower. Inoculated flower branches were incubated in a growth chamber (Weis Technik, Liedekerke, 205503/8/0001) at 24°C, 95% relative humidity, 12 hours of light (with an average intensity of 200 µmol/m²s).

The presence and spread of the bacteria was followed by confocal microscopy at 1, 2 and 3 days after inoculation. Samples for electron microscopy were taken at 4 days after infection.

2.3.4 Confocal laser scanning microscopy

Confocal imaging was done on a Zeiss LSM 510 Meta, equipped with an Argon Ion 2 laser, coupled to a Zeiss Axiovert 200 M inverted microscope frame. The laser power used at 488 nm is kept at 1% and 10 µW at the sample position to prevent photo bleaching (Zeiss, Zaventem, Belgium). The detector pinhole diameter is set to 69 µm. The images were obtained with a 10 x Plan-Neofluar objective with a numerical aperture of 0.3, image size 920 x 920 µm or 512 x 512 pixels. For GFP visualization, an HFT UV/488/543/633 filter is used to select the excitation illumination and a BP 510/20 (FWHM) IR to specify the emitted light. For chlorophyll visualization excitation at 488 nm is used, with respectively an UV/488/543/633 and a BP 650-710 IR emission path optical filter.

Biological samples are three-dimensional structures. To visualize these structures using confocal microscopy, Z-stacks were made. A series of 2 dimensional images (in x and y), or optical sections, are acquired at regular focus intervals. In order to create a representation of the three-dimensional object, such 'Z-stack' optical sections are layered on top of each other.

Another confocal technique used is the lambda-scan. A lambda-scan records a series of individual images within a wavelength range; each image will be detected at a specific emission wavelength. These images were fused together to create a spectrally resolved image (fig. 2.4) where each colour represents the emission signal of the representative spectral bin of given colour (e.g. a red colour represents emission in the red region). To be more certain that a BP 510/20 bright image region can be associated with GFP, a strong smooth decreasing GFP signal with a peak in the first spectral channel starting with 504 nm has to be seen (fig. 2.4). However autofluorescence especially from Conference anther material as well as scattered excitation light do also have a peak intensity in this first spectral channel. In general BP 510/20 brightness matches spectral classification, but spectral analysis was required to weed out misinterpretation caused by autofluorescence signal.

The flower organs that were studied were dissected from a blossom and placed on a microscope slide (fig. 2.5). The style, the stamen and the peduncle were studied as a whole. To study the hypanthium, the flower was placed on the microscope slide after petals and sepals were removed, and the entire flower was chopped into two pieces (fig. 2.5 b).

2.3.5 Transmission electron microscopy (*TEM*) and light microscopy (LM)

Flower parts were fixed for 20 hours at 4°C using vacuum infiltration in 2% v/v glutaraldehyde and 0.01% w/v malachite green, buffered in 0.05 M sodium PIPES (pH 7.5). The samples were rinsed 3 times 30 minutes in 0.05 M sodium-PIPES (pH 7.5) and post-fixed in 2% w/v osmium tetroxide, buffered in 0.2 M sodium cacodylate at 4°C for 2 hours. The tissues were rinsed once in 0.2 M sodium cacodylate and twice in distilled water before staining in 2% w/v uranyl acetate overnight at 4°C. The tissues were dehydrated in graded concentrations of acetone and impregnated and embedded in Spurr's epoxy resin. Ultra-thin sections (65 nm), obtained using a Leica Ultrcut UCT ultramicrotome, were mounted on 0.7%

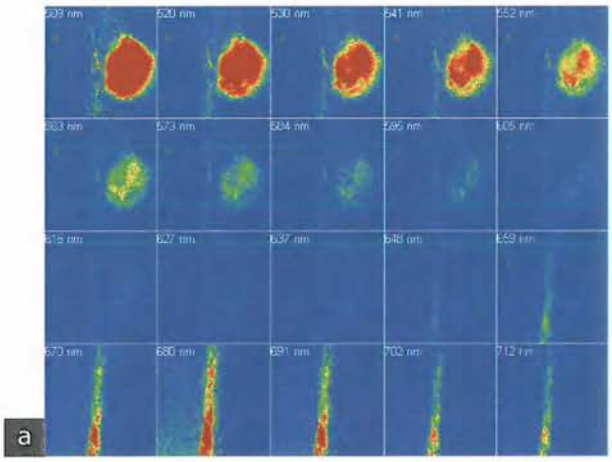

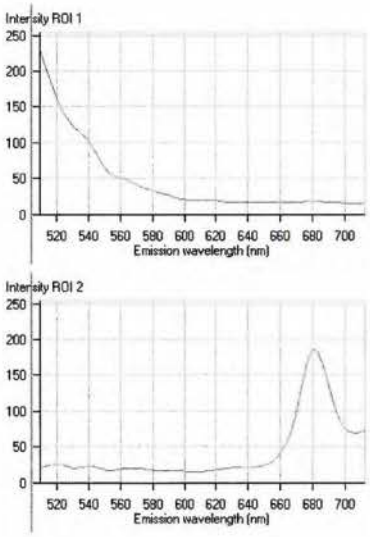

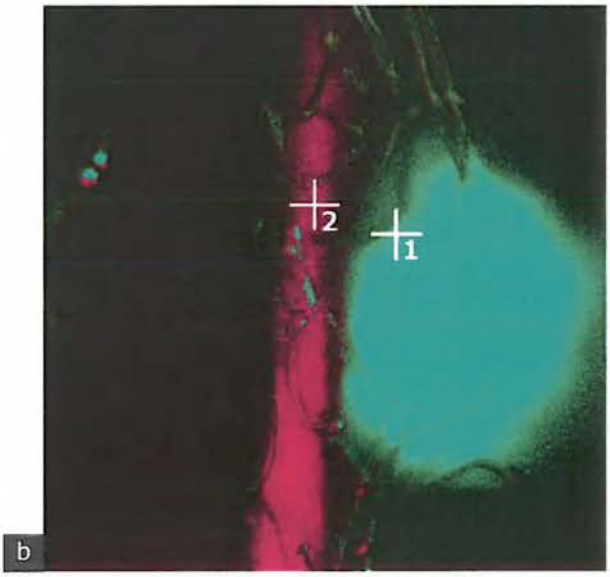

Figure 2.4:
The images show the results of a lambda scan of a peduncle of an infected Braeburn flower with an ooze drop. Image size is 920 x 920 µm.
a. Series of individual images within a wavelength range. The colour code of the individual images indicates the intensity of the signal.
b. Spectrally resolved image of a lambda scan. The green area represents the ooze drop where GFP producing bacteria are present. The emission spectrum of the first (1) region of interest (ROI) shows the typical GFP signal. The GFP peak is approximately at 510 nm. The red signal is from chlorophyll, present in the peduncle. ROI 2 illustrates the chlorophyll emission spectrum, with a peak near 680 nm.

w/v formvar coated copper grids 50 mesh). The sections were contrasted with uranyl acetate (4% w/v in 50% v/v ethanol) followed by lead citrate (4% w/v solution) and examined in a Philips EM 208 transmission electron microscope operated at 80 kV. Images were digitized with the MORADA 10/12 camera (Olympus, Germany).

From the same, in resin imbedded tissues, semi-thin sections (0.5 µm) were made for light microscopy. The sections were mounted on a gelatine coated microscope slide, coloured with methylene blue (0.1% w/v) and thionine (0.1% w/v) and sealed with Depex. The tissue samples were examined using a Nikon Eclipse 80i microscope and images were taken with a Nikon Coolpix 5400 camera.

2.4 Results and Discussion

Inoculation occurred on one-day-old flowers of respectively apple (Braeburn), pear (Conference) and common hawthorn (*Crataegus monogyna).* Inoculation was carried out on the anthers, stigma or hypanthium of the flowers of each plant type. The bacterial spread was followed by confocal microscopy and in addition TEM images ware taken.

Figure 2.5:
The image shows the Zeiss LSM 510 Meta confocal microscope (a) and the way of studying the different flower organs (b). The style, the stamen and the peduncle were studied as a whole. To study the stamen, for practical reasons, the stamen was removed from the flower. To study the hypanthium, the flower was placed on the microscope slide after petals and sepals were removed, and the entire flower was chopped into two pieces. Sepals and petals never show the presence of *E. amylovora* and were not discussed in the results.

In order to follow infection by confocal microscopy, infection was performed with *E. amylovora* strain BCCM-LMG2024, which contains a plasmid coding for the green fluorescent protein (GFP). To obtain a general overview of the tissue by confocal microscopy, chlorophyll fluorescence was used. All green flower parts contain plastids, which contain the chlorophyll molecules. Chlorophyll detection is an easy way to visualise the different flower parts by confocal microscopy.

2.4.1 Inoculation of the anthers

Visualisation of *E. amylovora* on the anthers by confocal microscopy was a real challenge due to the high background fluorescence levels. The high background fluorescence is probably due to the carotenoids and azulenes, present in the pollen (Roshchina et al., 1997). These molecules are fluorescent in the green spectral region and we found this background signal altering in function of time.

For *Crataegus* and Conference anthers, the emission spectra of the background fluorescence overlap with the GFP emission spectrum. For these flowers it was difficult to distinguish between GFP and background fluores-

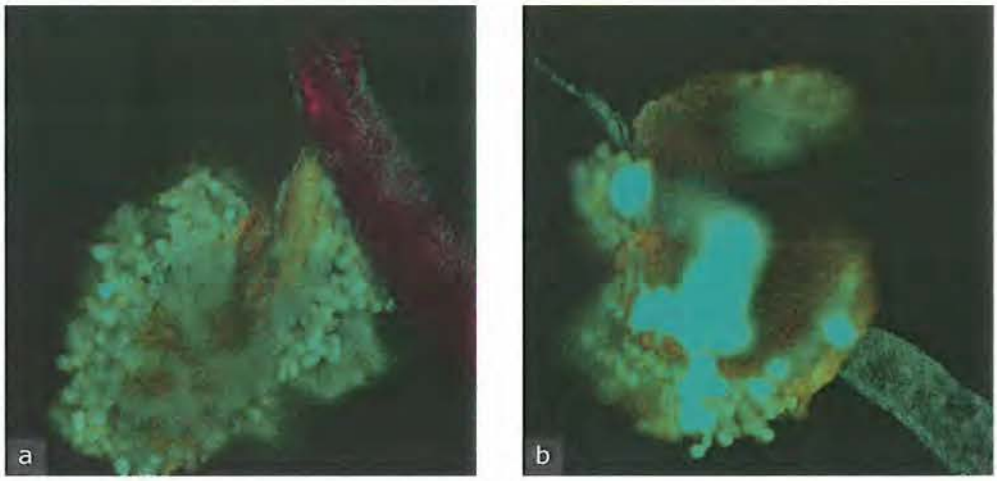

Figure 2.6:
Left: un-inoculated anther of a *Crataegus* flower; right: *Crataegus* anther inoculation with *E. amylovora* strain BCCM-LMG2024, three days after inoculation.
Both pictures are coded images of a lambda scan. A lambda-scan measures fluorescence at a series of wavelengths. Each colour represents the emission signal of the representative wavelength of the used colour. Image size of both images is 920 x 920 µm.
Note the high background fluorescence in the green area of the pollen of the un-inoculated anther (a). GFP is also fluorescent in the green region (max.: 509 nm) but the signal deriving from GFP shows a brighter signal. Note here the ultra bright green GFP-signal of the inoculated *Crataegus* anther (b). In the red region, chlorophyll fluorescence is visible (max.: 690 nm) near the filament.

cence. For *Crataegus* however there was a strong increase in fluorescence intensity in the green spectral region three days after inoculation indicating the presence of GFP producing *E. amylovora* (fig. 2.6).
Braeburn anthers show also a high background signal, but the emission spectrum is slightly different from the GFP spectrum (fig 2.7). For these flowers it was possible to recognize the GFP fluorescence near the anthers, even in presence of high background fluorescence levels.

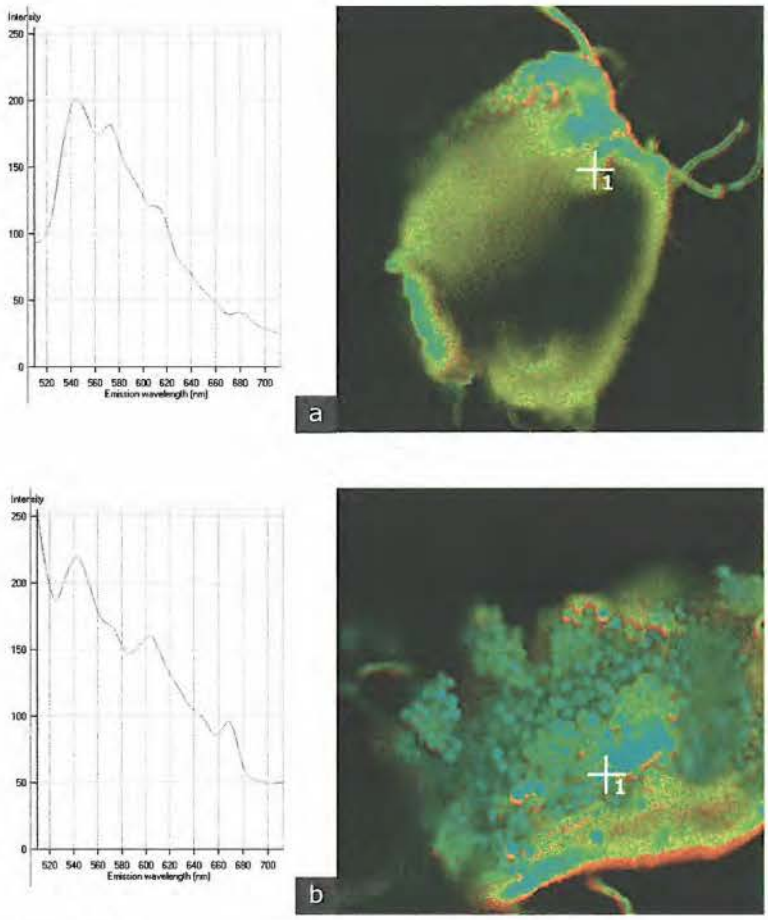

Figure 2.7:
Spectrally resolved images of a lambda scan. Image size is 920 x 920 µm. The first image (a) is a control anther of a Braeburn flower; image (b) shows a Braeburn anther three days after inoculation. Note in both cases the fluorescence spectra. For the control anther (a), there is a relative low fluorescence near 510 nm. The background fluorescence has a peak at approximately 540 nm. Near the inoculated anther (b) we can find areas with a peak near 540 nm (background signal) but also a peak near 510 nm, which corresponds with the GFP signal.

In most cases flowers remained symptomless after anther inoculation. However sometimes infection occurs. This could be due to contaminated pollen that fell inside the calyx cup. But we found also evidence for another infection route. Bacteria may move epiphytic via the small grooves of the filament (fig 2.8). A similar movement was already shown from the stigma to the hypanthium via the stylar groove (Spinelli et al. 2005). Such a transfer requires a continuous film of free water (Bubán et al., 2003), which could also be present in our case due to the high humidity during the incubation period (95% RH).

The TEM images of all studied flowers showed the presence of *E. amylovora* bacteria inside the locule of the anther. On the outside, the place of inoculation, only a few bacteria were visible. The epiphytic growing bacteria inside the locules did not invade the anther tissues and the anther tissues stayed completely unaffected in the presence of the bacteria.
Once on the anthers, bacteria can easily enter the locules via the dehiscence zone of the anther. Inside the locule, the bacteria grow epiphytically and contaminate the pollen. These contaminated pollen are now a new source of inoculation. Flower visiting insects can transport this contaminated pollen to other flower parts and also to other flowers. Figure 2.9 shows the presence of *E. amylovora* inside the locule and on the surface of the pollen of a Conference flower.

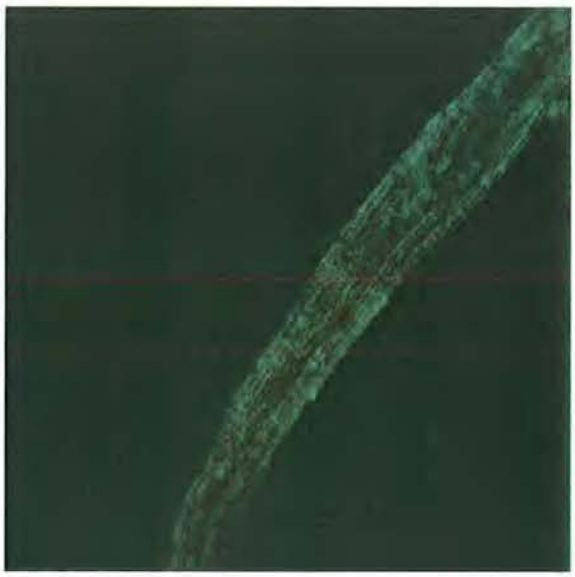

Figure 2.8:
Spectrally resolved image of a lambda scan. Image size is 920 x 920 µm. The image shows the filament of a Conference flower one day after inoculation near the anthers. The bright green signal deriving from GFP producing bacteria follows the small grooves of the filament. This indicates that bacteria may move via these grooves towards the calyx cup.

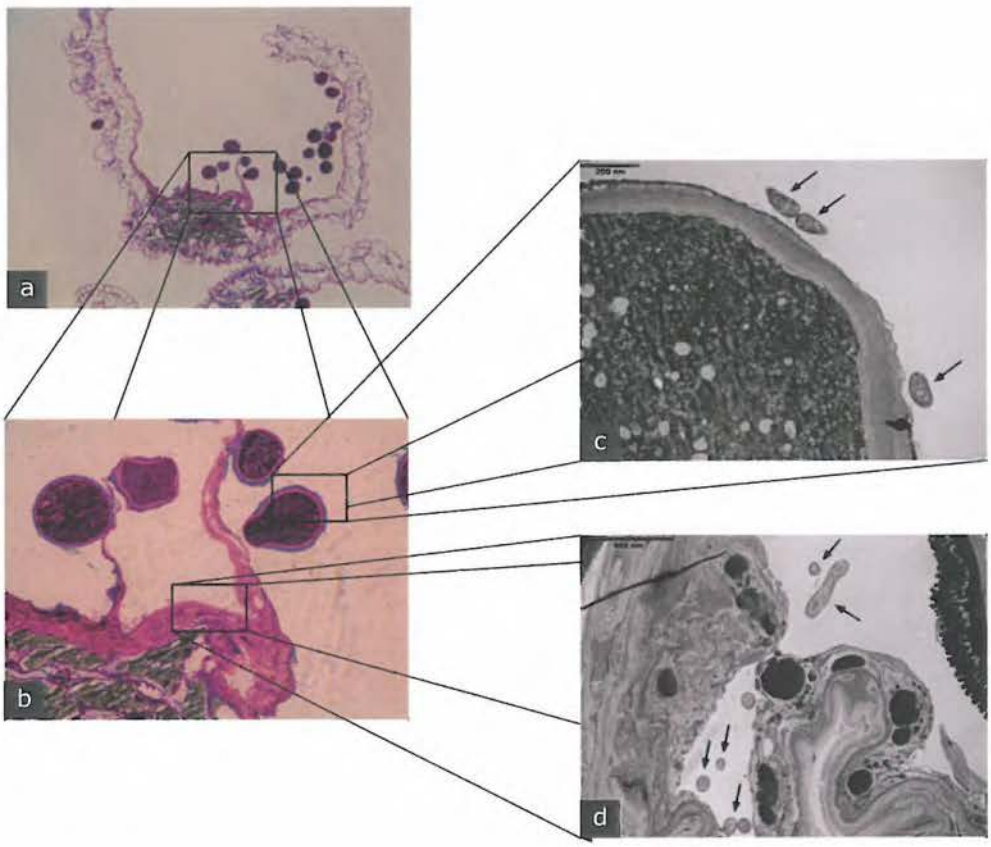

Figure 2.9:
Images of Conference anthers inoculated with *E. amylovora* 4 days after inoculation of the anthers. Image a. and b. are light microscopic pictures and c. and d. are transmission electron microscopic images.

a LM overview of anther locule with pollen inside and the dehiscene zone in the middle above.
b LM close up of the pollen.
c TEM image of pollen contaminated with *E amylovora*. Bacteria, indicated by the arrows, stick to the outside of the pollen grains.
d TEM image of epiphytic bacteria (arrows) inside the locule. Bacteria do not invade the anther tissue.

2.4.2 Inoculation of the stigma

The stigma is the pollen receptor at the top of the pistil. The stigma has commonly a somewhat glutinous or viscid structure. It forms a protected, hydrated environment and is well provided with nutrients. This makes the stigma the ideal environment for epiphytic multiplication of *E. amylovora.* Under natural circumstances, epiphytic populations of *E. amylovora* can reach up to 10^7 cfu per stigma (Johnson and Stockwell, 1998).
If inoculation occurs at this location, confocal images do not show a massive spreading of *E. amylovora* throughout the style to the ovary. However, *E. amylovora* invade massively the tissue of the stigma and the upper part of the style.
The images of figure 2.10 show the spectrally resolved sequence of a lambda scan of a control *Crataegus* stigma (a) compared with an inoculated one (b) three days after inoculation. Notice the intense GFP signal of *E. amylovora* on top of the pistil. Image (c) demonstrates how *E. amylovora* entered the upper part of the style of a Braeburn flower three days after inoculation. Figure 2.11 shows a Z-stack of the same style of the Braeburn flower. The successive images show the GFP-fluorescence at successive layers in the style tissue. These images prove the presence of *E. amylovora* inside the upper part of the style. In the lower tissues of the style was no massive spread of bacteria and remained symptomless (fig. 2.10c).
These confocal recordings explain why mostly no bacterial spread was found in other flower organs after inoculation near the stigma. However, sporadically infection of the entire flower was noticed. But for none of these flowers, a massive GFP signal, derived from *E. amylovora,* was detected inside the lower parts of the styles. This indicates that the bacteria may reach the hypanthium via a different route than via the style. In contrast to the stigma and style, the nectary appears to be the major site of bacterial entry. Rain, dew or a humid environment facilitates the movement of *E. amylovora* from the stigma to the calyx cup of the hypanthium where infection occurs.

The LM/TEM images showed the stigma as an ideal place for bacterial growth (fig. 2.12). *E. amylovora* was present at very high concentrations at the intercellular spaces of the stigmas of all flowers studied. As a consequence of the bacterial invasion, the cellular structure of the stigma became distorted. Plant cells engulfed by the bacteria lost there structure and collapsed completely. The images of figure 2.12 show both an infected and uninfected stigma of a Braeburn flower and give an idea about the

destructive character of *E. amylovora*. Also in the upper parts of the style, where *E. amylovora* was present, cellular structure was disrupted. In the lower parts of the style, near the ovary, no bacteria were present and the cellular structure remained intact. These observations were made for Braeburn, Conference and *Crataegus* as well.

Our data correspond with the findings of Wilson et al. (1989, 1990). They examined the growth and development of *E. amylovora* on only *Crataegus* stigmas. They found that *E. amylovora* developed in a biphasic manner, with an epiphytic phase up to 48h after inoculation, where bacteria were detected only in the intercellular spaces between the papillae on the stigma. After 48-72h, the bacteria invaded the secretory tissue below the papillae and formed lysoginous cavities between the collapsed papillae. From 71h onward, the bacteria completely covered the stigmatic surface and the layer of papillae had collapsed and was necrotic. Despite populations of 10^5-10^8 cfu per flower on the pistils, there was only a limited invasion of the tissue below and infection did not occur (Thomson, 2000).

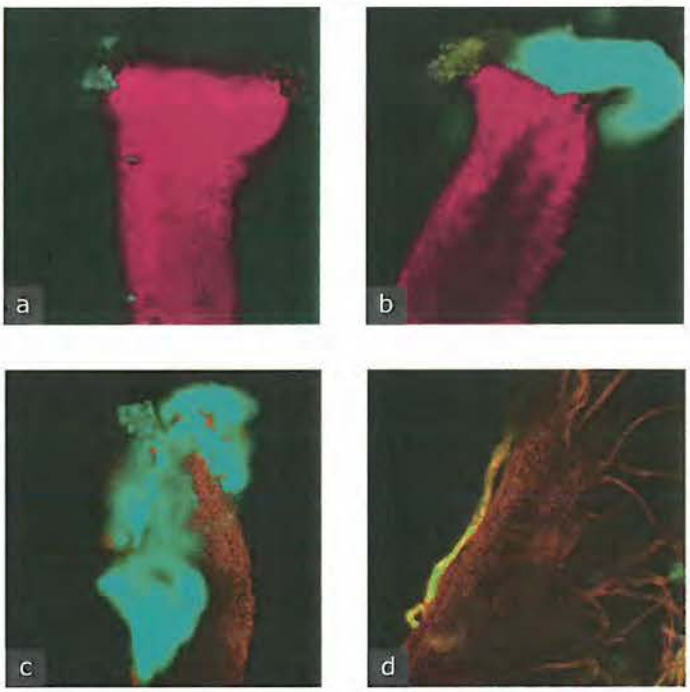

Figure 2.10:
Spectrally resolved image series. Image size of all images is 920 x 920 µm. The intense green colour represents the GFP fluorescence of *E. amylovora.* The red colour represents the chlorophyll fluorescence. These pictures are representative examples of host plant flowers showing controls and stigmas after inoculation with *E. amylovora*.
a Longitudinal section of a control stigma of *Crataegus*.
b Longitudinal section of an inoculated stigma of *Crataegus* 3 days after inoculation. Note the bright green colour, deriving from GFP of *E. amylovora,* present on top of the pistil.
c Longitudinal section of a Braeburn stigma 3 days after inoculation. The image shows also GFP fluorescence beneath the stigma, in the upper part of the style, which indicates the presence of *E. amylovora* inside this part of the style. Evidence for this is given in fig. 2.11.
d Longitudinal section of a Braeburn style, beneath the stigma, 3 days after inoculation. No bright green colour is present, indicating the absence of *E. amylovora* in the lower parts of the style.

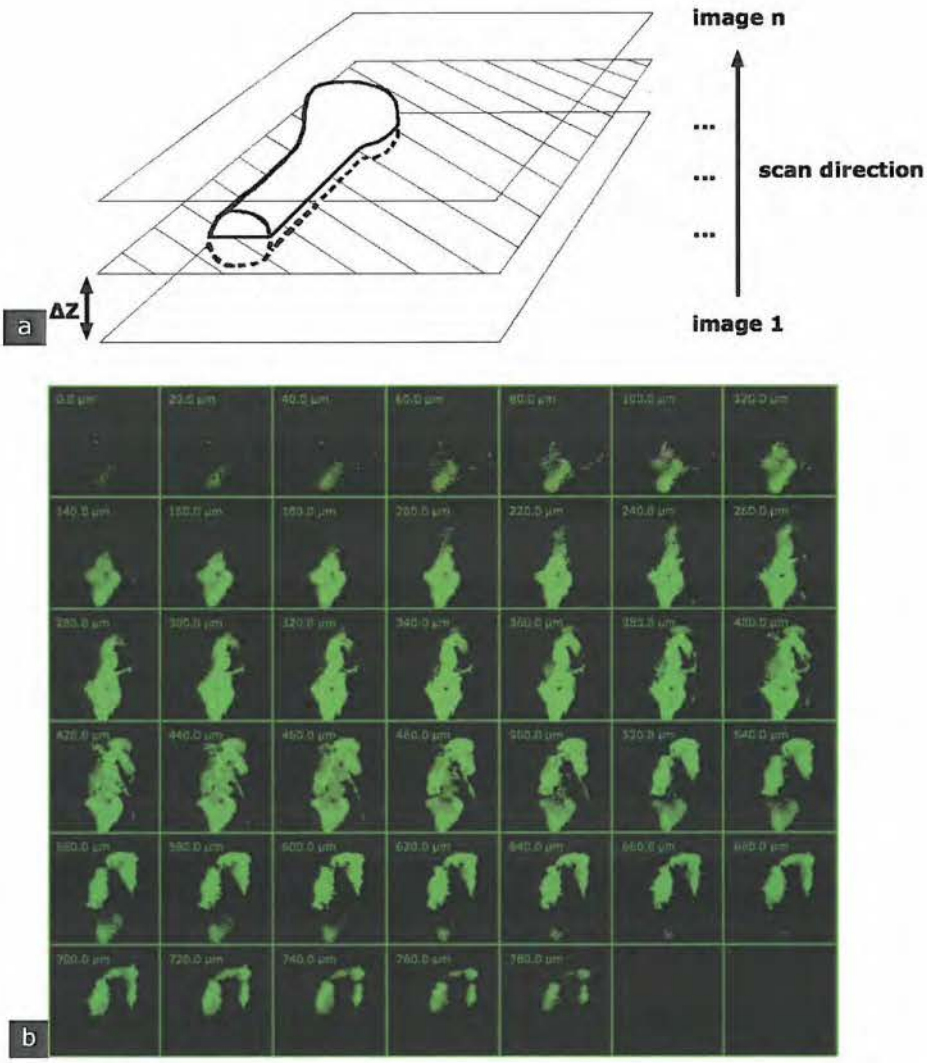

Figure 2.11:
Z-stack of a Braeburn style, three days after inoculation of the stigma. Fluorescence is measured in the green region (ex. 488 nm; em. 510-520 nm), where GFP-fluorescence, deriving from *E. amylovora,* is present. Image size is 920 x 920 µm.
This Z-stack is made from the same style represented in fig. 2.10c, to prove the presence of *E. amylovora* inside the upper part of the style.

a Schematic overview of the Z-stack confocal scan and the position of the upper part of the style. ΔZ is the Z-scan step size.

b Each image represents a successive layer of a longitudinal section of the stigma and the upper part of the style. Z-scan step size is 20 µm. The depth is displayed on each layer. The first and the last layers are longitudinal sections just next to the style. Fig. 2.10c corresponds with a dept of approximately 440 µm. The bright GFP-fluorescence is present in the layers in the middle of the upper part of the style (longitudinal section), illustrating the presence of E. amylovora inside this part of the style.

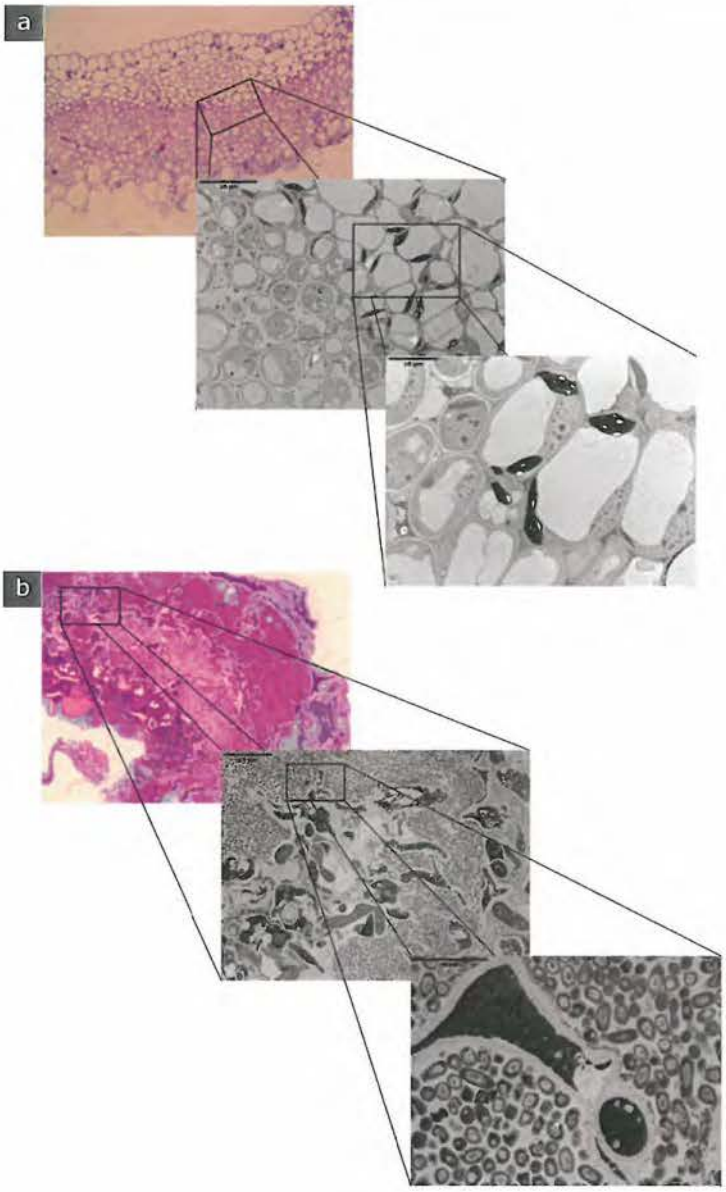

Figure 2.12:
All images show a cross section of the stigma of a Braeburn flower. The upper images show a control stigma (a). The lower images display a stigma four days after inoculation (b). The flowers were in both cases of the same age.
The control stigma shows well-arranged plant cells with a well-delineated cell kern, vacuole and chloroplasts. The inoculated stigma on the other hand exhibits the opposite. Notice the total loss of cellular structure of the infected stigma and massive presence of bacteria. The bacteria are the small round to egg-shaped structures at the highest magnification.
The colored images are light microscopic pictures and the black and white images are transmission electron microscopic pictures.

2.4.3 Inoculation of the calyx cup

Two or three days after application of *E. amylovora* near the calyx cup, almost all flowers appeared water soaked. Between the third and the fourth day, the hypanthium of some flowers starts to wilt and turn brown and black. At this stage, the first ooze drops appear near the peduncle. Subsequently the entire flower shrivels and turns completely black. This is the case for Conference, Braeburn and *Crataegus*.

Confocal observations at one day after inoculation illustrates already the presence of *E. amylovora* near the onset of the peduncle near the hypanthium. This means a spread of approximately 0.5 cm within 24 hours. At this stage no visual wilting symptoms were seen.

Symptoms appeared when massive GFP fluorescence originating from *E. amylovora* was present. This was the case one and two days after inoculation, near the upper cellular layers of the hypanthium. On the third day, massive GFP fluorescence showed up over the entire hypanthium as well as near the peduncle.

The images represented in figures 2.13, 2.14 and 2.15 show controls and infected *Crataegus* flowers, three days after inoculation of the calyx cup. Similar observations were made on Braeburn and Conference. The red pictures reflect chlorophyll fluorescence; they give an overview of the tissue structure. The green images display the green GFP fluorescence. Also it must be noticed that the control flowers show some background fluorescence in the green spectral regions, especially near the epidermis and the plant hairs.

The confocal images give an overall impression of the local concentration variations of the pathogen inside the flower. For a more detailed overview, TEM provides more information about the expansion of *E. amylovora* inside the flower.
TEM images of a *Crataegus* calyx cup show how *E. amylovora* infiltrates the flower via the nectarthodes, the nectar glands of the flower (fig. 2.16). These pictures display how the stomatal-like opening of the nectarthodes acts as an open gate for the bacteria. The pathogen can enter easily the intercellular spaces beneath the nectarthodes and from this vantage point *E. amylovora* can invade the entire flower en even the whole plant.

Once inside the hypanthium, *E. amylovora* starts to invade the flower tissue. The bacteria multiply inside the intercellular spaces and stimulate cell death of the plant cells in their environment, which is illustrated in figure 2.17. This reaction can be explained by the action of the bacterial TTSS. Proteins secreted through the TTSS interfere with the plant metabolism. Effectors of the TTSS evoke a hypersensitive response (Venisse et al., 2001), which is defined by the phenotypic characteristic of rapid and localized cell death (Lam et al., 2001). The plant cells collapse and once the cell wall starts to degrade, the bacteria can enter the new available space. Three to four days after inoculation, the confocal images prove the presence of *E. amylovora* inside the peduncle. At this stage, also the first ooze drops appear.

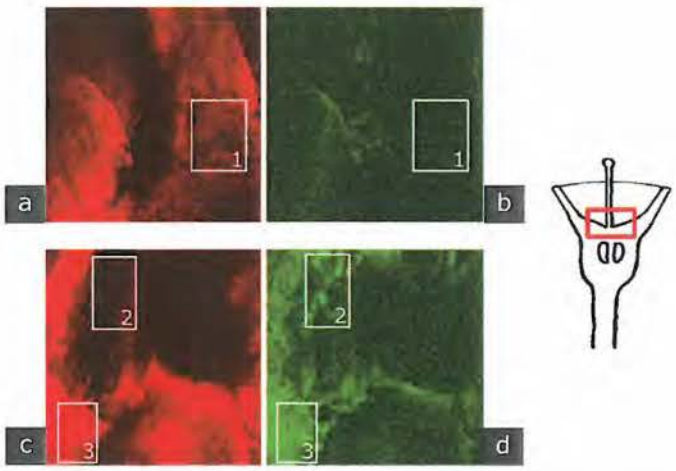

Figure 2.13:
Images of the calyx cup of *Crataegus*. The schematic flower on the right is a longitudinal section of a fruit principle and the location of the imaged area. Image size is 920 x 920 µm. Images (a) and (c) show red chlorophyll fluorescence for controls and flowers inoculated near the calyx cup. Similarly images (b) and (d) display the autofluorescence/GFP spectral band. Notice in the right corner of image (a) the onset of the style (1). The GFP fluorescence, originating from *E. amylovora* is clearly visible on image (d). Rectangle (2) shows the GFP-fluorescence deriving from epiphytic *E. amylovora* bacteria inside the calyx cup. These bacteria are not present inside the flower tissue because of the absence of chlorophyll fluorescence in this region. Rectangle (3) on the other hand indicates GFP-fluorescence deriving from bacteria inside the hypanthium tissue. At this location chlorophyll fluorescence of the hypanthium tissue and the bacterial GFP-fluorescence are both present.

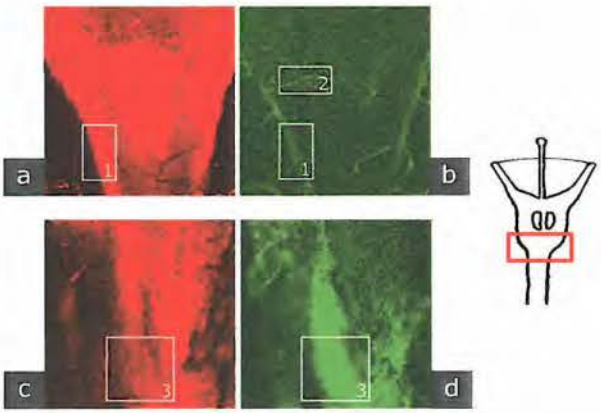

Figure 2.14:
Images of *Crataegus* flowers near the lowest part of the hypanthium and the onset of the peduncle The schematic flower on the right is a longitudinal section of a fruit principle and the location of the imaged area. Image size is 920 x 920 µm. Images (a) and (c) show red chlorophyll fluorescence for controls and flowers inoculated near the calyx cup. Similarly images (b) and (d) display the autofluorescence/GFP spectral band. (a) and (b) are images of the same an control flower. (c) and (d) show the lowest part of the hypanthium of a flower inoculated with *E. amylovora*. Note in image (b) the higher background fluorescence levels in the green area of the epidermis (1) and the plant hairs (2). Notice in image (d) the massive accumulation of GFP-fluorescence deriving from *E. amylovora* (3) in the hypanthium.

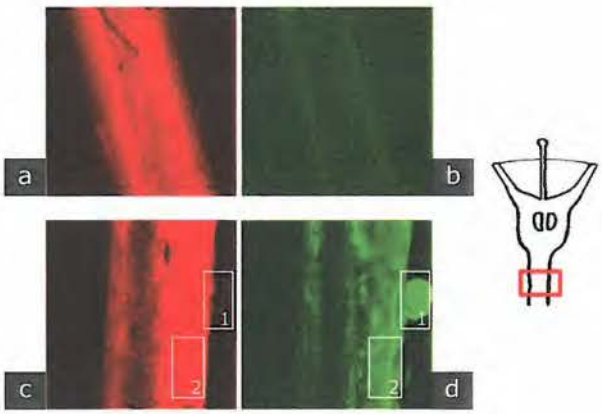

Figure 2.15:
Images of the peduncle of *Crataegus* flowers. The schematic flower on the right is a longitudinal section of a fruit principle and the location of the imaged area. Image size is 920 x 920 µm. Image (a) and (b) show respectively chlorophyll fluorescence and fluorescence in the green spectral area of the peduncle of a control flower. Image (c) and (d) display respectively chlorophyll and GFP-fluorescence of an infected flower, three days after inoculation of the calyx cup. Notice at image (d) the GFP fluorescence derived from *E. amylovora* inside the peduncle (1). On this site, chlorophyll fluorescence of the peduncle tissue and the bacterial GFP-fluorescence coexist on the same place. The brightly fluorescent spot (2) is the GFP-fluorescence of the bacteria localised in an ooze drop outside the peduncle, where no chlorophyll fluorescence is present.

Figure 2.16:
Nectarthode in the calyx cup of a *Crataegus* flower, four days after inoculation with *E. amylovora*. The colored images are light microscopic pictures and the black and white images are transmission electron microscopic pictures.

a Light microscopic overview of a nectarthode and its surroundings. Note the pink regions at the left side from the nectarthode. These regions consist of intercellular spaces and collapsed cells, which are invaded by E. amylovora. The little dark blue dots in this region represent the bacteria.

b TEM image of the stomatal-like opening of the nectarthode. E. amylovora bacteria were found inside this opening. The guard cell of the nectarthode is indicated with an asterisk.

c More detailed TEM image of the stomatal-like opening of the nectarthode. The bacterial contours can be distinguished (arrow).

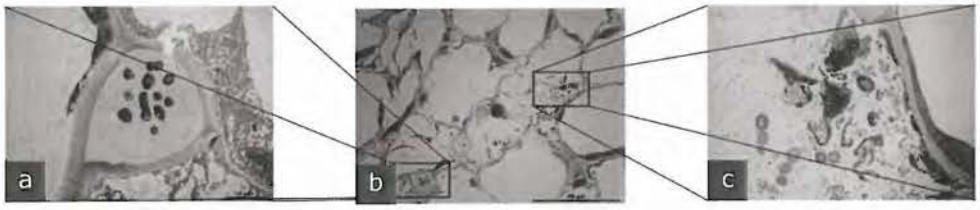

Figure 2.17:
Hypanthium of a Conference flower 4 days after inoculation near the calyx cup. All images are transmission electron microscopic pictures.

a Close up, which shows E. amylovora (arrow) inside the intercellular space.

b Overview of a region invaded with E. amylovora. Note the collapsed cells in the centre of the image.

c Close up, showing bacteria (arrow 1) invading the space that came available after cells die. Note the remains of cellular organelles (arrow 2) next to the bacteria.

2.5 Conclusion

The outcome of the present study is in agreement with earlier of blossom infections (Thomson, 2000; Vanneste and Eden-Green, 2000). The use of GFP-producing *E. amylovora* in combination with confocal microscopy allows to follow the infection process over time in the various plant parts. The stigma and the anther prove to be very important regions of epiphytic bacterial growth and major sources for disease dispersal throughout the orchard. In contrast to the stigma and the anther, the nectary appear to be the major site of bacterial entry. Once *E. amylovora* entered the flower via the nectarthodes, the pathogen can spread throughout the hypanthium and the peduncle, and from this point it can invade the entire plant.

The use of confocal microscopy in this study has a lot of advantages. It can be used for *in situ* studies, it gives very fast results and it can provide the spatial three-dimensional distribution through the plant parts over time. The technique allows the *in vivo* observation of the pathogen colonization on intact, viable plant tissues without any kind of staining. Bacteria can be detected even before visual symptoms were present and the fluorescence signal gives an overall impression of the local pathogen concentration variations inside the flower. The used confocal technique however, didn't produce images with detailed cellular structures. For more detailed images of the cellular structures, we were relying on the traditional microscopic techniques. These light microscopic and transmission electronic microscopic techniques however need a lot of preparation time before the tissue samples could be visualised. These traditional techniques also required a lot of time to screen the microscopic coupes for the presence of bacteria.

Future studies should use confocal microscopy to distinguish exact bacterial concentrations inside plant tissues over time. To do this, there exist theoretical models that help to interpret the accumulation of fluorescent GFP, both in bacterial cultures and in individual bacterial cells (Leveau and Lindow, 2001).

A possible challenge during future measurements is the reduction of the influence of the fluorescence background signal. We have seen that the fluorescence background is different for every type of tissue and that this background may and does change as a function of time for some plant parts. But even in presence of high background levels it is possible to distinguish between the GFP signal and background. One can differentiate

between different background and GFP fluorescence spectra. And even when there is an overlap in fluorescence spectra, fluorescence lifetime imaging microscopy (Holub et al., 2007) can be used to discriminate between the background and the GFP signal. The idea is that steady-state spectra may be identical and severely overlapping but nanoseccond fluorescence intensity decay imaging may show significant differences.
Another approach is the use of fluorescent proteins that emit outside the absorption zone of chlorophyll, caroteinoids and phenols. In these spectral regions there may be a reduced influence of the background fluorescence level. An example of such a fluorescent protein is the red fluorescent protein eqFP611, which already has been successfully used in subcellular localization studies in higher plants (Forner and Binder, 2007). In a next step, a photoswitchable fluorescent protein can be used. The genetically coded fluorescent protein can be induced with a light flash of a given wavelength (Leung et al., 2008). In this case, the quantity of fluorescent proteins can be controlled in order to restrict the influence on the bacterial behaviour.
These fluorescence techniques can be used to study the behaviour of different *E. amylovora* strains and different mutants to compare their behaviour inside plant tissues and to get a better understanding of the infection process and disease controll. Also the competition between *E. amylovora* and other organisms should be studied. Spinelli et al. (2005) studied already the influence of stigmatic morphology on flower colonization by *E. amylovora* and *Pantoea agglomerans* by confocal microscopy. This technique makes it also possible to study co-cultures of *E. amylovora* and their antagonists. These results can be used to predict the best timing and concentrations in the use of antagonists in orchard treatments to prevent severe fire blight outbreaks.

Chapter 3

Comparative proteome analysis of *E. amylovora in vitro* and *in planta*: oxidative stress by *E. amylovora*

3.1 Introduction

Oxygen, which appeared in the Earth atmosphere mainly as a product of photosynthesis, exists in air as the diatomic molecule O_2 (Madger, 2006). Today oxygen is essential for most living organisms, except for some anaerobic bacteria, and they depend on its presence in the environment. Living organisms need oxygen for the generation of energy in the form of ATP during the process of oxidative phosphorylation. This process is associated with the reduction of an O_2 molecule to water and it is the main process providing energy to aerobic organisms. Whereas in eukaryotic organisms oxidative phosphorylation occurs in mitochondria, in bacteria it occurs in the plasma membrane because they do not have intracellular membrane structures (Lushchak, 2001). These reactions generate reactive oxygen species (ROS) as part of normal cellular function.

ROS are ions or very small molecules that include oxygen ions, free radicals, and peroxides, both inorganic and organic. They are highly reactive due to the presence of unpaired valence shell electrons. These reactive oxygen species are able to attack all cellular components. Their interaction with proteins results in the modification of amino acids: oxidation of thiol groups of cysteine and methionine, the imidazole ring of histidine, and the rings of tyrosine, phenylalanine, and tryptophan, etc. Reactive oxygen species also attack DNA, producing chain breaks, modification of the carbohydrate parts and nitro bases, and this may lead to point mutation. Polyunsaturated fatty acids are especially sensitive to ROS attack, and this initiates a chain reaction that forms lipid peroxides (lipid-OOH) and so called lysolipids (Lushchak, 2001).

To protect themselves, potent protective mechanisms have evolved to allow cells to cope with this situation. Plant cells even make use of these ROS to defend themselves against pathogen invasions.

Fire blight provokes the typical hypersensitive reaction (HR, rapid and localized plant cell death at the infection site) in host plants combined with an oxidative burst in non-host plants. The oxidative burst is a rapid production of ROS released into the apoplast. The oxidative burst is characterized as a two-phase phenomenon. Phase I is an immediate and very transient ROS production, non-specifically stimulated by compatible, incompatible, and even saprophytic bacteria. In contrast, phase II is a massive, delayed (1-3 h after the addition of bacteria) and prolonged ROS production that is specifically stimulated by incompatible HR-causing bac-

teria and is therefore characteristic for the HR (Lamb and Dixon, 1997). ROS can act directly against phytopathogen attack by killing the microorganism. They have been also implicated in the destruction of the challenged plant cells, either through lipid peroxidation or as a threshold trigger for hypersensitive plant cell death (Venise et al., 2001). Moreover, ROS hinders microorganism penetration in plant tissues because it contributes to wall stiffening by facilitating peroxidase reactions catalysing intra- and inter-molecular cross-links between structural components of cell walls and lignin polymerisation (Ros Barceló, 1997). The resulting increase in mechanical barriers slows down pathogen penetration allowing plant cells to arrange defences that require more time to be activated. As H_2O_2 is a diffusible molecule in biological membranes, it also acts as intracellular signal, which is able to activate plant defence responses (Durner et al., 1997).
Oxidative burst seems to be an integral part of the incompatible response against biotrophic phytopathogens that allow plant cells to counteract their penetration by surrounding them with an extremely oxidative environment (De Gara et al., 2003).

Also in susceptible host plants, *E. amylovora* induces an oxidative burst, as does an incompatible pathogen. As shown by Venisse et al. (2003) this oxidative burst is the result of the combined action of two Hrp effectors of *E. amylovora*, HrpN and DspA, which are related with a functional type III secretion system (TTSS) in the bacterium.
Phytopathogenic bacteria use TTSS to inject effector proteins into plant cells. These proteins contribute to bacterial pathogenicity by interfering with plant defence signal transduction. HrpN and DspA both participate in the induction of an oxidative burst in host plants of *E. amylovora* during the compatible reaction. The rapid necrosis of invaded host plant tissues is associated with this particular compatible plant/bacterial interaction. Such a necrosis is not common to all compatible plant/bacterial interactions.

E. amylovora is capable to turn the defence mechanism of the plant, namely the HR and oxidative burst, into an infection mechanism. The bacteria can only take advantage of an oxidative burst during compatible reactions when they tolerate high concentrations of ROS and pose defence mechanisms to protect themselves against the influences of ROS.

3.2 Objective

The aim of this chapter was to obtain a better insight into which bacterial processes could be involved during infection and could play a key role during disease progress besides the known pathogenicity factors. We want to investigate which strategies *E. amylovora* follows to overcome the host plant defences usually elicited in tissues surrounding an oxidative burst. To achieve this goal, the proteomes of *E. amylovora* grown *in vitro* and *in planta* were compared using 2D-GE.

3.3 Materials and methods

3.3.1 Bacteria

The strain used in the experiments is the *Erwinia amylovora* strain PFB5, isolated from *Prunus salicina* (S.K. Mohan, Idaho, USA) and is kindly provided by Dr. Martine Maes (ILVO, Institute for Agricultural and Fisheries Research, Ghent).

3.3.2 Plant material

Maling 9 (M9 clone 29) apple rootstocks (9 mm diameter) were used in these experiments. Dormant rootstocks were potted in regular potting soil (5.5 litre potting volume) and transferred to the greenhouse under normal conditions (22°C, 60% relative humidity and a minimal light intensity of 150 µmol/m²s); one shoot was left on the plant to grow for several weeks. The M9 rootstock is known to be severely susceptible to fire blight (Van der Zwet & Keil, 1979).

3.3.3 Bacterial growth and isolation

In vitro:
Bacteria were grown at 24°C in fluid MM_2 medium (0.4% w/v L-asparagine; 0.2% w/v H_2HPO_4; 0.02% w/v $MgSO_4.7H_2O$; 0.3% w/v NaCl; 0.02% w/v nicotinic acid; 0.02% w/v thiamine hydrochloride) supplemented with 1% w/v sorbitol. Sampling occurred during the exponential phase when the optical density was 0.8 at 600 nm (UV-1602; Shimadzu, Deurne, Belgium). The bacteria were collected by centrifugation and were washed 3 times with phosphate buffered saline (PBS; 137 mM NaCl, 10 mM phosphate, 2.7 mM KCl, pH 7.4).

In planta:
Apple rootstocks were infected by cutting the leaf tip of the youngest fully developed leaf and dipping it into a bacterial suspension. This suspension contains bacterial cells of *E. amylovora* of an overnight culture diluted in PBS (10^8 CFU/ml). Infected plants were kept at 24°C and 99% relative humidity. Sampling occurred based on the infection stage. Samples were taken when the infection was systemic. At this stage the shoot tip appeared water soaked and ooze drops were present on the entire shoot. This was about 8 to 10 days after inoculation.
The bacteria were isolated from the plants using the following protocol. After disinfection of de shoot surface, the whole shoot was cut in little pieces. The shoot fragments were shaken for 20 minutes in a sterile buffer (phosphate buffer 120mM pH 8, 0.1% w/v sodium pyrophosphate, 0.1% v/v Tween-20, 25% w/v PVPP (ad fresh) together with glass beads (0.1 mm - 1 mm). During this stage bacteria migrated out the plant tissue into the buffer. The migrated bacterial fraction is representative for the entire bacterial population because bacteria migrated from the multiple wounds created on all shoot parts (the cutting sites and the wounds induced by the glass beads). The suspension is filtered through 2 Wattman filters, pore size 8 µm. The filtrate, which contains the bacteria, was centrifuged to collect the bacteria. The bacteria were washed 3 times with PBS before protein extraction.

3.3.4 Protein extraction

The washed bacteria were lysed with sample solution (7 M urea, 2 M thiourea, 2 % (w/v) CHAPS, 10 mM DTT, 0.5 % IPG Buffer). The lysate was sonicated for 1 min, shaken for 30 min at 20°C and centrifuged at 76 000 g for 90 min. Protein concentration was determined with the 2-D Quant Kit (GE Healthcare, Diegem, Belgium). The protein samples were stored at -70°C until further processing.

3.3.5 Two-dimensional gel electrophoresis

Two-dimensional gel electrophoresis (2D-GE) is a form of gel electrophoresis commonly used to analyze proteins. Protein samples are separated by two properties in two dimensions on 2D gels. In a first dimension, proteins are separated by their iso-electric point. This is called iso-electric focusing (IEF). Thereby, a gradient of pH is applied to a gel and an electric potential is applied across the gel, making one end more positive than the other. At all pHs other than their isoelectric point, proteins will be charged.

If they are positively charged, they will be pulled towards the more negative end of the gel and if they are negatively charged they will be pulled to the more positive end of the gel. The proteins applied in the first dimension will move along the gel and will accumulate at their isoelectric point; that is, the point at which the overall charge on the protein is 0 (a neutral charge). In a second dimension, proteins are separated by mass using sodium dodecyl sulphate polyacrylamide gel electrophoresis (SDS-PAGE). Before separating the proteins by mass, they are treated with sodium dodecyl sulfate (SDS). This denatures the proteins and binds a number of SDS molecules roughly proportional to the protein's length. Since the SDS molecules are negatively charged, the result is that all of the proteins will have approximately the same mass-to-charge ratio. An electric potential is applied and proteins will be attracted to the more positive side of the gel proportionally to their mass-to-charge ratio.

After overnight rehydratation of the Immobiline dry strips (NL pH 3-10; 24 cm; GE Healthcare) with destreak (GE Healthcare, Diegem, Belgium), protein samples (80 µg) were applied by cuploading. The proteins were separated by IEF at 20°C and 50µA/strip (500 V for 1 hour, gradient to 1000 V for 7 hours, gradient to 8000 V for 3 hours and 3 hours at 8000 V) on an IPGphor II (GE Healthcare, Diegem, Belgium) with a manifold strip holder. The IPG strips were subsequently incubated in equilibration buffer (50 mM Tris-HCl, 6M urea, 30% v/v glycerol, 2% w/v SDS, bromophenol blue containing 1% w/v dithiothreitol (DTT) for 15 min and in equilibration buffer containing 4.25% w/v iodoacetamide instead of DDT for an additional 20 min. After rinsing the strips with 1x SDS electrophoresis buffer (25 mM Tris, 192 mM glycine, 0.1% w/v SDS), strips were placed between the glass plates on top of the second-dimension gel (12.5% v/v polyacrylamide). Above the strips a small amount of agarose sealing solution (0.5% w/v agarose, 25 mM Tris, 152 mM glycine, 0.1% w/v SDS, 0.02% w/v bromophenol blue) was applied to prevent IPG strips from moving.
SDS-PAGE was carried out in an EttanDALTsix unit (GE Healthcare) which is provided with a power supply and cooling unit. The separation unit was filled with 1x SDS electrophoresis buffer and was cooled down to 4°C. Up to six gels were placed in the separation unit. The upper chamber was put in position and filled with 2x SDS electrophoresis buffer. The proteins were shifted from the first to the second-dimension (30 min at 20 mA/gel). Afterwards, protein separation was carried out for 3 hours at 30 mA/gel.

3.3.6 Staining

The proteins were visualized by silver staining according to Shevchenko et al., (1996). All steps were performed in stainless steel trays, each containing two gels. After electrophoresis, gels were fixed overnight in 50% v/v methanol, 5% v/v acetic acid (HAc) in water. The gels were then washed for 10 min with 50% v/v methanol in water and additionally for 10 min with water to remove the remaining acid. Afterwards, the gels were sensitized by an 1 min incubation in 0.02% w/v sodium thiosulfate, and were rinsed with two changes of distilled water for 1 min each. After rinsing, the gels were submerged in a 0.1% w/v silver nitrate solution and incubated for 20 min. After incubation, the silver nitrate was discarded and the gels were rinsed twice with water for 1 min and then developed in 2% w/v sodium carbonate containing 0.04% v/v formaline until no new spots appeared. Development was stopped in HAc/water 95/5 v/v, gels were rinsed with water and scanned with a digital scanner (Image scanner, UTA III; GE Healthcare, Diegem, Belgium).

3.3.7 Image analysis

2D-GE computer image analysis was carried out with Image Master 2D Platinum Software Version 5.0 (GE Healthcare, Diegem, Belgium). Image analysis was redone with the Delta 2D software of Decodon (Decodon, Greifswald, Germany). A T-test was performed, based on a Welch approximation. The overall threshold p value was 0.01 and the p-values were based on permutations. These settings allow the statistic evaluation of non-normal distributed samples (as 2D-GE results usually are) (cfr. Decodon software).
Spots that became differentially expressed with both the Image Master 2D Platinum Software and the Delta 2D software were included in the study.

3.3.8 Digestion

Differentially expressed pots were picked and trypsin-digested manually according to the method described by Shevchenko et al. (1996). After the gel pieces were excised and shrunk by dehydration in ACN, which was then removed, spots were kept at -20°C until further analysis. A volume of 10 mM DTT in 100 mM NH_4HCO_3 sufficient to cover the gel pieces was added, and the proteins were reduced for 1 h at 56 °C. After cooling to room temperature, the DTT solution was replaced with roughly the same volume of 55 mM iodoacetamide in 100 mM NH_4HCO_3. After 45 min incubation at room temperature, the gel pieces were washed with 100 mM

NH_4HCO_3 for 10 min, dehydrated by addition of ACN, swelled by rehydration in 100 mM NH_4HCO_3, and shrunk again by addition of the same volume of ACN. The liquid phase was removed, and the gel pieces were completely dried in a vacuum centrifuge. Incubation in 133 mM NH_4HCO_3 containing trypsin (12.5 ng/µl, Promega) for 45 min on ice was followed by an overnight incubation at 37°C in 50 mM NH_4HCO_3. From this point onwards, supernatants was removed and collected. Spots were washed with 20 mM NH_4HCO_3 and proteins were extracted in three consecutive steps using 5% formic acid in 50% ACN. The pooled supernatant was dried in a vacuum centrifuge; the pellet was dissolved in 5% v/v ACN in 100 mM HAc containing 4 pg/µl of cortisone and stored at -20°C until mass spectrometric analysis.

3.3.9 Mass spectrometry and database management

Protein digest were analysed by liquid chromatography coupled to electrospray ionization tandem mass spectrometry (LC-ESI-MS/MS) on a LCQ Classic (ThermoFinnigan, San Jose, USA) equipped with a nano-LC column switching system. Flow regulation was as described by Meiring et al (2002). The trapped sample was separated on the analytical column (Biosphere C18, 200 mm L x 0,05 mm ID, 5 µm; Nanoseparations, Nieuwkoop, The Netherlands) using a linear gradient from 5 to 60% v/v ACN in water containing 100 mM HAc for 55 min. The eluate from the analytical column was introduced in a nanoelectrospray device (ThermoFinnigan) and sprayed from a gold-coated fused silica emitter (5 µm ID; Nanoseparations). The LCQ automated protocols were used to optimise the ion optics and calibration parameters. The mass spectrometer was operated in a data-dependent acquisition mode to automatically switch between MS (m/z 300-1500 Thompson in centroid mode at a maximum injection time of 150 ms) and MS/MS acquisition on the three most intense precursor ions, controlled by Xcalibur 1.3 software. All MS/MS data were searched using MASCOT (Matrix Sciences, London, UK) and SEQUEST (ThermoFinnigan) against a database, which was constructed by downloading the complete genome of *Erwinia amylovora* (strain Ea273) from the Sanger Institute (www.sanger.ac.uk/Projects/E_amylovora) and translating the sequence in six frames. Homologues were found by searching the NCBI database (http://www.ncbi.nlm.nih.gov) using BLAST. SEQUEST/MASCOT mass tolerance for parent and fragment ions were 2.5/2.0 and 0.5/0.8, respectively. Carbamidomethylation of cysteine and oxidation of methionine, tryptophan and histidine were set as fixed and variable modification, respectively. Maximally two missed cleavages were allowed, and the neu-

tral loss of water and ammonia from b- and y-ions was taken into consideration. Each peptide used for protein identification had a significant ($p < 0.05$) individual ion score in Mascot, and/or with specific Sequest parameters (i.e. a cross-correlation value of > 2 for a doubly charged peptide and a delta correlation value of > 0.1).

3.3.10 *Experimental setup*

Two-dimensional gel electrophoresis (2D-GE) can give an overall view of proteins that are expressed by *E. amylovora* during given circumstances. It is an ideal tool to study the differences of the proteome under both conditions, namely *E. amylovora* grown *in vitro* and *E. amylovora* grown *in planta*.

For each condition, three biological independent samples were taken. Of each sample, equal protein amounts were analyzed to obtain the proportion of the studied proteins against the total protein content. Silver stained gels of three biological independent samples of each condition revealed reproducible protein spot patterns. After image analysis, the spots that fitted the applied criteria for differentially expressed protein spots, were picked and subjected to LC-ESI-MS/MS for identification. The spectra were processed using MASCOT (Matrix Science, www.matrixscience.com) and SEQUEST (ThermoFinnigan). The sequences were identified by searching an in-house database of genomic sequences of *E. amylovora*. To elucidate protein function, homologues were found by BLAST searching the NCBI non-redundant database. Figure 3.1 gives a schematic overview of this workflow. A more detailed description of the used methods is given in the previous sections of materials and methods.

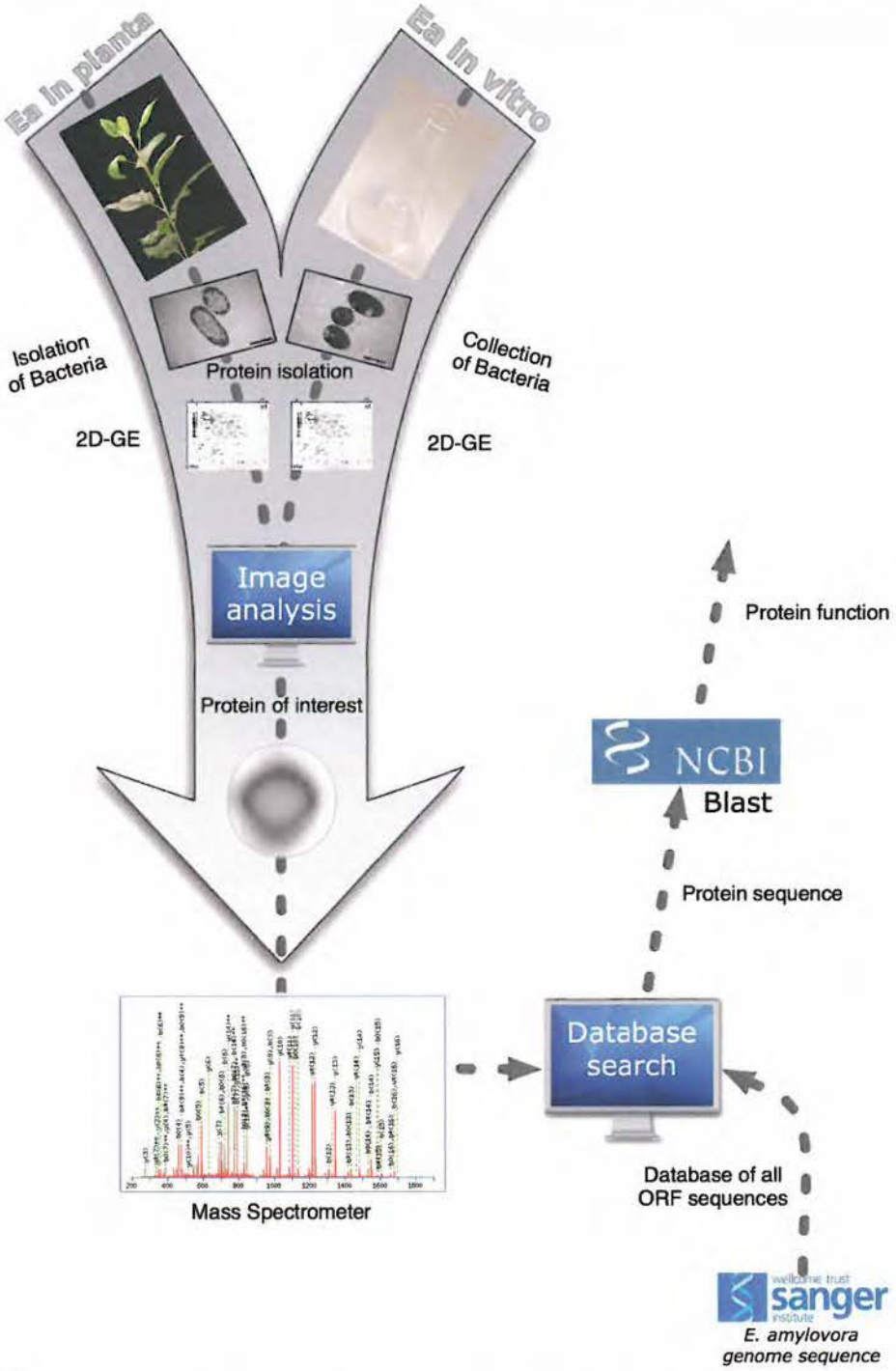

Figure 3.1:
Schematic overview of the experimental workflow of the 2D-GE experiment. Ea stands for *E. amylovora*.

3.4 Results and Discussion

In order to find factors involved in the infection process of *E. amylovora*, the bacterial proteome was studied. To perform this study, bacteria grown *in vitro* were compared with bacteria in their natural environment, namely during infection. The protein expression profiles of *E. amylovora* in both conditions were measured against each other. An overview of the experimental setup is given in section 3.3.10 and illustrated in figure 3.1.

The image analysis of the 2D-gels with the Image Master 2D Platinum Software (GE Healthcare) resulted in 175 proteins that were differentially expressed between both groups (*E. amylovora* grown *in vitro* and *E. amylovora* grown *in planta)*. From this group of proteins, 127 proteins were successfully identified. Afterwards, image analysis was redone with the Delta 2D software of Decodon to verify the results of the Platinum Software because Decodon has another approach to analyze 2D-gels. Only the 96 spots that became differentially expressed with both software packages and were successfully identified we included in the study.

Figure 3.2 shows an example of the silver-stained protein profile of *E. amylovora*, grown *in planta*. The indicated spots are the proteins that were differentially expressed between both groups: *in vitro* and *in planta*. Table 3.1 displays the identifications of the selected spots and whether these spots are up or down regulated.

Regarding the functional diversity, the major part of the proteins identified via 2D-GE are involved in oxidative stress related processes (fig. 3.3). Also amino acid and carbohydrate metabolism play a considerable role in the infection process. But still, for many of identified proteins, the biological function remains unclear.

Overall, 26% of all proteins that were significant differentially expressed in *E. amylovora* grown *in vitro* and *in planta*, could be linked to oxidative stress or to oxidative stress related processes. Almost all (with the exception of two) of these oxidative stress related proteins of *E. amylovora* are more expressed during infection. This is the first study indicating the high priority of the oxidative stress defence during the infection process of *E. amylovora.*

After induction of an oxidative burst in host plant tissues, these findings could explain how *E. amylovora* copes the devastating influences of ROS.

In the following parts we'll focus on these oxidative stress defence related proteins and discuss their possible protective role against ROS.

The bacterial protective systems against ROS could be divided into three groups and are described in the discussion:

- prevention of ROS
- free radical chain termination and detoxification of radicals by enzymes and quenchers
- repair of damaged elements

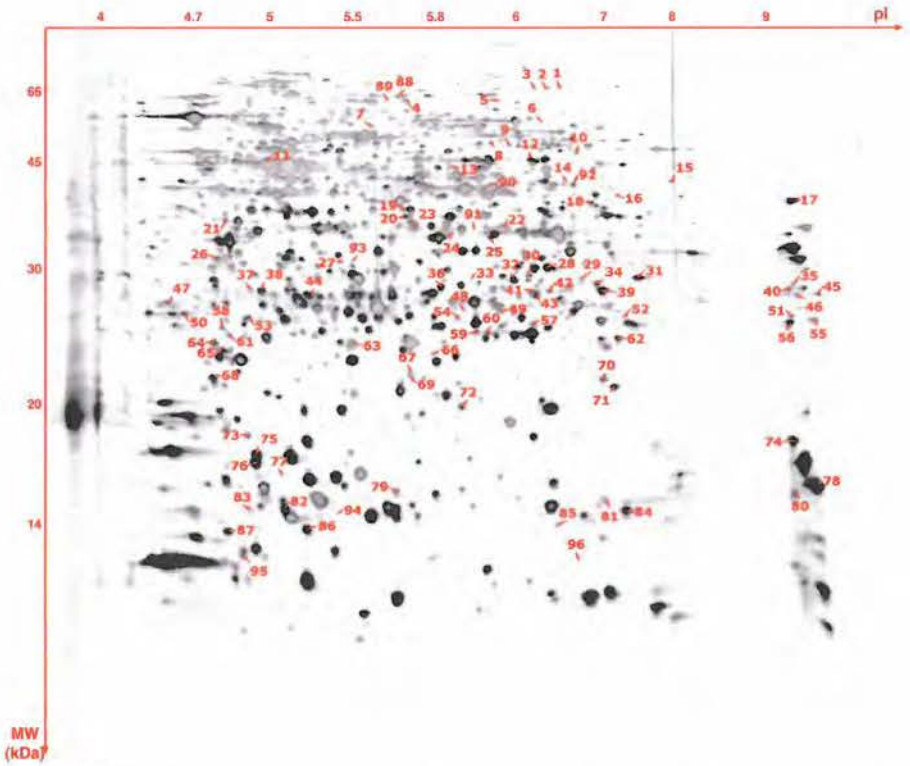

Figure 3.2:
2D pattern of *E. amylovora* grown *in planta* and visualised with silver staining. Proteins were separated in two dimensions. In a first dimension, proteins were separated by isoelectric point (pI). The acidic proteins are located on the left side of the gel, the basic proteins on the right side. The separation in the second dimension is based on a separation by molecular weight (MW). The largest proteins are situated in the upper part of the gel, the smaller proteins in the lower part.
Proteins that were differentially expressed in both conditions (*in vitro* versus *in planta*) are marked.

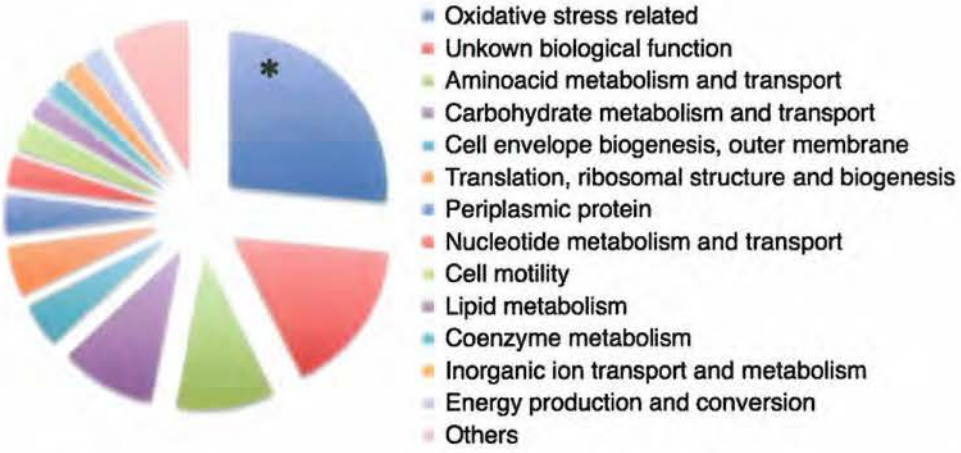

Figure 3.3:
Functional annotation of proteins of E. amylovora that were differentially expressed in both conditions: in vitro and in planta. The proteins were classified according to their function as mentioned on the NCBI database or based on literature references. The chart can be read clockwise starting with the blue part: "oxidative stress related", indicated with the asterisk.

Spot nr.	Fold change	Identification
1	2.04	AmsF
2	2.44	AmsF
3	2.13	AmsF
4	-2.09	Transketolase
5	1.85	Acetyl-coenzyme A synthetase
6	-4.5	Periplasmic oligopeptide-binding protein
		Malate:quinone oxidoreductase
7	-2.06	Glucans biosynthesis protein D
8	2.78	Enolase (2-phospho-D-glycerate hydrolyase)
9	2.63	probable glycosyl hydrolase
10	2.33	3-isopropylmalate dehydratase large subunit (LeuC)
11	-1 .62	Enolase (2-phospho-D-glycerate hydrolyase)
12	1.85	alkaline phosphatase
13	1.67	Peptidase B (Aminopeptidase B)
14	10	Putative aminotransferase
15	3.03	Sn-glycerol-3-phosphate ABC type periplasmic binding protein
16	-2.97	Gamma-glutamyltranspeptidase
17	4.35	Periplasmic sulphate binding protein
18	2.44	Dihydroorotase
19	6.67	Phenylalanyl-tRNA synthetase alpha chain
20	3.13	Transaldolase A (TalA)
21	3.13	Predicted periplasmic lipoprotein involved in iron transport
22	2.56	Outer membrane protein A
23	5.88	Outer membrane protein A
		Dihydrodipicolinate synthase (DapA)
24	5	Probable oxidoreductase
25	7.69	Putative oxidoreductase YghA
26	1.96	Putative antibiotic biosynthesis protein (Pab)
27	2.5	GTP-binding protein (EngA)
28	5	Aliphatic sulfonates binding protein (SsuA)
29	1.82	Probable pyruvate dehydrogenase multienzyme complex (AceF)
30	7.69	phosphogluconate dehydrogenase, NAD-binding, putative-like protein
31	2.78	histidine-binding periplasmic protein
32	-1.57	predicted hydrolase
33	-5.41	predicted hydrolase
34	3.13	Glutamate-aspartate ABC transporter ATP-binding component (GltL)
35	14.29	FKBP-type peptidyl-prolyl cis-trans isomerase FkpA (Rotamase)
36	7.69	amidohydrolase 2

Spot nr.	Fold change	Identification
37	4.17	Putative peroxiredoxin/glutaredoxin family protein
38	3.33	Deoxyribose-phosphate aldolase 2 (DeoC2)
39	2.13	Uridylate kinase (PyrH)
40	7.14	Ubiquinone/menaquinone biosynthesis methyltransferase (UbiE)
41	11.11	hypothetical protein
42	4.76	Conserved hypothetical protein YdiA
43	1.72	tRNA/rRNA methyltransferase
44	1.41	Trehalose phosphatase (OtsB)
45	8.33	CsuC protein, similar to fimbrial chaperone proteins
46	4	Putative short chain dehydrogenase
47	2.33	Elongation factor Tu-A (TufA)
48	2.33	hypothetical protein ETA_27180
49	2.08	Queuosine biosynthesis protein (QueC)
50	6.67	Elongation factor Ts FKBP-type peptidyl-prolyl cis-trans isomerase FkpA (Rotamase)
51	14.29	Thiamine-phosphate pyrophosphorylase (ThiE)
52	2.86	Conserved hypothetical protein YmcB
53	6.67	Enolase-phosphatase (MasA)
54	3.7	Conserved hypothetical protein YbgI
55	5	Putative ABC superfamily transport protein (YrbC)
56	11.11	cAMP-regulatory protein (Crp)
57	3.13	Orotidine 5'-phosphate decarboxylase (PyrF)
58	5	imidazole-4-carboxamide isomerase (HisA)
59	3.85	3-oxoacyl-[acyl-carrier-protein] reductase (FabG)
60	4	Manganese superoxide dismutase (SodA)
61	3.45	Elongation factor Ts
62	3.23	Glutathione S-transferase (Gst)
63	5.56	Putative alkyl hydroperoxide reductase subunit C (AhpC)
64	2.5	acyl carrier protein phosphodiesterase (AcpD) Imidazole glycerol phosphate synthase subunit HisH (HisH)
65	3.7	Oligoribonuclease (Orn)
66	3.85	Thiol:disulfide interchange protein DsbA (DsbA)
67	5.56	Putative alkyl hydroperoxide reductase subunit C (AhpC)
68	2.04	ATP synthase, F1 complex, delta subunit (AtpH)
69	4	Putative alkyl hydroperoxide reductase subunit C (AhpC)
70	5.88	hypothetical protein ETA_25210 (YajQ)
71	5.88	Putative oxidoreductase YieF (YieF)

Spot nr.	Fold change	Identification
72	4.55	Osmotically inducible protein Y (OsmY)
73	5	Shikimate kinase I (AroK)
74	12.5	Peptidyl-prolyl cis-trans isomerase A (Rotamase A) (PpiA)
75	14.29	DNA protection during starvation protein (Dps)
76	8.33	DNA protection during starvation protein (Dps)
77	2.56	hypothetical protein ETA_06200
78	2.38	Outer membrane protein
		30S ribosomal protein S8 (RpsH)
79	2.86	2-C-methyl-D-erythritol 2,4-cyclodiphosphate synthase (IspF)
		Outer membrane protein
80	5.56	unknown (similar to VirK of Xanthomonas axonopodis)
		Outer membrane protein
81	3.33	hypothetical protein ETA_08850
82	1.54	heat-stable nucleoid-structuring protein (Hns)
83	4.17	hypothetical protein ETA_09730
84	3.33	Elongation factor Tu-A (TufA)
85	4	Outer membrane protein
86	6.25	Small heat shock protein IbpA (16 kDa heat shock protein A)
87	3.85	hypothetical protein ECA0009
88	-2.44	Peptidyl-dipeptidase (Dcp)
89	-3.3	Catalase
90	-1.48	branched-chain amino acid-binding protein (LivK)
91	-4.92	Dihydrodipicolinate synthase (DapA)
92	2.56	Glyceraldehyde 3-phosphate dehydrogenase A (GapA)
93	-4.71	FliC
94	-6.48	Organic hydroperoxide resistance protein (ohr)
95	-2.31	Chemotaxis regulator transmits chemoreceptor signals to flagelllar motor components (CheY)
96	-3.11	hypothetical protein ETA_04270

Table 3.1:
Identification results of the selected spots. Spot numbers are indicated in figure 3.2. Average fold change of spot expression, either upregulated (+) or downregulated (-) in *E. amylovora* grown *in planta*, compared with *E. amylovora* grown *in vitro*.

3.4.1 ROS prevention

ROS prevention could be understood as the prevention of further ROS formation but also as the prevention of ROS entering the bacterial cells.

The entering of ROS could be prevented by the bacterial capsule, composed of exopolysaccharides. In our experiment we found a two times increased expression in *E. amylovora,* grown *in planta,* of AmsF (prot nr. 1,2 and 3). AmsF belongs to the *ams* operon, which is involved in the synthesis of the exopolysaccharide amylovoran. Exopolysaccharides form a protective capsule around the bacteria *E. amylovora* and could play a protective role against ROS. Such a protective role of the extracellular capsule of phytopathogenic bacteria against oxidative stress has been proposed by Kiraly et al. (1997). In *E. amylovora* however, this protective feature has not been evidenced against H_2O_2 by Venisse at al (2003).

Once inside, ROS can cause severe damage. Superoxide for instance, is not extremely reactive by itself. However, it has been shown that it favours the Fenton reaction (see equation 1) by reducing free ferric iron, leading to production of hydroxyl radicals, which can damage any biological macromolecules (Touati, 2000).

$$H_2O_2 + Fe^{2+} \rightarrow Fe^{3+} + OH^{\cdot} + OH^{-} \qquad (1)$$

It is thought that the strict regulation of iron metabolism and its coupling with regulation of defences against oxidative stress, is an essential factor for life in de presence of an excess of ROS. Due to its potential damaging effects, in bacteria, iron solubilisation and metabolism is strictly regulated at two levels: the entrance to the cell and inside the cell (Cabiscol et al., 2000).
We found the expression protein nr. 21, called "Predicted periplasmic lipoprotein involved in iron transport", more than 3 times increased in *E. amylovora* grown *in planta.* This protein belongs to the group of membrane-bound receptors and is responsible for iron entrance in bacterial cells. Because of this feature, this protein could be indirectly be involved in the prevention of further ROS generation in *E. amylovora.*

3.4.2 Detoxification of ROS

ROS attacking bacteria most frequently include both radicals ($O_2^{\circ-}$, OH^-, $^{\cdot}OH$, $NO^{\cdot}$) and non-radicals substances (H_2O_2 and singlet oxygen, $^1O_2$). The high reactivity and short lifespan of hydroxyl radicals and singlet oxygen prevent cells from developing mechanisms of their elimination. Conversely, $O_2^{\circ-}$ and H_2O_2 are relatively stable and cells possess enzymes degrading these ROS (Vorob'eva, 2004). These anti-oxidative enzymes are an important first line defence against oxidative stress.

In our experiment, we found 12 proteins, differentially expressed between *E. amylovora* grown *in vitro* and *in planta*, which posses an anti-oxidative feature or are involved in the regulation of these anti-oxidative proteins.

A first group of detoxifying enzymes, which needs attention, are the superoxide dismutases (SOD). These proteins represent a group of enzymes that catalyse the dismutation of superoxide ($O_2^{\circ-}$) and the formation of hydrogen peroxide (H_2O_2) (see equation 2).

$$2\ O_2^{\circ-} + 2\ H^+ \rightarrow H_2O_2 + O_2 \qquad (2)$$

There are three classes of SODs in bacteria. A first class of bacterial SODs are cofactored by copper and zinc ([Cu,Zn]-SODs; encoded by *sodC*) and are located in the periplasm or are lipid anchored in the outer envelope. The other two classes, the manganese- and iron-cofactored SODs are found in the cytosol (Dunn et al., 2003).
The activity of SOD containing iron (Fe-SOD) does not rely on growing conditions. This is in contrast to the manganese-containing SOD (Mn-SOD) activity, which depends on growing conditions and is sensitive to external oxidative stress. In *E. amylovora,* Mn-SOD was shown to be 4 times more expressed *in planta* (prot. nr 60).
The Mn-SOD enzyme is coded by the *sodA* gene. At least six global effectors of gene *sodA* transcription have been identified (Lushchak, 2001). The SoxRS system, for instance, plays an important role in this process. This system is a sensor of superoxide and nitric-oxide stress and enhances ~45 proteins in response to superoxide, including Mn-SOD (Green and Paget, 2004). The *sodA* transcript is also post-transcriptional regulated by aconitases.

Protein nr. 10 in our experiment is identified as "3-isopropylmalate dehydratase large subunit" (LeuC) and belongs to the aconitase protein

family. This protein is more than 2 times more expressed in *E. amylovora in planta*. Most members of the aconitase family are enzymes, which share four domains in common and contain a single [4Fe-4S] cluster essential for catalytic activity.
During exposure of the cell to peroxide or superoxide-mediated oxidative stress, the iron sulfur [4Fe-4S] clusters of aconitase are disassembled and the catalytic activity is lost. For some members of the aconitase family is shown that the resulting apo-proteins bind specific mRNAs, causing enhanced transcript stability or inhibition of translation (Green and Paget, 2004). In that way, aconitases have a dual role as enzymes and post-transcriptinal regulators.
It has been shown that *E. coli* aconitases modulate the translation of *sodA* (manganese superoxide dismutase). It would appear that the aconitases can act positively (AcnA) and negatively (AcnB) to control translation of the *sodA* message. This dual control may help fine-tuning the *sodA* expression with respect to growth phase and environmental stress (Tang et al., 2002). Whether there is such a relation between LeuC and mRNAs of anti-oxidative proteins has not been established yet.

The functioning of SOD enzymes accomplishes the conversion of superoxide into hydrogen peroxide and increases the level of hydrogen peroxide. The latter is not very toxic, but in the presence of superoxide anion and transition metal ions, it can be converted into the very toxic hydroxyl radical. Peroxidase enzymes eliminate H_2O_2 by using it for the oxidation of a substrate (S). Catalases dismutate H_2O_2 directly to O_2 (see equations 3 and 4).

Peroxidase reaction:
$SH_2 + H_2O_2 \rightarrow S + 2H_2O$ (3)

Catalase reaction:
$2\ H_2O_2 \rightarrow 2H_2O + O_2$ (4)

By comparing the proteome of *E. amylovora in vitro* and *in planta,* 5 proteins, which were differentially expressed in both groups, were identified as a peroxidase or a catalase.

The proteins 63, 67 and 69 were all identified as "Putative alkyl hydroperoxide reductase subunit C" (AhpC), which act as a peroxidase. All these protein spots were at least 4 times more expressed in *E. amylovora,* grown

in planta. Multiple spots are identified as the same protein. This could be explained by the fact that proteins can become degraded, processed or post-translationally modified. Such modifications reveal different products of the same protein with different pI and/or MW. AhpC is an NAD(P)H-dependent peroxidase that rapidly reduces hydroperoxide as well as organic hydroperoxides (Seaver and Imlay, 2001). AhpC belongs to the *oxyR* regulon. OxyR is a sensor for peroxide stress. In the presence of peroxide, OxyR activates the expression of the *oxyR* regulon, which includes several detoxifying enzymes such as *ahpC* (Green and Paget, 2004).

Surprisingly, the protein (nr 89) that was identified as a catalase, is more than 3 times less expressed *in planta* compared with *E. amylovora* grown *in vitro*. This could be explained as follows: *Escherichia coli* produces two catalases or hydroperoxidases (HP), namely HPI and HPII. The levels of the two catalases respond to different stimuli. HPI synthesis is induced by environmental H_2O_2 and HPII synthesis is induced during growth into the stationary phase (Mulvey et al., 1990). The catalase enzyme, we found differentially expressed, is a homolog of HPII of *E. coli*. This explains the higher expression of this enzyme *in vitro*, as the sampling *in vitro* occurred at the end of the exponential phase, maybe at the beginning of the stationary phase.

Protein nr 94 is also a peroxidase, namely "Organic hydroperoxide resistance protein" (Ohr). The Ohr proteins were identified as a family of bacterial proteins involved in the detoxification of organic hydroperoxides (Lesniak et al., 2008). This enzyme is more than 6 times less expressed *in planta*. This peculiar finding is difficult to explain because of the presence of oxidative species released by the host plant of *E. amylovora*. However, *ohr* has a unique pattern of oxidative stress-induced expression, unlike other genes involved in protection against oxidative stress. In several bacteria, *ohr* expression is highly induced by treatment with low concentrations of organic peroxides. In contrast, exposure to other oxidants or stresses does not induce *ohr* expression (Sukchawalit et al., 2001).

In the bacterial defence against oxidative stress, thioredoxin-dependent systems play also an important role. Protein nr. 37 and 66, respectively identified as "Putative peroxiredoxin/glutaredoxin family protein" and "Thiol:disulfide interchange protein DsbA", belong to this group of proteins. Both are approximately 4 times more expressed in *E. amylovora* grown *in planta* compared to *E. amylovora* grown *in vitro*. Protein nr. 37 belongs to the peroxiredoxin (PRX) family, PRX5-like subfamily. PRX5 has

been shown to reduce hydrogen peroxide, alkyl hydroperoxides (ROOH) and peroxinitrite (NCBI database). Protein nr. 66 contains a thioredoxin domain. These thioredoxins act as disulfide oxidoreductases (equation 5) and are the electron donors for thioredoxin peroxidases in both prokaryotic and eukaryotic cells (equation 6). Oxidized thioredoxin is reduced by thioredoxin reductase at the expense of NADPH (Carmel-Harel and Storz, 2000).

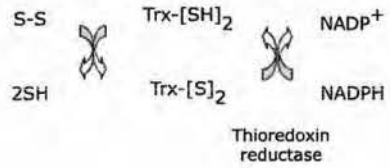

(5)

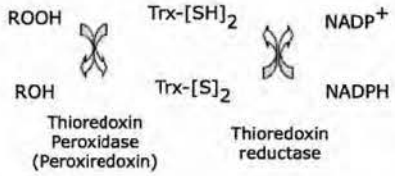

(6)

NADPH provides the reducing equivalents for biosynthetic reactions but also for oxidation-reduction involved in the protection against the toxicity of ROS. The pentose phosphate pathway meets the need of all organisms for a source of NADPH. This pathway consists of two phases: the oxidative phase, where NADPH is generated, and the non-oxidative stage. Protein nr. 30, identified as phosphogluconate dehydrogenase belongs to the oxidative stage of the penthose phosphate pathway. This protein is more than 7 times more expressed in *E. amylovora* grown *in planta* compared with *E. amylovora* grown *in vitro*. This illustrates the importance of reducing power in bacteria during the infection process. The enzyme transaldolase (nr. 20), belonging to the non-oxidative stage of the penthose phosphate pathway, is also more expressed during infection. Transketolase (nr. 4) however, is more expressed in bacteria in *E. amylovora* grown *in vitro.*

A last group of detoxifying proteins are involved in the ubiquinone/menaquinone biosynthesis and metabolism.
Protein nr. 40, which is more than 7 times more expressed in *E. amylovora* grown *in planta,* is identified as "Ubiquinone/menaquinone biosynthesis methyltransferase" (UbiE). This protein is involved in the ubiquinone/menaquinone biosynthesis. Reduced ubiquinone (UQ), also called ubiquinol (UQH_2) plays a role in oxidative stress management. Beside its

function in electron-transport chains, UQH_2 is able to function as a lipid-soluble antioxidant. UQH_2 scavenges lipid peroxyl radicals and thereby prevents a chain reaction causing oxidative damage to polyunsaturated fatty acid of biological membranes, a process known as lipid peroxidation (Soballe and Poole, 2000).
Also noticeable is the almost 6 times augmented expression (in *E. amylovora* grown *in planta)* of the protein (nr. 71) identified as "Putative oxidoreductase YieF". YieF in *E. Coli* is known as a chromate reductase, but it is also a putative H_2O_2-quenching quinone reductase. YieF was shown to possess quinone reductase activity, which appears to guard against oxidative stress by preventing redox cycling of quinones, which would otherwise generate ROS, and by maintaining a pool of reduced quinone in the cell that is able to quench ROS directly (Ackerley et al., 2004).

3.4.3 Repair of damaged cell components

Besides ROS prevention and detoxification, is the repair of damaged cells a crucial defence mechanism against ROS. In fact, all cellular components of *E. amylovora* are attacked by ROS, which are released by the oxidative burst of the host plant during infection. The repair of damaged components is especially important for *E. amylovora* during infection, because it is critical for the survival of injured cells.

The experiment showed that at least 8 proteins, involved in repair mechanisms are more expressed in *E. amylovora* during infection compared with *E. amylovora* grown *in vitro.*

A first group of proteins is involved in the repair and the protection of DNA. A protein identified as an Oligoribonuclease (Orn) (prot. nr. 65) is 3.7 times more expressed in *E. amylovora* during infection. Orn belongs to the DnaQ-like exonuclease superfamily. This is a structurally conserved group of 3'-5' exonucleases, which catalyze the excision of nucleoside monophosphates at the DNA or RNA termini in the 3'-5' direction. The members of the DnaQ-like exonuclease superfamily have a function in DNA replication, recombination, but also in the repair of damaged DNA. (http://www.ncbi.nlm.nih.gov/Structure)
The proteins nr. 75 and 76, which are respectively more than 14 and 8 times higher expressed in *E. amylovora* during infection are both identified as "DNA protection during starvation protein" (Dps). It has been shown that in response to hydrogen peroxide, *E. coli* shows a 180 times induction of the transcript level of the Dps protein (Zheng et al., 2001).

This strong induction indicates that Dps plays an important role in the oxidative stress defence. Dps is a DNA binding protein, which belongs to the OxyR regulon. By binding the DNA, it can directly prevent oxidative damage, particularly DNA strand breaks and certain types of base damage (Martinez and Kolter, 1997). Dps concerns no repair mechanism, but is a direct protection mechanism of the DNA.

A following group of proteins, involved in repair mechanisms, are responsible for the stabilizing and correct folding of proteins.
A first protein in this group is more than 3 times more expressed in *E. amylovora* grown *in planta*. This protein (prot. nr. 62), Glutathione S-transferase (GST) belongs to a family of enzymes that is capable of multiple reactions with a multitude of substrates. GST's are involved in a stunning variety of metabolic processes and afford protection against oxidative stress but also ensure the correct folding, synthesis, regulation of enzymes and multi-enzyme complexes. GSTs catalyse the conjugation of reduced glutathione via the sulfhydryl group, to electrophilic centres on a wide variety of substrates. Some of these represent compounds that may arise during oxidative damage to cell components, such as endogenous lipids, DNA hydroperoxides and hydroxyalkenals (Vuilleumier, 1997).
Another protein in this group is the "Small heat shock protein IbpA" (prot. nr. 86) which has a more than 6 times higher expression in *E. amylovora* grown *in planta*. Small heat shock proteins (sHsp), including IbpA, function as molecular chaperones. sHsps bind to and stabilize unfolded proteins to protect them from aggregation. It has been shown that over expression of *ibpA* in *Escherichia coli* increases the resistance to superoxide stress. It is likely that IbpA may function towards the defence against oxidative stress by themselves or in cooperation with some other Hsps, such as DnaK and Hsp33 (Kitagawa et al., 2000). In response to hydrogen peroxide, *Escherichia coli* shows a 29 times induction of the *ibpA* transcript level (Zheng et al., 2001).
The last proteins in this group of chaperones are peptidyl-prolyl isomerases (Ppiases). The proteins nr 35 and 50, are both identified as "FKBP-type peptidyl-prolyl cis-trans isomerase FkpA" and protein nr. 74 is identified as "Peptidyl-prolyl cis-trans isomerase A" (PpiA). These proteins are respectively 14.29; 6.67 and 5 times more expressed in *E. amylovora* during infection. These Ppiases are predicted to facilitate the proper folding of proline-containing substrates and play an important role in the envelope folding. FkpA is also known as a chaperone. The expression of FkpA is σ^E regulated while PpiA is controlled by the Cpx two-component system. The Cpx and the σ^E pathway sense both environmental cues. They perceive

periplasmic or envelope stress as a result of effects on protein folding in this distinct cellular compartment. These pathways are important during the bacterial adaptation to unfavourable circumstances such as oxidative stress (Raivio and Silhavy, 2001).

A final group of proteins of interest are proteins, whose genes are strongly induced during bacterial oxidative stress, but whose function remains unclear. In our experiment we found "Osmotically inducible protein Y" (OsmY) and "Periplasmic sulphate binding protein" (Sbp) at least 4 times more expressed in *E. amylovora* during infection.
OsmY is a periplasmic protein and is associated with membrane functions and is responsive to oxidative stress. The precise function of OsmY however, remains unclear (Bernstein et al., 1999).
As response to hydrogen peroxide, many genes of *E. coli* are induced. One of these genes is the *sbg* gene. The *sbg* gene is 12 times more expressed in the presence of hydrogen peroxide and belongs to the 30 most strongly hydrogen peroxide-induced genes. The function of Sbp in oxidative stress defence remains unclear (Zheng et al., 2001).

3.5 Conclusion

Erwinia amylovora evokes an oxidative burst in host plants. Until now, it's unclear how *E. amylovora* can overcome this plant defence mechanism. This study illustrates the importance of the oxidative stress defence during host-plant infection. This may be an explanation why *E. amylovora* escapes host plant oxidative burst.

From our research many indications are found that a considerable number of oxidative defence mechanisms are involved in *E. amylovora* during the infection process. This finding, however, is not surprising, since *E. amylovora* evokes an oxidative burst in host plants (Venisse et al., 2001). The bacterial pathogenicity factors HrpN and DspA both participate in this induction of an oxidative burst during the compatible interaction (Venisse et al., 2003). To overcome this oxidative burst, *E. amylovora* must display an effective oxidative defence mechanism.

In bacterial cells, various regulatory sensors are active, monitoring the cellular redox state. In response to oxidative stress or redox imbalance, new metabolic pathways are initiated, the repair or bypassing of damaged cellular components is coordinated and systems that protect the cell from further damage are induced (Green and Paget, 2004).

OxyR and SoxRS are examples of such redox sensors, which are also involved in the *E. amylovora* infection process. The first factor activates anti-oxidative genes in response to the appearance of hydrogen peroxide; the second induces anti-oxidative enzymes in the presence of superoxide. OxyR serves as a ROS-sensor and as a transcription activator: the oxidized and reduced forms of this factor have different conformations and a change in its conformation serves as a cellular emergency signal. OxyR contains six residues of the amino acid cysteine, of which two (Cys_{199} and Cys_{208}) are critical for building up stress response. These cysteines can be modified by H_2O_2, reactive nitrogen species or can be glutathionylated by oxidized glutathione. These modifications produce distinct forms of OxyR with altered DNA-binding characteristics, leading to the activation of the *oxyR* regulon (Vorob'eva, 2004). The *oxyR* regulon includes several detoxifying enzymes such as the AhpC enzyme, which was strongly induced in our experiment in *E. amylovora* during infection. But also Dps is one of the proteins belonging to the *oxyR* regulon.
Excess O_2^- is sensed by the SoxRS system. It senses the production of ~45 proteins in response to superoxide, including AcnA and the detoxifying protein Mn-SOD, which are also stronger expressed in our experiment in *E. amylovora* grown *in planta*. Other proteins of the *soxRS* regulon are involved in DNA repair (endunuclease IV), maintaining cellular reducing power (glucose-6-phosphate dehydrogenase) and central metabolism (superoxide-stable fumarase). Activating of the *soxRS* regulon is achieved by SoxR activating expression of the transcription factor SoxS. Oxidation facilitates SoxR-dependent distortion of the *soxS* promotor DNA to form a transcriptionally active complex with RNA polymerase. Once the source of the oxidative stress is removed, SoxR is rapidly reduced, thereby switching off expression of the SoxRS regulon (Green and Paget, 2004).

Beside activation of the *oxyR* and *soxRS* regulon, also other mechanisms involved in the oxidative stress defence are activated during infection. These proteins are involved in ROS prevention and prevention of ROS entering the bacterial cells, such as proteins involved in iron transport and bacterial capsule formation. But also proteins involved in ROS detoxification and repair were not all OxyR and SoxRS regulated. We saw also interplay between ROS regulated stress mechanisms and other stress related pathways. Examples of these are de Ppiases, which are periplasmic, or envelope stress related proteins. These findings indicate that during infection not only ROS related defence mechanisms are involved but also other general stress related pathways are activated.

Although several proteins expressed during plant-pathogen interaction have been highlighted, not all proteins involved in this process showed up. To illustrate this: only two (of the ~45) proteins of the *soxRS* operon showed up in our experiment. Only a small amount of novel information has been obtained and can be explained by the fact that key proteins are expressed in low abundance and are therefore not detected by current proteomic tools. Indeed, only the most abundant proteins are detected in two-dimensional gels and successfully identified by MS (Mehta et al., 2008). But also other techniques, such as micro array are not the Holy Grail. Studies revealed that the levels of mRNA do not necessarily predict the levels of the corresponding proteins in the cell (Jones et al., 2004). In our experiment, the posttranscriptional regulation of Mn-SOD by the apo-AcnA is a good example for this.

Because of the impediments of the technique, we probably only saw the perceptible part of a larger situation and to date no comparable studies have been published so far. Nevertheless, the results show the importance of the oxidative stress defence in *E. amylovora* during infection. Because the evocation of the oxidative burst in the host-plant and the possibility of *E. amylovora* to escape this plant defence mechanism, it is clear that *E. amylovora* shifts the defence mechanisms of the host-plant into an attack strategy. The infected host-plans will turn black due to a massive apoptotic death, partly because of the occurrence of the evoked hypersensitive response and oxidative burst. *E. amylovora* must have evolved a strategy to escape this oxidative burst and must resist high concentrations of ROS to survive. By further progression of *E. amylovora* inside host-plant tissues, the bacteria will go on evoking an oxidative burst in the surrounding plant cells, which will lead to the further devastation of the host plant.

This study reveals a part of the mystery, how *E. amylovora* succeeds in avoiding the plant defence mechanisms. But beside the importance of the oxidative stress defence in *E. amylovora,* also other components are involved during infection. Future studies must reveal these components and show possible associations between the different pathogenicity factors and their relation with the plant defence system.

Chapter 4

Comparative proteome analysis of four *E. amylovora* strains, differing in virulence degree, *in vitro* and *in planta*

4.1 Introduction

The disease, fire blight, is caused by the bacterium *Erwinia amylovora*. It is a common and very serious bacterial plant disease. *E. amylovora* infects approximately 75 plant species, all in the family of the *Rosaceae*. The principle and most susceptible hosts are in the sub-family *Pomoidae*. From the economic point of view, apple and pear are very important hosts.

Many genes and gene products have been identified and characterized as being involved in the ability of *E. amylovora* to cause fire blight in host plants.
An important group of virulence factors are involved in the production of a type III secretion system (TTSS) and the effector proteins delivered via this TTSS into host plants. The TTSS in *E. amylovora* controls the ability of *E. amylovora* to cause disease in susceptible host plants and to elicit the hypersensitive response in host and non-host plants. Those genes are clustered into a 40-kb genomic region, termed the Hrp pathogenicity island (PAI) (Oh and Beer, 2005; Venisse et al.,2003).
Additionally, other major *E. amylovora* virulence factors contribute to pathogenesis and plant colonization, including the exopolysaccharides (EPS) amylovoran and levan. EPS has been suggested to play a role in disturbance and obstruction of the plant vascular system (Denny, 1995) and to protect the bacterial cells from plant defense reactions (Kiraly et al. 1997). EPS production differs in wild-type *E. amylovora* strains and data on *in vitro* amylovoran production per cell could account for the differences in aggressiveness found in *E. amylovora* strains (Maes et al., 2001). Another known virulence factor is the iron-scavenging siderophore desferrioxamine. Siderophores allow *E. amylovora* to overcome conditions of iron limitation encountered in host tissues but act also as protective agents against iron toxicity (Dellagi et al., 1998). A more detailed overview of the virulence factors of *E. amylovora* is given in section 1.3.

Many genetic studies of virulence genes in *E. amylovora* have been performed. With the increase in genomic and postgenomic studies, a large amount of information is available and advances have been achieved in the understanding of defence mechanisms in plants, as well as the pathogenicity strategies used by the pathogen. At present the functional assignment of given proteins is considered to be the main challenge in postgenomic studies. Transcriptional changes do not reflect the complete cellular regulatory mechanism, as post-transcriptional processes, which alter the amount of active protein, such as synthesis, processing post-

translational modification and degradation, are not taken into account. Thus, complementary approaches, such as proteome-based expression profiling, are needed to obtain a full picture of the regulatory elements. Moreover, several studies have revealed that the levels of mRNA do not necessarily predict the levels of the corresponding proteins in the cell (Jones et al., 2004). The different stabilities of mRNAs and different efficiencies in translation can affect the generation of new proteins. Once formed, proteins also differ significantly in their stability and turnover rate, which makes proteomic investigation even more important (Mehta et al., 2008).

4.2 Objective

The aim of this study is to contribute to a better understanding of the infection process of *E. amylovora.* In analysing different *E. amylovora* strains we want to complement todays view on host-plant infection processes. To include *E. amylovora* strains with different virulence degrees we also tried to shed light on the origins of the differences in degree of aggressiveness. To achieve this goal, a DIGE-approach has been used.

The previous chapter illustrated the importance of the bacterial oxidative stress defence mechanisms during infection. Now, the question arose whether there might be a relation between the efficiency of these defence mechanisms and the virulence degree of different wild type *E. amylovora* strains. To figure this out, we studied the *in vitro* growth capacity of different *E. amylovora* strains during artificially induced oxidative stress.

4.3 Material and methods

4.3.1 Bacteria and plant material

The strains used in the experiments are the *Erwinia amylovora* strains LMG2024, PD437, PFB5 and BG16.
Strain LMG2024 is isolated from *Pyrus communis* (Belgian coordinated collections, Ghent university). Strain PD437 is also isolated from *Pyrus communis* (plantenziektenkundige dienst, Wageningen, The Netherlands). Strain PFB5 is isolated from *Prunus Salicina* (S.K. Mohan, Idaho, USA). Strain BG16 is isolated from *Malus sylvestris* (Dr. S. Bobev, Plovdiv, Bulgaria) and has collection number SBG 225/12.
Based on amplified fragment length polymorphism (AFLP) analysis, all strains are genetically very similar but differ in degree of virulence

(Maes et al., 2001). LMG2024 and PD437 are normal virulent strains. PFB5 is a highly virulent strain and BG16 is a very high virulent strain.
All strains are kindly provided by Dr. Martine Maes (ILVO, Institute for Agricultural and Fisheries Research, Ghent).
The used plant material is described in section 3.3.2.

4.3.2 *In vitro* bacterial growth in presence of H_2O_2

The *Erwinia amylovora* strains LMG2024, PD437, PFB5 and BG16, were grown in presence of H_2O_2 in liquid MM_2 medium (0.4% L-asparagine; 0.2% H_2HPO_4; 0.02% $MgSO_4.7H_2O$; 0.3% NaCl; 0.02% nicotinic acid; 0.02% thiamine hydrochloride) supplemented with 1% sorbitol. Bacteria at initial concentration of 10^6 cells/ml were exposed to concentrations of H_2O_2 ranging from 0.062 to 2 mM. (0 mM; 0.062 mM; 0.125 mM; 0.25 mM; 0.5 mM; 1 mM and 2 mM H_2O_2). Bacterial growth was assessed manually by optical density measurements at 600 nm (UV-1602; Shimadzu). Each concentration of H_2O_2 was tested in triplicate and experiments were performed twice.

4.3.3 Differential in-gel electrophoresis (DIG*E)*

DIGE is a method for prelabelling protein samples prior 2-dimensional electrophoresis for differential analysis. The DIGE system uses multiplexing, which is the simultaneous co-separation of multiple fluorescently labelled samples on one gel. DIGE also includes an internal standard on each gel. This means that each protein has its own internal standard, which minimizes gel-to-gel variation and significantly increase accuracy and reproducibility.

The bacterial strains LMG2024, PD437, PFB5 and BG16 were grown *in vitro* and *in planta*. Bacterial growth and isolation intended for proteomic studies were performed as described in section 3.3.3. Aliquots amounting to 50 µg of protein were labelled with CyDyes: Cy3 and Cy5. The labels were swapped to minimize effect of dye-specific binding properties. The internal standard was labelled with Cy2 and was prepared by mixing aliquots of each protein sample. IEF and SDS-PAGE were performed as described in section 3.3.5 with a minor modification: electrophoresis was performed overnight. Protein spots were visualized using an Ettan DIGE Imager (GE Healthcare).

4.3.4 Image analysis

2D-DIGE image analysis was carried out with DeCyder Software Version 6.5 (GE Healthcare). A 2-way anova test was performed to find strain related and treatment (*in vitro* versus *in planta*) related differences in protein expression patterns.

Bacterial proteins that differ in treatment (*in vitro* versus *in planta*), with a p-value threshold of 0.01, were maintained. These proteins were integrated in the results comparing bacteria grown *in vitro* versus *in planta* (section 4.4.1).

In a first step to find virulence related strain dependent differences, proteins with a strain related difference were retained. The p-value threshold was also 0.01. A selection of these proteins was made. Only the proteins that showed a possible correlation between strain dependent differences and the virulence degree of the used *E. amylovora* strains were retained (section 4.4.2).

All maintained spots were pricked and digested as described in 3.3.8

4.3.5 Mass spectrometry

Protein digests were analyzed using MALDI-TOF/TOF. First 2 µl aliquot of each protein digest was desalted using C_{18} ZipTips (Millipore) and eluted onto a MALDI target plate (anchorchip 600 µm, Bruker) with 2 µl 1% v/v TFA (trifluoracetic acid) in 50% v/v ACN. The samples were allowed to dry after which 0,5 µl of MALDI matrix solution containing CHCA (Sigma) was added. Samples were analyzed using a MALDI-TOF/TOF instrument (Ultraflex II, Bruker). Following peptide mass fingerprinting and MALDI TOF-TOF analysis, spectra were calibrated in FlexAnalysis using the Peptide Calibration Standard (Bruker). Data files were searched with MASCOT (Matrix Science) against a homemade database of *E. amylovora* (see section 3.3.9). Protein digests with no significant result were analyzed using LCQ as described in section 3.3.9.

4.4 Results

4.4.1 Proteomic approach in comparing different *E. amylovora* strains grown *in vitro* or *in planta*.

Of each strain (LMG2024, PD437, PFB5 and BG16), four biological independent samples of each growing condition (*in vitro* or *in planta*) were taken. The sampling methods are described in section 3.3.3. Proteins

were isolated and of each sample, equal protein amounts were analyzed to obtain the proportion of the studied proteins against the total protein content. Differential in-gel electrophoresis (DIGE) analysis was performed and gel images were examined using the DeCyder software (GE Gealthcare). An overview of the workflow of a proteomics experiment is illustrated in figure 3.1.

We were interested in strain dependent differences that may be correlated with the degree of virulence of the used *E. amylovora* strains. Besides this main goal we also studied the proteins of the different *E. amylovora* strains, which were for all strains differentially expressed in the bacteria grown *in vitro* compared with bacteria grown *in planta.* Figure 4.1 shows an example of a 2D-DIGE protein profile of *E. amylovora.* The indicated spots are all proteins of interest that were successfully identified. Proteins of interest are proteins that may be correlated with the degree of virulence or are proteins differentially expressed *in vitro* versus *in planta.*

To interpret the results, one needs to take account of the following features:

- Multiple spots are identified as the same protein. This could be explained by the fact that proteins can become degraded, processed or post-translational modified. Such modifications reveal different products of the same protein but with different pI and/or MW. These modifications of the same protein are present on a 2D-DIGE spot pattern as different spots. The used identification method, MS/MS spectrometry, does not distinguish between the different modifications.
- Sometimes, a single spot exhibits different proteins. In this case different proteins with the same pI and MW coexist in the same spot on a 2D-DIGE spot pattern.

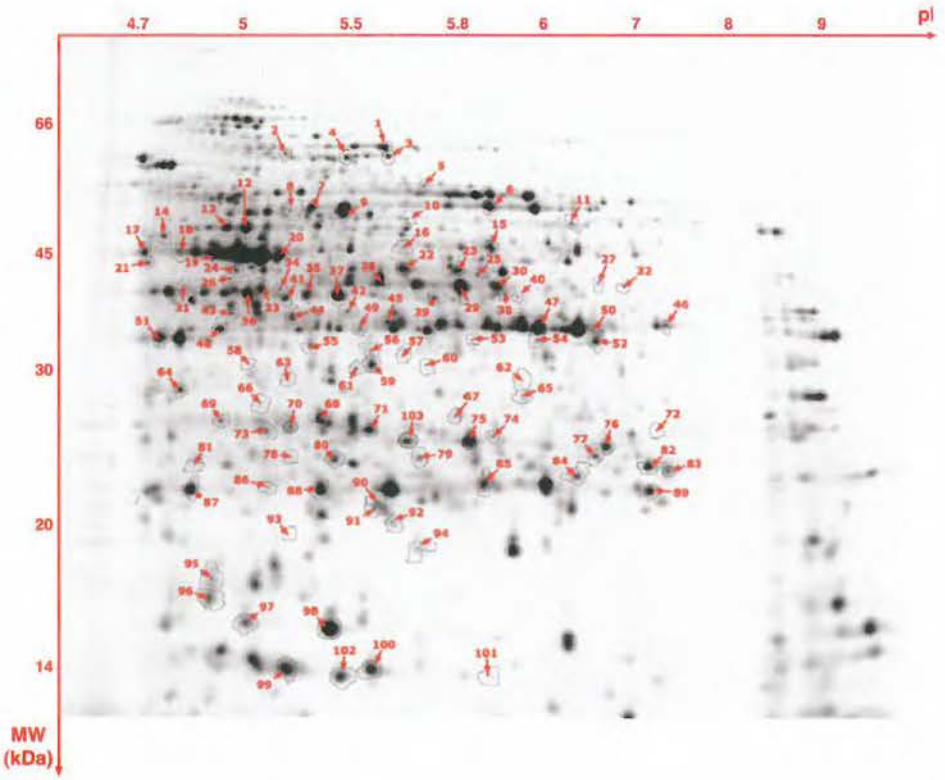

Figure 4.1:
2D-DIGE profile of *E. amylovora*. Proteins were separated in two dimensions. In a first dimension, proteins were separated by iso-electric point (pI). The acidic proteins are located on the left side of the gel, the basic proteins on the right side. The separation in the second dimension is based on a separation by molecular weight (MW). The largest proteins are situated in the upper part of the gel, the smaller proteins in the lower part.
Proteins of interest that were successfully identified are marked. Proteins of interest are proteins that may be correlated with the degree of virulence or are proteins differentially expressed *in vitro* versus *in planta*.

In vitro versus *in planta*

In this part of the survey, we want to investigate which proteins for all studied *Erwinia amylovora* strains are at the same moment differentially expressed when the bacteria were grown *in vitro* compared to *in planta.* In this section we didn't study strain dependent differences. For each protein, the mean expression value of all "*in vitro*" values was compared with the mean expression value of all *in planta* values. The different strains were not taken into account. Strain dependent differences are discussed in the next section.

In total, 91 proteins were identified, which were differentially expressed *in vitro* versus *in planta.* 55 proteins are significantly more expressed in bacteria grown *in vitro.* The other 36 proteins were more expressed for all studied *E. amylovora* strains, during infection (*in planta*). Table 4.1 (in addendum I) gives an overview of all identified differentially expressed proteins grown *in vitro* versus *in planta*. Figure 4.2 shows an overview of the portions of the different protein functionalities for each group of proteins (more expressed *in vitro* or more expressed *in planta*).

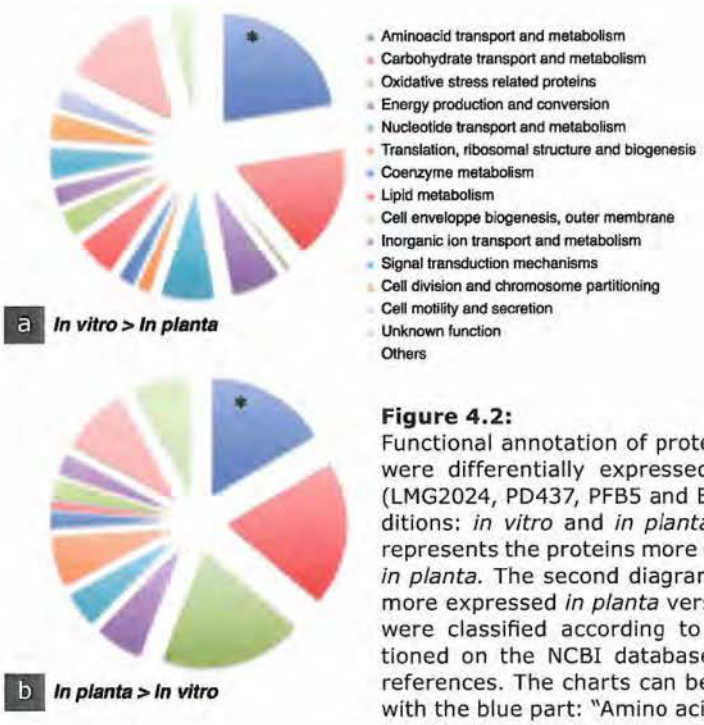

Figure 4.2:
Functional annotation of proteins of *E. amylovora* that were differentially expressed for all studied strains (LMG2024, PD437, PFB5 and BG16) between both conditions: *in vitro* and *in planta.* The first pie chart (a) represents the proteins more expressed *in vitro versus in planta.* The second diagram (b) shows the proteins more expressed *in planta* versus *in vitro.* The proteins were classified according to their function as mentioned on the NCBI database or based on literature references. The charts can be read clockwise starting with the blue part: "Amino acid transport and metabolism" indicated with an asterisk.

Amino acid and carbohydrate metabolism:

The majority of the differences between bacteria grown *in vitro* versus *in planta* are localized at the amino acid and carbohydrate metabolism and transport. In the category of amino acid metabolism and transport, the majority of the differentially expressed proteins are involved in the amino acid synthesis and transport. In the carbohydrate group, most proteins that were differentially expressed between bacteria *E. amylovora* grown *in vitro* versus *in planta*, are involved in the glycolysis and the pentose phosphate pathway. The large differences in expression in those protein groups suggest substantial dissimilarities in general metabolism between *E. amylovora* grown *in vitro* compared with *E. amylovora* during infection. Some spots, identified as the same protein appear in the group of proteins more expressed *in vitro*, but also in the group of proteins more expressed during infection. Examples of such proteins are DabE (prot. nr. 63 and 32), GapA (prot. nr. 47, 49, 50, 68 and 76), Pgk (prot. nr. 36 and 46), TpiA (prot. nr. 75 and 103) and Gnd (prot. nr. 12 and 13) (see abbreviations). So, we found different spots, identified as the same protein, indicating the presence of different modifications of the same protein. Some modifications of the same protein are more present in bacteria grown *in vitro* others more in bacteria during infection. This reflects the different growing conditions, which can lead to dissimilar modifications of the same protein. These modifications can contribute to an altered function of the specific protein.

Oxidative stress related mechanisms:

Considerable differences between *E. amylovora* grown *in vitro* and *in planta* were also found at the level of oxidative stress defence. In all studied *E. amylovora* strains we found an abundance of oxidative stress related proteins more expressed in bacteria *in planta* compared with bacteria grown *in vitro*. The proteins manganese superoxide dismutase (SodA) (prot. nr. 85) and putative alkyl hydroperoxide reductase subunit C (AhpC) (prot. nr. 81, 86 and 88) are both ROS detoxifying enzymes and both are more expressed in *E. amylovora* during infection. Superoxides, such as SodA, represent a group of enzymes that catalyse the dismutation of superoxide and the formation of hydrogen peroxide (H_2O_2). Peroxidase enzymes, such as Ahpc, dismutate H_2O_2 to O_2.

Most cellular components are attacked by ROS. The prevention of the harmful influences of ROS on cellular elements and the repair of damaged elements plays a crucial role in the defence mechanism against ROS. Several proteins involved in oxidative stress defence, more expressed in *E. amylovora in planta* belong to this protecting and repairing group of proteins. These proteins are glutatione-S-transferase (Gst), DNA protecting during starvation protein (Dps), Recombinase A (RecA) and Putative ATP-dependent Clp protease proteolytic subunit (ClpP1).
Proteins nr. 95 and 96, which were expressed respectively more than 7 and 11 times higher in *E. amylovora* during infection are both identified as "DNA protection during starvation protein" (Dps). Dps is a DNA binding protein. By binding the DNA, it can directly prevent oxidative damage, particularly DNA strand breaks and certain types of base damage (Martinez and Kolter, 1997). Dps concerns no repair mechanism, but is a direct protection mechanism of the DNA. Once DNA damage occurred, DNA repair mechanisms trigger the mending of the DNA. One of these enzymes is RecA (prot. nr. 21), 1.5 times more expressed in *E. amylovora* during infection. The RecA protein is a recombinase functioning in recombinational DNA repair in bacteria (Cox, 2007).
Glutathione S-transferase (Gst) (prot. nr. 89), two times more expressed *in planta*, belongs to a family of enzymes that is capable of multiple reactions with a multitude of substrates. GST's are involved in a stunning variety of metabolic processes and provide protection against oxidative stress but also ensure the correct folding, synthesis, regulation of enzymes and multi-enzyme complexes (Vuilleumier, 1997).

The last protein, more expressed in *E. amylovora* during infection, involved in oxidative stress defence is Putative ATP-dependent Clp protease proteolytic subunit (ClpP1) (prot. nr. 81). Clp proteases were first identified in *Escherichia coli* and consist of an ATPase specificity factor (ClpA or ClpX) and a proteolytic domain (ClpP) that contains a consensus serine protease active site. Clp proteolytic complexes are responsible for adaptation to multiple stresses, such as oxidative stress, by degrading accumulated and misfolded proteins. In *Staphylococcus aureus* ClpP has also a strong regulatory impact on the expression of genes encoding proteins that are involved in the pathogenicity and adaptation of the pathogen to several stresses (Michel et al., 2006).

The only protein involved in oxidative stress, which is more expressed in *E. amylovora in vitro* compared with bacteria during infection is the Xenobiotic reductase, XenA (prot. nr. 38). XenA is an oxidoreductase of un-

known physiological function that has also been proposed to be a member of the oxidative stress response system and appears also in response to aromatic compounds (Blehert et al., 1999).

Motility:

We found also large differences of the cell motility protein, flagellin (FliC). Spot 58, 66 and 72 are identified as FliC. These proteins were all significantly more expressed in all studied *E. amylovora* strains grown *in vitro* compared with *E. amylovora* during infection. Spot nr. 66 is even more than 17 times higher expressed *in vitro* versus *in planta*. These findings are in correspondence with earlier studies. *E. amylovora* displays motility in fluid medium but in the plant after infection, *E. amylovora* switches off its flagellar system (Cesbron et al., 2006).

Amylovoran precursor formation:

We saw also a significantly higher expression of protein nr. 43 in *E. amylovora* during infection versus *E. amylovora* grown in fluid MM_2 medium, supplemented with sorbitol. This protein is identified as Glucose-1-phosphate uridylyltransferase (GalU). GalU is involved in the production of the activated sugar molecule UDP-glucose. Activated sugar molecules are the basis of polysaccharide synthesis. The formation of amyloveran depends on UDP-sugars, i.e. UDP-galactose, UDP-glucose and UDP-glucuronic acid. They have to be synthesized within the cells from the pool of highly energetic compounds, such as ATP or UDP. GalU is required for the conversion of glucose-1-phosphate to UDP-glucose, necessary for the amylovoran synthesis. UDP-glucose is also a precursor of UDP-galactose and UDP-glucuronic acid. AmsM has homology to GalU and GalF of *E. coli*. The latter protein has been associated to GalU as a subunit (Geider, 2000).

Heat-stable nucleoid-structuring protein:

Another interesting protein is protein nr. 100, identified as "heat-stable nucleoid-structuring protein" (Hns). This protein is significantly more expressed in all studied *E. amylovora* grown *in planta* compared with bacteria grown *in vitro.* Hns plays a fundamental role in the bacterial nucleoid organization. In addition to a role in nucleoid organization, Hns functions as a pleiotropic regulator of gene expression. Hns directly or indirectly regulates adaptation to different environmental conditions (Dorman, 2004).

Quorum sensing:

Besides the bacterial feature to adapt to environmental conditions, bacteria have evolved mechanisms to coordinate cellular functions in response to population density. One such mechanism, quorum sensing (QS), involves the production and detection of intercellular signals (called autoinducers, or pheromones) in the surrounding environment. Autoinducers (AIs), observed in a broad range of bacteria, are known to modulate critical functions including virulence factor production; plasmid conjugal transfer; activation of secretion systems; swarming, swimming, and twitching motility; biofilm formation; and bioluminescence (Withers et al., 2001).
In our experiment, we found three proteins involved in the AI-production, differentially expressed between bacteria grown *in vitro* and *in planta*, and this for all studied *E. amylovora* strains. These proteins are LuxS-Like protein (LuxS) (prot nr. 91), Malonyl CoA-acyl carrier protein transacylase (FabD) (prot nr. 58 and 61) and 3-oxoacyl-[acyl-carrier-protein] reductase (FabG) (prot nr. 85). These differences indicate the importance of quorum sensing in the different expression profiles of *E. amylovora* grown in both growing conditions, *in vitro* and *in planta*.
In the Gram-negative *Erwinia* species, at least two QS systems exist and are defined by the nature of the chemical signals involved: N-acyl homoserine lactones (N-AHLs; also called AI-1 signals), synthesized by the LuxI family of proteins; and the AI-2 signal. AI-2 is furanosyl borate diester (Chen et al., 2002), which is synthesized by the LuxS enzyme (Reading and Sperandio, 2006).
N-AHL signals are made by a wide range of Gram-negative bacteria. They are characterized by an invariant homoserine lactone ring, to which a variable acyl side chain is attached. Each cell in the bacterial population has the capacity to make the QS signal, which indicates their presence to other cells in the population (Bernard and Salmond, 2007). FabG and FabD are involved in the formation of the acyl side chain of the N-AHL molecules. In *Pseudomonas aeruginosa* FabG activity is correlated with the length of the acyl side chain (Hoang et al., 2002).
The AI-2 is synthesized in two enzymatic steps. The gene responsible for the last enzymatic step of AI-2 production is *luxS* (Gao et al. 2008). In our experiment, LuxS was found significantly more expressed in *E. amylovora* grown *in vitro* compared with *E. amylovora* during infection.

Thiamine related proteins:

Thiamine is an essential cofactor that is required for processes of general metabolism amongst all organisms. Thiamine pyrophosphate (TPP) is the active form of vitamin B_1. TPP plays an essential role in most, if not all, organisms and is required at several central points of anabolic and catabolic intermediary metabolism, such as the pentose-phosphate pathway and the Krebs cycle (Frank et al., 2007).

Translation of transcripts encoding enzymes required for the thiamine biosynthesis or import is impeded by riboswswitching in the presence of thiamine (Frank et al., 2007). A riboswitch is apart of an mRNA molecule that can directly bind a small target molecule and whose binding of the target affects the gene's activity. The *in vitro* growing medium of *E. amylovora* contains thiamine. So its no surprise we found proteins involved in thiamine transport and metabolism differentially expressed *in vitro* versus *in planta*. The thiamine transport protein TbpA (prot. nr. 46) is about 2.5 times more expressed *in planta*. In the study described in chapter 3 we found the protein thiamine-phosphate pyrophosphorylase (prot. nr. 51; table 3.1), involved in thiamine synthesis, even 14 times more expressed *in planta*.

TPP is also the cofactor of some enzymes that were differentially expressed in bacteria grown *in vitro* versus *in planta*. The enzymes acetolactate synthase (BudB)(prot. nr. 5) and pyruvate dehydrogenase multienzyme complex (IpdA)(prot. nr. 9) are more expressed *in planta*. Transketolase however, is less expressed in *E. amylovora* grown *in planta*. The expression of thiamine-related genes is down regulated in presence of thiamine by riboswitching (Serganov et al., 2006). Why IpdA and BudB are more expressed *in planta* compared with *E. amylovora* grown *in vitro* can be explained by riboswitching and the presence of thiamine in the *in vitro* growing medium. Why transketolase is less expressed in *E. amylovora* grown *in planta* compared with in *E. amylovora* grown *in vitro* cannot be explained by riboswitching.

Potential virulence related strain dependent differences

In this study we searched for proteins, potentially involved in the virulence degree of different *E. amylovora* strains. To achieve this, not all proteins that were differently expressed between the different strains, were examined. Only the proteins that meet the requirements for being

potentially involved in the virulence degree of the different *E. amylovora* strains were studied. In an ideal situation, a protein of interest is a protein with a maximum difference in expression between the normal virulent strains (LMG2024 and PD437) and the very highly virulent strain (BG16). Moreover, the expression of the highly virulent strain, PFB5, should be in the middle of the expression of the same protein of the normal and the very virulent strains. However, we couldn't find any protein that matches these conditions. By this strategy, we tried to come up with elements that may be the foundation for the differences in aggressiveness between the studied *E. amylovora* strains.

The virulence degree of different *E. amylovora* strains is most probably not the result of one single gene. It could be the result of an interplay of a variety of genes and gene products leading to a higher degree of virulence. This is the reason why we also tried to scan for proteins, of which the expression level is different between the normal virulent strains (LMG2024 and PD437) and one of the higher virulent strains (PFB5 or BG16).

Protein nr.	Protein name
14	Threonine synthase (ThrC)
26	Conserved hypothetical protein YbiS
28	Fructose bisphosphate aldolase class II (Fba)
31	Methyltransferase
35	Phospho-2-dehydro-3-deoxyheptonate aldolase, Tyr-sensitive (AroF)
	Aspartate aminotransferase (AspC)
37	Phospho-2-dehydro-3-deoxyheptonate aldolase, Tyr-sensitive (AroF)
40	hypothetical protein plu1873
51	Elongationfactor Ts
53	ABC superfamily high affinity Zn transport protein (ZnuA)
70	2,3-bisphosphoglycerate-dependent phosphoglycerate mutase(GpmA)
94	Protein YceI
99	no homologs found; conserved cupin domain
102	Nucleoside diphosphate kinase (Ndk)

Table 4.2:
Identification results of the selected spots, which are potentially related with the virulence degree of the different *E. amylovora* strains. Spot numbers are indicated in figure 4.1.

In the end, we had a selection of 13 proteins that may be correlated with the virulence degree of the strains. The next paragraphs will give an overview of these proteins. The expression patterns are depicted in figure 4.3 (in addendum II) and table 4.2 is an overview of the protein names of these selected proteins.

Protein nr. 14 showed a lower expression in the more virulent strains (BG16 and PFB5). This protein is identified as threonine synthase (ThrC) and catalyzes the final steps of the threonine biosynthesis. Protein 28 was also less expressed in the higher virulent strains BG16 and PFB5 grown *in planta*. For all strains grown *in vitro,* the expression of this protein remained more or less the same. Protein 28 was identified as fructose bisphosphate aldolase (class II) and is involved in the carbohydrate metabolism in the gluconeogenesis and glycolysis. Protein 53 is the last protein where the expression *in planta* is lower in the highly virulent strains (PFB5 and BG16) compared with the normal virulent strains (LMG2024 and PD437). This protein was also significant more expressed in bacteria during infection, for all studied strains. The expression of protein 53, *in vitro,* remained for all strains nearly unchanged. This protein is identified as "ABC superfamily high Zn transport protein" (ZnuA). ZnuA has been shown to function as initial receptors in the ATP-binding cassette (ABC) uptake of Zn^{2+}.

In the highly virulent *E. amylovora* strain BG16, the proteins nr. 26 and 70 were less expressed in comparison with the other studied strains. Protein 26 is identified as "conserved hypothetical protein Ybis". This protein has an unknown function and is found in a range of bacteria. The conserved region contains a conserved histidine and cysteine, suggesting that these proteins have an enzymatic activity. Several members of this family contain peptidoglycan-binding domains. So these proteins may use peptidoglycan or a precursor as a substrate. Protein nr. 70 is identified as "2,3-bisphosphoglycerate-dependent phosphoglycerate mutase" (GpmA) and is involved in the gluconeogenesis and glycolysis.

The following group of proteins showed a higher expression level in the more virulent strains (BG16 and PFB5) in bacteria grown *in vitro* and/or *in planta.* These are the proteins nr. 94, 99, 102 and 40. Protein 94, identified as "protein YceI", was significantly more expressed in all studied *E. amylovora* strains during infection. The highest expression occurs in BG16 and PFB5 grown *in planta*. The function of this protein is unclear. Also for protein 99, the function remains unknown. This protein has a cupin-

conserved domain, but we found no homologs in related bacteria such as *Erwinia tasmaniensis* and *Escherichia coli*, where for most *E. amylovora* proteins homologs were found. Protein 99 showed a higher expression level for all strains grown *in vitro* and was more expressed is strain PFB5 and BG16. Another protein with unknown function is protein nr. 40, identified as "hypothetical protein plu1873". This protein is less expressed *in planta* and showed only in vitro a higher expression level for the more virulent strains PFB5 and BG16 compared with the normal virulent strains LMG2024 and PD437. This expression pattern was also more or less the same for protein nr. 102, identified as "nucleoside diphosphate kinase".

The last group of proteins that may be involved in the degree of virulence showed a higher expression level in *E. amylovora* strain BG16, compared with the other studied strains. The expression level of BG16 is higher both, *in vitro* and *in planta* for the proteins nr. 35, 37 and 51 (see table 4.2 for identification results). Protein 35 and 37 were both more expressed in all strains grown *in vitro* and protein 51 is more expressed during infection for all strains. Protein nr 31, identified as methyltransferase, showed only in BG16 grown *in vitro* a higher expression level, compared with the other strains.

4.4.2 *In vitro* bacterial growth in the presence of H_2O_2

The previous chapter illustrated the importance of oxidative stress related mechanisms during infection. To analyse whether there is a relation between the virulence degree of different *E. amylovora* strains and the resistance against oxidative stress, growth curves of different *E. amylovora* strains in the presence of different hydrogen peroxide concentrations were compared. These growth curves showed that the strains PD437 and PFB5 were much more resistant to H_2O_2 than the strains LMG2024 and BG16 (fig. 4.4). This effect was already visible when 0.25 mM H_2O_2 was present in the medium. The differences were more pronounced when 2 mM H_2O_2 was present. When no H_2O_2 was present, there was no difference in growing capacity between the different strains.
The strains LMG2024 and PD437 are normal virulent strains, strain PFB5 is high virulent, BG16 is a very highly virulent strain. Owing to the virulence of the different *E. amylovora* strains, there is no relation between virulence degree and growing capacities in the presence of H_2O_2.

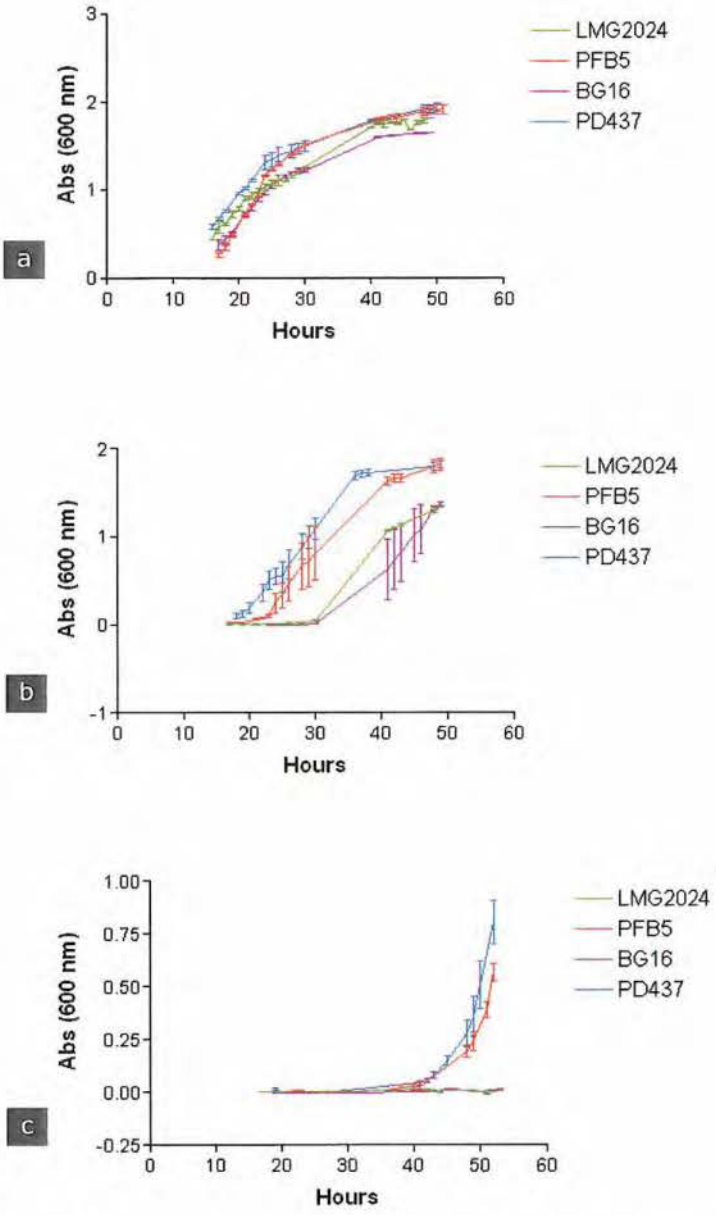

Figure 4.4:
Growth curves of different *E. amylovora* strains (LMG2024, PFB5, BG16 and PD437) in presence of 0 mM H_2O_2 (a), 0,25 mM H_2O_2 (b) and 2 mM H_2O_2 (c).

4.5 Discussion

4.5.1 Potential virulence differences

Wild type *Erwinia amylovora* strains can differ in degree of virulence. In this study we tried to find proteins that are involved in the virulence degree. To include *E. amylovora* strains with different virulence degrees we tried to shed light on the origins of the differences in degree of aggressiveness. To achieve this goal, a DIGE-approach has been used. Based on their expression profile, thirteen spots that were significantly different expressed between the various strains were retained. The representative proteins of these spots could possibly be involved in the degree of aggressiveness of the studied strains. The description of these proteins is given in section 4.4.1. Study of the literature however didn't show any relationship between the functions of these proteins and a possible role in the infection process. There was also no clear relation to bacterial virulence. This makes it very doubtful that these candidates are really involved in the virulence degree of the different *Erwinia amylovora* strains. Maybe we didn't find a suitable candidate because of the restrictions of the 2D-DIGE technique and the used experimental setup. During this experiment we analyzed the bacterial proteome only at one sampling time. Studying a time course can give more nuanced results. Another option is that we probably didn't look at the right place. In our study, only proteins inside the bacteria were included. Secreted proteins were not incorporated and maybe one (or more) of these secreted proteins forms the foundation for the differences in aggressiveness between the different *E. amylovora* strains.

A previous study by Maes et al. (2001) showed that the *in vitro* amylovoran production per cell could account for the differences in aggressiveness found in wild-type *E. amylovora* strains. Our 2D-DIGE study didn't come up with enzymes involved in the amylovoran production. We only found the higher expression of the enzyme GalU, more expressed in *E. amylovora* during infection compared with bacteria grown *in vitro*. The expression of this protein, which is involved in the production of amylovoran precursors, didn't show a correlation with the virulence degree of the studied strains. To investigate whether "amylovoran synthesis enzymes" are associated with the virulence degree of different wild type *E. amylovora* strains, other techniques must be applied. This can be done, for instance, by real time quantitative PCR.

In chapter 3, the importance of the bacterial oxidative stress defence during infection was illustrated. Maybe there might be a relation between oxidative stress defence mechanisms and the virulence degree of *E. amylovora.* We intended to investigate whether these mechanisms are also involved in the virulence degree of the different *E. amylovora* strains. Are the more virulent strains more resistant against higher concentrations of ROS? To answer this question, *E. amylovora* strains differing in virulence were artificially exposed to oxidative stress. We compared growth curves of different *E. amylovora* strains in the presence of hydrogen peroxide. However, the differences in growing capacities of the different strains in the presence of H_2O_2 showed no correlation between virulence degree and the growing capacities in the presence of H_2O_2. Also the 2D-DIGE study didn't show the potential involvement of oxidative stress defence mechanisms in the degree of virulence of different *E. amylovora* strains.

4.5.2 Processes involved in *E. amylovora* during infection

Despite the negative results in our quest for proteins potentially involved in the virulence degree, we analysed the proteins differing *in vitro* versus *in planta*. With this study we want to confirm the results of chapter 3 (involvement of oxidative stress defence mechanisms during infection) and we want to give an overview of the other factors differing *in vitro* versus *in planta.*

The DIGE study revealed also the importance of oxidative defence mechanisms during infection in all studied *E. amylovora* strains. But not all proteins involved in this process, which were significantly expressed in the 2D-GE experiment of chapter 3, were also found to be significant in the DIGE experiment of this chapter and visa versa. Important players in the oxidative defence mechanisms were in both studies significantly more expressed *in planta* versus *in vitro.* Proteins that were found in common were the detoxifying enzymes SodA and AhpC, the anti-oxidative enzyme Gst and the DNA protecting protein Dps. The DNA repair enzyme RecA and the chaperone ClpP1 were found significantly more expressed *in planta* during the DIGE experiment of this chapter and were not found significantly expressed in the experiment of chapter 3. The previous chapter described how *E. amylovora* evokes an oxidative burst in host plants and how the bacteria arm themselves with an arsenal of oxidative defence related proteins. The similar results in both studies support the theory that *E. amylovora* adapts to extreme unfavourable conditions and how *E. amylovora* can overcome plant defence mechanism and can go on with blighting plant tissues.

The use of different bacterial growth conditions provides also information how bacteria behave in particular environments. Comparing *E. amylovora* grown *in vitro* with *E. amylovora* in their natural environment, namely during infection, can provide interesting knowledge about the bacterial infection process.
In order to find factors involved in the infection process of *E. amylovora*, the bacterial proteome was studied. The study of the proteome by two-dimensional differential in-gel electrophoresis (2D-DIGE) gives an overall exhibition of all proteins that are expressed by *E. amylovora* during growth in two conditions: *in vitro* and *in planta.* By using different *E. amylovora* strains, we tried to find mechanisms that are generally involved in infection for all studied strains.

Bacteria continuously respond to signals from external and internal environments. Quorum sensing (QS) is one of the mechanisms that bacteria have evolved to coordinate cellular functions in response to population density. It involves the production and detection of intercellular signals or autoinducers (AIs) in the surrounding environment. These AIs modulate critical bacterial functions including virulence factor production; plasmid conjugal transfer; activation of secretion systems; swarming, swimming, and twitching motility; biofilm formation; and bioluminescence (Withers et al., 2001). In *E. amylovora,* at least two QS systems exist: a first one involves AI-1 signals and the second AI-2 signals (Bernard and Salmond, 2007). The gene responsible of the final enzymatic step of AI-2 production is LuxS (Bernard and Salmond, 2007) and LuxS is one of the proteins that has been significantly more expressed in *E. amylovora* grown *in vitro* compared with *E. amylovora* grown *in planta.* It is shown by Gao et al. (2008) that *E. amylovora* exhibited maximum functional AI-2 activity in the late-exponential and early stationary growth phases and diminished during the stationary phase. This finding is consistent with our results, showing a higher expression of LuxS in *E. amylovora* grown *in vitro*, where sampling occurred at the end of the exponential phase.
LuxS is present in a wide phylogenetic range of Gram-negative and Gram-positive bacteria. The chemical structure of AI-2 appears to be conserved, possibly allowing interspecies communication. Thus it was hypothesized that AI-2 might be a universal signal molecule. Inactivation of *luxS* in a variety of bacteria has produced a range of effects, from no observable pathogen phenotype (e.g., in *Helicobacter pylori* and *Proteus mirabilis*) to altered production of virulence determinants (e.g., in *Porphyromonas gingivalis, Streptococcus pyogenes*, and *Clostridium perfringens*) and decreased virulence (in *Neisseria meningitides*, *Streptococcus pneumoniae*,

and *Vibrio vulnificus*). It is also reported that *E. amylovora* has *luxS* dependent AI-2 activity, and that inactivation of *luxS* affects some phenotypes including virulence in planta (Gao et al. 2008). Inactivation of *luxS* in *E. amylovora* impaired extracellular polysaccharide (EPS) production, tolerance for hydrogen peroxide, and reduced virulence on pear leaves, but *luxS* inactivation also impaired motility (Gao et al. 2008). These findings indicate a possible relation between LuxS function and the regulation of the flagellar system in *Erwinia amylovora*. In our experiment we found besides a higher expression of LuxS in *E amylovora* grown in vitro, a 17 times higher expression of flagellin (FliC) compared with *E. amylovora* during infection.
Motility of *E. amylovora* appears to help the bacterium in its invasion of host plant tissues. However, bacterial cells seem non-motile after their entry into the apoplast, which explains the differences of the FliC expression profiles between *E. amylovora* grown *in vitro* and *in planta*. Motility is needed in an initial step of the infection process, e.g. movement towards infection sites, adherence or penetration, but appears unnecessary afterwards. In the plant after infection, *E. amylovora* switch off their flagellar system. Switching off flagellar synthesis may be vital for the bacteria because flagellins are often considered as general elicitors of antimicrobial plant defence responses (Cesbron et al., 2006).

QS in *Erwinia* allows coupling of the accumulation of small, diffusible signalling molecules to the regulation of gene expression. The accumulation of these signals may indicate an increase in population density, colonization of a surface or the diffusibility of the QS signal itself (Barnard and Salmond, 2007). Beside AI-2, *E. amylovora* produces also AI-1 signals. AI-1 signals or N-acacyl homoserine lactones (N-AHLs) are characterized by an invariant homoserine lactone ring, to which a variable acyl side chain is attached. The proteins FabG and FabD, which were significantly different expressed in bacteria grown *in vitro* compared with *E. amylovora* during infection, are involved in the formation of the acyl side chain of the N-AHL molecules. FabD is more expressed in vitro while FabG is more than 3 times more expressed in *E. amylovora* during infection. In *Pseudomonas aeruginosa* FabG activity is correlated with the length of the acyl side chain (Hoang et al., 2002). The different expression of FabG *in vitro* and *in planta* may also in *E. amylovora* lead to the production of N-AHLs with different acyl side chains. One may suggest that different N-AHL signals may lead to different expression profiles.

The population density is not the only physical or chemical parameter that bacteria sense and respond to by altering gene expression. However, the QS system appears to be able to operate as a kind of central 'hub' at which cues from multiple inputs can be integrated to control gene expression in an appropriate way. Another regulator of gene expression in response to different environmental circumstances is the heat-stable nucleoid-structuring protein (Hns). Hns is significantly more expressed in all studied *E. amylovora* strains during infection versus *E. amylovora* grown *in planta.*

Hns plays a fundamental role in the bacterial nucleoid organization. In addition to a role in nucleoid organization, Hns functions as a pleiotropic regulator of gene expression. Hns directly or indirectly regulates adaptation to different environmental conditions. The small acidic protein is known as a general negative regulator of gene expression. Two mechanisms of transcriptional regulation by Hns have been proposed: Hns might have an indirect effect on the expression of promoters by altering the status of DNA-supercoiling (Mojica and Higgins, 1997) or it can directly inhibit transcription by preferential binding to promoter regions (Afflerbach et al., 1999). However, Hns can also activate genes by repressing a repressor (Dorman, 2004).

E. amylovora contains two *hns* genes. One *hns* gene is located on the *E. amylovora*-specific plasmid; the other *hns* gene is located on de genome. Both *hns* genes of *E. amylovora* showed 63% homologies to each other (Hildebrand et al., 2006). In our experiment we found the plasmid encoded Hns protein significantly more expressed in *E. amylovora* during infection compared with *E. amylovora* grown *in vitro.* This finding indicates a possible role of Hns during host plant infection.

Hildebrand et al. (2006) demonstrated already a delayed virulence on pear slices for *hns* mutant *E. amylovora* strains. Also EPS production and motility were affected in the *hns* mutant *E. amylovora* strains. Furthermore, studies have shown that most Hns bound DNA have been horizontally acquired (Oshima et al., 2006). Since the Hrp pathogenicity island of *E. amylovora* is the result of horizontal gene transfer (Oh and Beer, 2005), the question arises whether the expression of the genes encoded by the Hrp pathogenicity island are effected by Hns.

Our understanding of the action of Hns is still fragmented and a comprehensive assessment of the action of Hns in bacterial cells is still lacking.

An important virulence factor of *E. amylovora* is the exopolysaccharide (EPS) amylovoran. Expression of amylovoran synthesis also depends on various environmental conditions, such as temperature, salt or carbon

sources(Geider, 2000). To regulate its EPS production, a network of regulatory proteins seems to come into play, including global regulators, such as Hns (Geider, 2000). So it is not surprising that we found proteins that were involved in amylovoran production differentially expressed in *E. amylovora* grown *in vitro* versus *in planta.*
One of the findings is a higher expression of the enzyme GalU in all studied *E. amylovora* strains during infection, compared with the same strains grown *in vitro*. GalU is required for the conversion of glucose-1-phosphate to UDP-glucose. UDP-glucose, in its turn, is a precursor of UDP-galactose and UDP-glucuronic acid. These UDP-sugars are necessary for the synthesis of amylovoran, the most important EPS of *E. amylovora* (Geider, 2000). The higher expression of GalU during infection may lead to an efficient production of the amylovoran precursors. This finding underlines the importance of the amylovoran production during infection.

Our results showed large differences in *E. amylovora* grown *in vitro* versus *in planta.* Adaptation to different environmental conditions seems to be very important in the infection process of *E. amylovora.* Not only proteins involved in oxidative stress defence, QS-signalling, motility and EPS production are associated with this adaptation process. A large group of differentially expressed proteins are those proteins involved in protein and carbohydrate metabolism and transport. This underlines the importance of the general metabolism and the adaptation behaviour in different growing conditions. Because of the presence of different spots identified as the same protein, the occurrence of different modifications of the same protein plays also an important role. The cellular responses to changing conditions are commonly mediated by the reversible covalent modification of existing molecules such as proteins and phospholipids. Proteins can be altered by a diverse set of post-translational modifications that include phosphorylation, methylation, acetylation, ubiquitylation and hydroxylation. These modifications often function together to control the activities of individual proteins and multiprotein signalling pathways. Each of these modifications can be recognized by specific protein-interaction domains, which therefore read out the dynamic state of the proteome and transmit this information to the molecular machines that organize cellular behaviour. Such modification-dependent interactions can be configured to produce complex forms of regulation that involve, for example, auto regulation, cooperative interactions, sequential interactions, inhibition and mutually exclusive interactions (Seet et al., 2006).

The adaptation to different environmental conditions is an important tool for *E. amylovora*. Sensing the environment and interacting at an appropriate way makes it possible for *E. amylovora* to infect host plants, to spread into host plant tissues and to overcome extreme conditions such as plant defence mechanisms. This property makes from *E. amylovora* a successful pathogen.

Chapter 5

Summary and general conclusions

Erwinia amylovora is the causal agent of the bacterial disease, called fire blight. Fire blight is particularly destructive to most species of the *Malaceae* and some species in other families of the *Rosales.* Apple and pear trees are from the economic point of view, the most important host species but also woody ornamentals such as hawthorn, pyracantha and cotoneaster are susceptible to fire blight. The bacterium enters plant tissue via blossoms or wounds, and spreads within intercellular spaces and vascular tissue, killing blossoms, shoots, branches and in the most severe cases entire plants (Vanneste and Eden-Green, 2000). The severity of the disease results from its destructive character on the one hand and the lack of effective control methods by growers on the other hand.

The main objective of this work was to gain a better insight into the infection process of *E. amylovora*. In chapter 2, we studied the bacterial propagation during flower infections by different microscopic tools. In chapters 3 and 4 we analyzed the proteins involved during the infection process. We also searched for factors that play a role in the virulence degree of different wild type *E. amylovora* strains.

Microscopic study of blossom infections

In spring primary infection occurs generally through the flowers and moves up to the shoots and branches. Because of the importance of blossoms as primary infection site, we first investigated the microbial spread of *E. amylovora* after inoculation of different parts of the flowers. We examined Braeburn, Conference and *Crataegus* blossom infections by confocal, light and transmission electron microscopic (TEM) techniques. This was done to verify and refine the current understanding of blossom infections by *E. amylovora.*

When the anthers were inoculated, most flowers remained symptomless. Nevertheless, bacteria could enter the locule of the anther, grow epiphytically and contaminate the pollen. In the orchard, this contaminated pollen is a new inoculum source and could be spread to other flower parts and even to other flowers. During our study, contaminated pollen that fell into the calyx cup could explain why some flowers became infected after anther inoculation. But we found also that bacteria may move epiphytically via the small grooves of the filament towards the calyx cup. Also when inoculation occurred near the stigma, the bacteria were mostly restricted to the inoculation site. The microscopic results emphasized the importance of the stigma as an ideal environment for epiphytic populations of

E. amylovora. The results demonstrated also how the bacteria entered the upper layers of the style. The lower part of the style remained for all studied flowers symptomless. In orchard, during humid conditions, the bacteria can flush into the nectarium of the calyx cup, where infection occurs (Bubán et al., 2003). Once present at the nectarium, under favourable conditions, bacteria penetrate through the nectarthodes and invade the tissues of the host plant (Vanneste and Eden-Green, 2000). This is also confirmed by our TEM study of *Crataegus* flowers, after inoculation of the calyx cup. In the nectarium we found bacteria in the stomatal-like opening of the nectarthodes. For all studied blossoms (Braeburn, Conference and *Crataegus*), *E. amylovora* invaded the entire hypanthium, when bacteria were applied near the calyx cup. TEM pictures illustrated the presence of the bacteria in the intercellular spaces and displayed the collapsed hypanthium tissue in the bacterial environment. Confocal observations at one day after inoculation illustrates already the presence of *E. amylovora* near the onset of the peduncle near the hypanthium. At this stage no visual wilting symptoms were seen. Symptoms appeared when massive GFP fluorescence originating from *E. amylovora* was present. This was the case one and two days after inoculation, near the upper cellular layers of the hypanthium. On the third day, massive GFP fluorescence showed up over the entire hypanthium as well as near the peduncle.

Proteome analysis of *E. amylovora*

The second section of this work focused on the proteins of *E. amylovora* involved in the infection process. For this study, we used shoots of the susceptible M9 rootstock to perform this study. During the growing season shoots are always present and play also an important role in the infection cycle. To perform this study, shoot infection resulted in sufficient non-wooden infected plant material.

In a first proteomic study presented in chapter 3, our goal was to study bacterial processes involved in the infection process. Especially proteins involved in the oxidative stress defence were studied. To perform this, the protein profile of *E. amylovora* grown *in vitro* was compared with the protein profile of *E. amylovora* in their natural environment, namely during host plant infection, in our case the susceptible apple rootstock M9. This was carried out by two-dimensional gel electrophoresis (2D-GE), a technique that gives an overall view of proteins that are expressed. The study ended up with 96 identified proteins that were differently expressed

under both conditions. Regarding the functional diversity, the major part of these proteins is involved in oxidative stress related processes. We focussed on this group of proteins because of their known importance in the adaptation process of the bacteria to oxidative stress. In susceptible host plants, *E. amylovora* induces a hypersensitive response and an oxidative burst, as does an incompatible pathogen. The release of reactive oxygen species (ROS) during the oxidative burst is the result of the combined action of two Hrp effectors of *E. amylovora*, HrpN and DspA (Venise et al., 2003). These proteins are injected by the type III secretion system (TTSS) into the host plant cells and interfere with plant defence signal transduction. HrpN and DspA participate in the induction of an oxidative burst, a process known to protect the plant against pathogen invasions. Despite this massive release of toxic ROS, *E. amylovora* is capable to survive and to devastate host plant tissue. Moreover, *E. amylovora* shifts the defence mechanisms of the host-plant into an attack strategy. Virulent *E. amylovora* strains must have evolved a strategy to escape this oxidative burst and must resist high concentrations of ROS to survive. By further progression of *E. amylovora* inside host-plant tissues, the bacteria will go on evoking an oxidative burst in the surrounding plant cells, which will lead to the further devastation of the host plant. The infected host plants will turn black due to a massive apoptotic death.
Evidence for the presence of massive defence mechanisms of the bacteria against ROS was found in our experiments, where numerous proteins involved in oxidative stress processes, showed up. This indicates the high priority of the oxidative stress defence during the infection process of *E. amylovora.* These protection mechanisms could be divided into three major groups: 1) prevention of ROS generation and ROS induced damage; 2) detoxification of ROS and quenching of chain propagation; 3) repair of damaged components. This study reveals a part of the mystery, how *E. amylovora* succeeds in deluding the plant defence mechanisms.

In a second proteomic study (chapter 4) we attempted to confirm the findings of the study presented in chapter 3, where only one *E. amylovora* strain was studied. To achieve this we did a DIGE experiment, comparing the proteome of *E. amylovora* grown *in vitro* and *in planta*. For this study four different wild type *E. amylovora* strains were involved. We wanted also to give an overview of the other factors differing *in vitro* versus *in planta* beside the factors involved in oxidative stress defence.

This experiment also showed the importance of oxidative defence mechanisms during infection in all studied *E. amylovora* strains. This is a confirmation of the results in chapter 3. These proteins were induced in *E. amylovora* during infection. *E. amylovora* first evokes an oxidative burst in the host plant. As a response on the massive released of ROS, bacteria express an arsenal of defence mechanisms against ROS.

Beside proteins related with ROS defence, other proteins involved in environmental adaptation factors of *E. amylovora* were studied. A mechanism, called quorum sensing (QS), has been evolved in bacteria to respond to population density. It involves the production and detection of intercellular signals or autoinducers (AIs) in the surrounding environment. Our study revealed that different environmental conditions (*E. amylovora* grown *in vitro* or *in planta*) affect the expression of enzymes involved in AI formation. An altered AI signal will lead to an altered bacterial response. An example of such an enzyme involved in AI formation, differentially expressed in *E. amylovora* grown *in vitro* versus *in planta*, is LuxS. Inactivation of *luxS* in *E. amylovora* impaired extracellular polysaccharide (EPS) production, tolerance for hydrogen peroxide, and reduced virulence on pear leaves, but *luxS* inactivation also impaired motility (Gao et al. 2008). These findings indicate a possible relation between LuxS function and the regulation of the flagellar system in *Erwinia amylovora*. This relation has been confirmed in our experiment. Besides a higher expression of LuxS in *E amylovora* grown *in vitro*, we found also a 17 times higher expression of flagellin (FliC) in *E. amylovora* grown *in vitro*.

However, QS is not the only factor involved in the adaptation to environmental conditions. If we look again to the relation between motility and QS, we can define other players affecting motility. In *E. amylovora,* motility is also affected by the heat-stable nucleoid-structuring protein (Hns) (Oshima et al., 2006). In our study we found Hns differentially expressed in *E. amylovora* grown *in vitro* versus *in planta.* Hns is a protein that plays a fundamental role in the bacterial nucleoid organization but functions also as a pleiotropic regulator of gene expression. Hns directly or indirectly regulates adaptation to different environmental conditions. Furthermore, studies have shown that most Hns bound DNA, have been horizontally acquired (Oshima et al., 2006). Since the Hrp pathogenicity island of *E. amylovora* is the result of horizontal gene transfer (Oh and Beer, 2005), the question whether the expression of the genes encoded by the Hrp pathogenicity island are effected by Hns can be put forward. Since most genes encoded by the Hrp pathogenicity island of *E. amylovora* are involved in the bacterial pathogenicity, one may suggest that Hns may regulate these pathogenicity factors in response to environmental conditions.

The results demonstrated the importance of environmental adaptation: proteins involved in oxidative stress defence, motility, QS and Hns-signaling were associated with this adaptation process. This experiment showed also other large differences between *E. amylovora* grown *in vitro* versus *in planta*. A large group of differentially expressed proteins are those proteins involved in protein and carbohydrate metabolism and transport. This underlines the importance of the general metabolism in the adaptation to different environmental conditions.
Sensing the environment and interacting in an appropriate way makes it possible for *E. amylovora* to infect host plants, to spread into host plant tissues and to overcome extreme conditions such as host plant defence mechanisms. This property makes from *E. amylovora* a successful pathogen.

The initial objective of chapter 4 was to find potential virulence related strain dependent differences. Using wild type *E. amylovora* strains, differing in virulence, we tried to find factors that might be involved in the degree of pathogenicity. Due to the importance of the oxidative stress defence mechanisms of *E. amylovora* during infection, our first idea was a possible relation between these defence mechanisms and the degree of virulence of the different *E. amylovora* strains. The results however didn't show any relation between oxidative stress related mechanisms and the degree of virulence of the studied strains.
Previous studies (Maes et al., 2001) revealed the relation between amylovoran production and the differences in virulence of wild-type *E. amylovora* strains. However, our study didn't come up with enzymes involved in the amylovoran production. To investigate whether "amylovoran synthesis enzymes" are associated with the virulence degree of different wild type *E. amylovora* strains, further studies are necessary.
The proteomic study of the different *E. amylovora* strains also didn't come up with suitable candidates of proteins that may be involved in the degree of pathogeniity. These results also indicate the necessity of further studies. Maybe we didn't find a suitable candidate because of the restrictions of the 2D-DIGE technique and experimental setup used. During this experiment we analyzed the bacterial proteome only at one sampling time. Studying a time course can give more nuanced results. Another option is that we probably didn't look at the right place. In our study, only proteins inside the bacteria were studied. Secreted proteins were not incorporated and maybe is one (or more) of these secreted proteins involved in the virulence degree the different *E. amylovora* strains. This could be a reasonable explanation because many known proteins involved in the

infection process are proteins that are translocated. Proteins encoded by the Hrp pathogenicity island are suitable candidates. Some of these proteins form the TTSS, a specialized protein-secretion pathway that directs the secretion of proteins through the bacterial envelope and even mediates the translocation into eukaryotic host cells. Other genes of the Hrp pathogenicity island code for proteins that are secreted through this pathway and interfere with various host-cell functions. Beside the differences in amylovoran production, maybe one of these proteins secreted by the TTSS may be involved in the degree of aggressiveness of *E. amylovora.*

Future research includes a further characterization of the bacterial proteome to acquire an entire overview of proteins involved in the infection process of *E. amylovora.* It would be useful to study proteins that become translocated and their possible interactions with host-cell functions. A first step in this direction is already made by Nissinen et al. (2007). They studied *in vitro* the secretome of *E. amylovora.* In a following step, it would be interesting to compare the secretome of wild type *E. amylovora* strains differing in degree of virulence. Also the development of techniques to study these secreted proteins and their interaction with host plant molecules during infection are necessary.
Another interesting approach is the study of the bacterial transcriptome this could be achieved by real time quantitative PCR or by micro array. This strategy provides interesting additional information since there is not always a straight relation between mRNA expression and the corresponding protein level. Also interesting is the study of the metabolome of *E. amylovora.* Metabolic profiling can give an instantaneous snapshot of the bacterial physiology. To integrate proteomic, transcriptomic and metabolomic information we get a more complete picture of the pathogen and the relation with its host.
A proper characterization of a pathogen and a good understanding of the infection process form also the foundation of the development of durable control methods.

Chapter 6

Samenvatting

Bacterievuur is een plantenziekte veroorzaakt door de bacterie *Erwinia amylovora*. De meeste planten, behorende tot de *Malaceae,* zijn gevoelig voor deze ziekte. Ook enkele plantensoorten in andere families van de *Rosales* worden getroffen door bacterievuur. Vanuit economisch standpunt zijn appel- en perenbomen de belangrijkste waardplanten maar ook tal van houtachtige ornamentele planten worden aangetast. Enkele bekende voorbeelden zijn: meidoorn, vuurdoorn, kweepeer, lijsterbes en cotoneaster. De bacterie kan de plant binnendringen via de bloesems of verwondingen. Vervolgens kan *E. amylovora* zich verspreiden via de intercellulaire ruimtes en de vaatbundels van de waardplant waarbij het een spoor van vernieling achterlaat. Bloemen, scheuten en takken sterven af en in zeer ernstige gevallen sterven zelfs gehele planten af (Vanneste and Eden-Green, 2000). Bacterievuur is een zeer ernstige ziekte: enerzijds omwille van zijn destructieve karakter, anderzijds door het gebrek aan effectieve bestrijdingsmiddelen.

Het belangrijkste doel van dit werk is een beter inzicht krijgen in het infectieproces van *E. amylovora*. In hoofdstuk 2 bestuderen we de bacteriele verspreiding bij bloeseminfecties. Hierbij wordt gebruik gemaakt van verschillende microscopische benaderingen. In hoofdstuk 3 en 4 worden proteïnen geanalyseerd die een rol spelen tijdens het infectieproces. Er wordt ook gezocht naar factoren die een invloed kunnen hebben op de virulentiegraad van verschillende wild type *E. amylovora* stammen.

Microscopische studie van bloeseminfecties

De primaire infectie in de lente vindt meestal plaats ter hoogte van de bloemen. Van hieruit verspreidt de ziekte zich naar de scheuten en takken van de waardplant. Omdat bloesems zo een belangrijke rol spelen bij de primaire infectie, hebben we gekozen om de bacteriële verspreiding ter hoogte van de bloemen te bestuderen nadat bepaalde bloemdelen werden geïnoculeerd met de bacterie. We bestudeerden bloeseminfecties van Baeburn, *Crataegus* en Conference. Met deze studie trachten we de bestaande kennis omtrent bloeseminfecties te staven en te verfijnen. Dit trachtten we te bereiken door de combinatie van confocaalmicroscopische, lichtmicroscopische en transmissie electronenmicroscopische (TEM) technieken.
Na inoculatie ter hoogte van de helmknoppen, vertonen de meeste bloemen geen ziektesymptomen. *E. amylovora* kan wel de helmhokken binnendringen en de pollen contamineren. Ter hoogte van de helmhokken

dringen de bacteriën het plantenweefsel echter niet binnen. In de boomgaard kunnen gecontamineerde pollen zich verspreiden naar andere bloemen en vormen zo een nieuwe bron van infectie. Gecontamineerde pollen die terecht komen ter hoogte van de calyx cup, kunnen verklaren waarom toch enkele bloemen een infectie vertonen na inoculatie ter hoogte van de helmknoppen. De resultaten laten ook zien hoe *E. amylovora* via de smalle groeven langs de buitenzijde van de helmdraad zich kunnen verspreiden richting bloembodem. Ook na inoculatie ter hoogte van de stempel, blijven de bacteriën hoofdzakelijk beperkt tot deze zone. De microscopische resultaten bevestigen het belang van de stempel als ideale omgeving voor epifytische *E. amylovora* populaties. We zien ook hoe *E. amylovora* binnen dringt in het bovenste gedeelte van de stijl. Het onderste gedeelte van de stijl blijft steeds vrij van symptomen. Onder vochtige omstandigheden kunnen bacteriën in de bloembodem spoelen, waar de infectie kan plaatsvinden (Bubán et al., 2003). Eens aanwezig in de calyx cup, zullen de bacteriën onder gunstige omstandigheden via de nectarklieren het plantenweefsel binnendringen (Vanneste en Eden-Geen, 2000). Dit bevestigt ook onze TEM studie van *Crataegus*-bloemen, na inoculatie ter hoogte van de calyx cup. We vinden de bacteriën terug in de openingen van de nectarklieren. Van hieruit verspreidt *E. amylovora* zich binnen de gehele bloembodem. Beelden opgenomen door TEM illustreren de aanwezigheid van de bacteriën in de intercellulaire ruimtes en tonen ook het beschadigde plantenweefsel in de nabijheid van de bacteriën. Confocale waarnemingen illustreren de aanwezigheid van *E. amylovora* ter hoogte van de aanzet van het bloemsteeltje aan de bloembodem, dit reeds één dag na inoculatie ter hoogte van de calyx cup. In dit stadium zijn nog geen zichtbare symptomen aanwezig. De symptomen doen zich voor wanneer massale GFP fluorescentie, afkomstig van *E. amylovora*, aanwezig is. Dit doet zich voor twee dagen na inocultatie ter hoogte van de bovenstel cellulaire lagen van de bloembodem. Na drie dagen is er massaal veel GFP aanwezig ter hoogte van de gehele bloembodem en het steeltje. Rond dit tijdstip verschijnen ook de eerste ooze druppels.

Proteoomanalyse van *E. amylovora*

De tweede sectie van dit werk concentreert zich rond het proteoom van *E. amylovora* en welke proteïnen betrokken zijn in het infectieproces. Voor deze studie maken we gebruik van scheuten van de gevoelige M9 onderstam.

In een eerste proteoomstudie , voorgesteld in hoofdstuk 3, worden proteïnen bestudeerd die betrokken zijn in het infectieproces. Onze focus ligt hier vooral op proteïnen die betrokken zijn in de bescherming tegen oxidatieve stress. Voor deze studie wordt het proteïneprofiel van *E. amylovora* opgegroeid *in vitro* vergeleken met het proteïneprofiel van *E. amylovora* in zijn natuurlijke omgeving, tijdens infectie van een M9 onderstam. Dit proteïneprofiel wordt opgesteld door middel van tweedimensionale gelelectroforese (2D-GE), een techniek waarbij we een overzicht krijgen van de geëxpresseerde proteïnen. De studie resulteert in 96 geïdentificeerde proteïnen die verschillend tot expressie komen. Een belangrijk aandeel van deze proteïnen is betrokken in oxidatieve stress gerelateerde processen. Wij focussen ons dan ook op deze groep omwille van hun belang in het adaptatieproces van de bacteriën aan oxidatieve stress. In gevoelige waardplanten induceert *E. amylovora* en hypersensitieve respons en een massale vrijstelling van reactieve zuurstofvormen (ROS). Dit is het resultaat van een gecombineerde actie van twee Hrp effectoren , HrpN en DspA (venise et al., 2003). Deze proteïnen worden door middel van het type III secretiesysteem (TTSS) geïnjecteerd in de cellen van de waardplant, waar ze interfereren met de signaaltransductie van de plant. HrpN en DspA zijn betrokken in de massale vrijstelling van ROS door de waardplant, een reactie die ook wel oxidatieve burst genoemd wordt en gekend is om planten te beschermen tegen pathogene invasies. Ondanks deze oxidatieve burst is *E. amylovora* in staat om te overleven en de waardplant te vernietigen. Virulente *E. amylovora* stammen moeten een strategie ontwikkeld hebben om te overleven bij hoge ROS concentraties. Bij de verdere verspreiding van de bacterie in het plantenweefsel, zal *E. amylovora* in de omliggende plantencellen een oxidative burst veroorzaken. Dit zal leiden tot de verdere vernietiging van de waardplant. Geïnfecteerde plantendelen zullen zwart worden omwille van massale appoptotische celdood.
Onze experimenten tonen dan ook de aanwezigheid van defensiemechanismen tegen ROS. Tal van proteïnen betrokken in de defensie tegen ROS worden terug gevonden. Deze studie heeft een stukje van de puzzel kunnen oplossen hoe *E. amylovora* erin slaagt om de defensiemechanismen van de plant te omzeilen.

In een tweede proteoomstudie (hoofdstuk 4) trachten we de bevindingen van de voorgaande proteoomstudie (hoofdstuk 3) te bevestigen. Voor dit onderzoek is er een DIGE experiment uitgevoerd waarbij ook nu weer het *in vitro* en *in planta* proteoom van *E. amylovora* werd vergeleken maar dit keer voor 4 verschillende *E. amylovora* stammen. Naast factoren betrok-

ken in ROS defensie wordt er gedurende deze studie ook gekeken naar proteïnen betrokken in het infectieproces.

Net als voorgaande studie toont ook dit experiment het belang aan van de verdediging tegen oxidatieve stress. Hiernaast worden ook andere factoren bestudeerd die een rol spelen in de aanpassing van *E. amylovora* aan zijn omgeving. Bacteriën hebben een mechanisme ontwikkeld waarbij ze kunnen reageren op de populatiedensiteit. Dit proces wordt ook wel quorum sensing (QS) genoemd. QS is gebaseerd op de bacteriële productie en detectie van intercellulaire signalen of autoinducers (AIs). Onze studie toont aan dat verschillende groeicondities (*E. amylovora in vitro* versus *in planta*) de expressie beïnvloeden van enzymen, betrokken in de AI formatie. Een ander AI signaal zal leiden tot een andere bacteriële respons. Een voorbeeld van zo'n enzym betrokken in AI formatie is LuxS. Inactivatie van LuxS leidt bij *E. amylovora* onder andere tot een verminderde motiliteit (Gao et al., 2008). Deze bevinding duidt op een mogelijke relatie tussen de functie van LuxS en de regulatie van het flagellair systeem in *E. amylovora*. Deze mogelijke relatie wordt ook terug gevonden in ons experiment. Bij *in vitro* gekweekte bacteriën ten opzichte van *E. amylovora in planta,* vinden we een hogere expressie van LuxS, maar ook een hogere expressie van het flagelline (FliC), een proteïne betrokken in de flagelformatie.

QS is echter niet de enige factor die betrokken is in de aanpassing van bacteriën aan verschillende omstandigheden. Het "heat-stable nucloid-structuring protein" (Hns) zal naast QS ook een rol spelen in de motiliteit van *E. amylovora* (Oshima et al., 2006). In onze studie vinden we Hns differentieel geëxpresseerd bij bacteriën *in vitro* versus *in planta*. Hns speelt ook een belangrijke rol in de organisatie van het bacteriële nucleoïd. Hiernaast zal Hns ook direct of indirect de adaptatie aan verschillende omgevingsomstandigheden reguleren. Studies hebben aangetoond dat Hns bindt ter hoogte van DNA dat verkregen is door horizontale gentransfer (Oshima et al., 2006). Aangezien het Hrp pathogenisiteits eiland van *E. amylovora* het resultaat is van horizontale gentransfer (Oh en Beer, 2005), rijst de vraag in welke mate Hns deze pathogenisiteitsfactoren zal beïnvloeden in respons op verschillende omgevingscondities.

De resultaten demonstreren het belang van bacteriële adaptatie aan zijn omgeving. Proteïnen betrokken in ROS defensie, motiliteit, QS en Hns-signalisatie zijn allemaal betrokken met dit adaptatieproces. Dit experiment toont ook grote verschillen tussen bacteriën *in vitro* en *in planta* op het gebied van het algemeen metabolisme. Deze bevinding onderstreept het belang van het algemeen metabolisme in dit adaptatieproces.

De omgeving correct aanvoelen en op een gepaste manier reageren is een zeer belangrijke strategie van *E. amylovora.* Op deze manier kan *E. amylovora* waardplanten infecteren, zich verspreiden binnenin de plant en defensiemechanismen van de plant omzeilen. Deze eigenschappen maken van *E. amylovora* een succesvol pathogeen.

De initiële opzet van hoofdstuk 4 is het vinden van proteïnen die mogelijk een rol spelen in de virulentiegraad van verschillende *E. amylovora* stammen. Om deze reden worden vier *E. amylovora* stammen bestudeerd met een verschillende virulentiegraad. Omwille van het belang van ROS defensiemechanismen, is ons idee dat er een mogelijke relatie was tussen deze ROS defensiemechanismen en de stamafhankelijke virulentie. De resultaten tonen echter geen relatie in deze richting.
Voorgaande studies (Maes et al., 2001) tonen een relatie aan tussen amylovoran productie en de virulentiegraad van verschillende wild type *E. amylovora* stammen. Onze studie kan echter geen relatie leggen tussen de virulentiegraad en proteïnen betrokken in de productie van amylovoran.
De proteoomstudie van de verschillende *E. amylovora* stammen levert geen geschikte kandidaat-proteïnen op, die mogelijk betrokken zijn in de virulentiegraad. Hierdoor dringen verdere studies zich op. Misschien vinden we geen geschikte kandidaten omwille van de beperkingen van de gebruikte technieken en de gevolgde experimentele procedure. Voor dit experiment analyseren we het bacteriële proteoom op slechts één tijdstip. Een studie in functie van de tijd zal ons in ieder geval een meer genuanceerd beeld geven van het infectieproces. Een andere mogelijkheid kan ook zijn dat we niet op de juiste plaats kijken. Wij kijken in onze studie enkel naar proteïnen binnenin de bacteriële cel. Gesecreteerde proteïnen worden door deze studie niet in beschouwing genomen en misschien is net één of meerdere van deze gesecreteerde proteïnen betrokken in de virulentiegraad van verschillende *E. amylovora* stammen.

Toekomstig onderzoek moet zich toespitsen op het verder karakteriseren van het bacteriële proteoom om een volledig overzicht te krijgen van het infectieproces van *E. amylovora.* Ook de gesecreteerde proteïnen en hun mogelijke interacties met de cellen van de waardplant moeten bestudeerd worden.
De studie van het infectieproces moet zich ook niet alleen beperken tot proteoom. Door informatie van proteoom, het metaboloom en het transcriptoom te integreren krijgt men een vollediger beeld van het pathogeen en zijn relatie met de waardplant.

Een goede karakterisatie van een pathogeen en een goed begrip van het infectieproces vormen ook de basis voor de ontwikkeling van duurzame bestrijdingsmiddelen.

References

Abramovitsch R.B., Anderson J.C. and Martin G.B. (2006) Bacterial elicitation and evasion of plant innate immunity. Nutere Rev. Mol. Cell Biol. 7:601:611.

Ackerley D.F., Gonzalez C.F., Park C.H., Blake II R., Keyhan M. and Matin A. (2004) Chromate-reducing properties of soluble flavoproteins from *Pseudomonas putida* and *Escherichia coli.* Appl. Environ. Microbiol. 70:873-882.

Afflerbach H., Schroder O. and Wagner R. (1999) Conformational changes of the upstream DNA mediated by H-NS and FIS regulate E. coli RnB P1 promotor activity. J. Mol. Biol. 286:339-353.

Agrios G.N. (2005) How plants defend themselves against pathogens. In: Plant Pathology. Elsevier Academic Press, pp 207-248.

Aldridge P., Metzger M. and Geider K. (1997) Genetics of sorbitol metabolism in *Erwinia amylovora* and its influence on bacterial virulence. Mol. Gen. Genet. 256:611-619.

Aldwinckle H.S. and Beer S.V. (1979) Fire blight and its control. Hortic. Rev. 1:423-474.

Aldwinckle H.S., Bhaskara Reddy M.V. and Norelli J.L. (2002) Evaluation of control of fire blight infection of apple blossoms and shoots with SAR inducers, biological agents, a growth regulator, copper compounds, and other materials. Acta Hortic 590:325–331.

Alfano J.R. and Collmer A. (1997) The type III (Hrp) secretion pathway of plant pathogenic bacteria: trafficking harpins, Avr proteins, and death. J. Bacteriol. 179:5655-5662.

Alfano J.R. and Collmer A. (2004) Type III secretion system effector proteins: double agents in bacterial desease and plant defence. Annu. Rev. Phytol. 42:385-414.

Atichartpongkul S., Loprasert S., Vattanaviboon P., Whangsuk W., Helmann J.D. and Mongkolsuk S. (2001) Bacterial Ohr and OsmC paralogues define two protein families with distinct functions and patterns of expression. Microbiology-SGM 147:1775-1782.

Barnard A.M.L. and Salmond G.P.C. (2007) Quorum sensing in *Erwinia* species. Anal. Bioanal. Chem. 387: 415–423.

Bellemann P., Bereswill S., Berger S. and Geider K. (1994) Visualisation of capsule formation by *Erwinia amylovora* and assays to determine amylovoran synthesis. International Journal of Biological Macromolecules 16:290-296.

Bellemann P. and Geider K. (1992) Localization of transposon insertions in pathogenicity mutants of *Erwinia amylovora* and their biochemical characterization. J. Gen. Microbiol. 138:931-940.

Bennett R.A. and Billing E. (1978) Capsulation and virulence in *Erwinia amylovora*. Annals of Applied Biology 89:41-45.

Bernstein C., Bernstein H., Payne C.M., Beard S.E. and Scheider J. (1999) Bile salt activation of stress response promotors in *Escherichia coli.* Current Microbiology 39:68-72.

Billing E., Baker L.A.E., Crosse J.E and Garret C.M.E. (1961) Characteristics of Englisch isolates of *Erwinia amylovora* (Burril) Winslow et al. Journal of Applied Bacteriology 24,195-211.

Blehert D.S., Fox B.G. and Chambliss G.H. (1999) Cloning and sequence analysis of two *Pseudomonas* flavoprotein xenobiotic reductases. J. Bacteriol. 181:6254-6263.

Bogdanove A.J., Beer S.V., Bonas U., Boucher C.A., Collmer A., Coplin D.L., Cornelis G.R., Huang H.C., Hutcheson S.W., Panopoulos N.J. and Van Gijsegem F. (1996) Unified nomenclature for broadly conserved *hrp* genes of phytopathogenic bacteria. Mol. Microbiol. 20:681-683.

Bogdanove A.J., Bauer D.W. and Beer S.V. (1998) *Erwinia amylovora* secretes DspE, apathogenicity factor and functional AvrE homolog, through the Hrp (type III secretion) pathway. J. Bacteriol 180:2244-2247.

Bogdanove A.J., Kim J.F., Wei Z., Kolchnsky P., Charkowski O.A., Conlin A.K., Collmer A. and Beer S.V. (1998) Homology and functional similarity of an hrp-linked pathogenicity locus, *dspEF*, of *Erwinia amylovora* and the avirulence locus avrE of *Pseudomonas syringae* pathovar *tomato*. Proc. Natl. Acad. Sci. USA 95:1325-1330.

Bogs J., Bruchmüller I., Erbar C. and Geider K. (1998). Colonization of the host plants by the fire blight pathogen *Erwinia amylovora* marked with genes for bioluminescence and fluorescence. Phytopathology 88:416-421.

Bradburry J.F. (1986) Guide to plant pathogenic bacteria. 332 pp. CAB International, Wallingford, UK.

Braun J. and Stösser R. (1985) Structure of stigma and style and their effect on pollen germination, pollen tube growth and fruit set in apple. Angewandte Botanik 59, 53-65.

Broggini G.A.L., Duffy B., Holliger E., Scharer H.J;, Gessler C. and Patocchi A. (2005) Detection of the fire blight biocontrol agent *Bacillus subtilis* BD170 (Biopro (R) in a Swiss apple orchard. Eur J Plant Pathol 111:93–100.

Bubán T., Orosz-Kovács Zs. and Frakas Á. (2003) The nectary as the primary site of infection by *Erwinia amylovora* (Burr.) Winslow et al.: a mini review. Plant Syst. Evol. 238:183-194.

Bugert P. and Geider K. (1995) Molecular analysis of the *ams* operon required for exopolysaccharide synthesis of *Erwinia amylovora*. FEBS Lett. 400:252-256.

Burril T.J. (1883) New species of *Micrococcus*. Am.Naturalist.

Cabiscol E., Tamarit J. and Ros J. (2000) Oxidative stress in bacteria and rotein damage by reactive oxygen species. Internatl. Microbiol. 3:3-8.

Caldas T.D., El Yaagoubi A. and Richarme G. (1998) Chaperone properties of bacterial elongation factor EF-Tu. J. Biol. Chem. 273:11478-11482.

Carmel-Harel O. and Storz G. (2000) Roles of the glutathione- and thioredoxin-dependent reduction systems in the *Escherichia Coli* and *Saccharomyces Cervisiae* responses to oxidative stress. Annu. Rev. Microbiol. 54:439-61.

Cesbron S., Paulin J.-P., Tharaud m., Barny M.-A. and Brisset M.-N. (2006) The alternative σ factor HrpL negatively modulates the flagellar system in the phytopathogenic bacterium *Erwinia amylovora* under *hrp*-inducing conditions. FEMS Microbiol. Lett. 257:221-227.

Chen X., Schauder S., Potier N., Van Dorssealaer A, Pelczer I., Bassler B.L. and Hughson F.M. (2002) Structural identification of a bacterial quorum-sensing signal containing boron. Nature 415:545-549.

Collmer A., Lindeberg M., Petnicki-Ocwieja T., Schneider D.J. and Alfano J.R. (2002) Genomic mining type III secretion system effectors in *pseudomonas syringae* yields new picks for all TTSS prospectors. Trends Microbiol. 10,462-469.

Cornelis G.R. and Van Gijsegem F. (2000) Assembly and function of type III secretory systems. Annu. Rev. Microbiol. 54:735-774.

Covey R.P., fischer W.R. (1990) Timely cutting of fire blight infections reduces losses. Acta Horticulturae 273,351-353.

Cox M.M. (2007) Regulation of Bacterial RecA Protein Function. Crit. Rev. Biochem. Mol. 42:41-63.

Cruz A.T., Cazacu A.C. and Allen C.H. (2007) *Pantoea agglomerans*, a plant pathogen causing human disease. J. Clin. Microbiol. 45:1989-1992.

Dangl J.L. and Jones J.D.G. (2001) Plant pathogens and integrated defence responses to infection. Nature 411:826-833.

Deckers T. (1996) Fire Blight: the present state of its occurrence in Belgium and phytosanitary measures to control the problem. Parasitica 52(3):127-131.

De Gara L., de Pinto M.C. and Tommasi F. (2003) The antioxidant systems vis-à-vis reactive oxygen species during plant-pathogen interaction. Plant physiology and biochemistry 41:863-870.

Dellagi A., Brisset M.N., Paulin J.P. and Expert D. (1998) Dual role od desferrioxamine in *Erwinia amylovora* pathogenicity. Mol. Plant Microbe Interact. 11:734-742.

Denny T.P. (1995) Involvement of bacterial polysaccharides in plant pathogenesis. Annu. Rev. Phytopathol. 33:173-197.

Dong H., Delaney T.P., Bauer D.W. and Beer S.V. (1999) Harpin induces disease resistance in Arabidopsis through the systemic acquired resistance pathway mediated by salicylic acid and the *NIM1* gene. Plant J. 20:207-215.

Dong H.P., Peng J., Bao Z., Meng X., Bonasera J.M., Chen G., Beer S.V. and Dong H. (2004) Downstream divergence of the ethylene signalling pathway for harpin-stimulated Arabidopsis growth and insect defence. Plant Physiol. 136:3628-3638.

Dorman C.J. (2004) H-Ns: a universal regulator for a dynamic genome. Nat. Rev. Microbiol. 2:391-400.

Dunn K.L.R., Farrant J.L., Langford P.R. and Kroll J.S. (2003) Bacterial [Cu,Zn]-Cofactored Superoxide Dismutase Protects Opsonized, Encapsulated *Neisseria meningitidis* from Phagocytosis by Human Monocytes/Macrophages. American Society for Microbiology 71:1604-1607.

Durner j., Shah J. and Klessig D.F. (1997) Salicylic acid and disease in plants. Trends Plant Sci. 2:266-274.

Evans J.R., Evans R.R., Regusi C.L. and Rademacher W. (1999) Mode of action, metabolism, and uptake of BAS 125W, prohexadione-calcium. HortScience 34:1200-1201.

Expert D., Dellagi A. and Kachadourian R. (2000) Iron and fire blight: role in pathogenicity of desferrioxamine E, the main siderophore of *Erwinia amylovora*. . In Fire Blight. The disease and its causative agent, *Erwinia amylovora*. Vanneste J.L. (ed), CABI Publishing, Oxon, pp 179-195.

Felix G. and Boller T. (2003) Molecular sensing of bacteria in plants. The highly conserved RNA-binding motif RNP-1 of bacterial cold shock proteins is recognized as an elicitor signal in tobacco. J. Biol. Chem. 278:6201-6208.

Forner J. and Binder S. (2007) The red fluorescent protein eqFP611: application in subcellular localization studies in higher plants. BCM Plant Biology 7:28-39.

Frank A.A.W., Leeper F.J. and Luisi B.F. (2007) Structure, mechanism and catalytic duality of thiamine-dependent enzymes. Cell. Mol. Life Sci. 64:892-905.

Galán J. E. and Collmer A. (1999) Type III secretion machines: bacterial devices for protein delivery into host cells. Science 284:1322-1328.

Gao Y., Song J., Hu B., Zhang L., Liu Q. and Liu F. (2008) The *luxS* Gene Is Involved in AI-2 Production, Pathogenicity, and Some Phenotypes in *Erwinia amylovora*. Curr. Microbiol. 7:473-483.

Gaudriault S., Malandrin L., Paulin J.P. and Barny M.A. (1997) DspA, an essential pathogenicity factor of *Erwinia amylovora* showing homology with AvrE of *Pseudomonas syringae*, is secrerted via Hrp secretion pathway in a DspB dependent way. Mol Microbiol 26:1057-1069.

Gaudriault S., Paulin J.P. and Barny M.A. (2002) The DspB/F protein of *Erwinia amylovora* is a type III secretion chaperone ensuring efficient intrabacterial production of the Hrp-secreted DspA/E pathogenicity factor. Mol Plant. Pathol. 3:313-320.

Geider K. (2000) Exopolyseccharides of *Erwinia amylovora*: Structure, biosynthesis, regulation, role in pathogenicity of amylovoran and levan. In Fire Blight. The disease and its causative agent, *Erwinia amylovora*. Vanneste J.L. (ed), CABI Publishing, Oxon, pp 117-140.

Geider K., Baldes R., Bellemann P., Metzger M. and Schwartz T. (1995) Mutual adaptation of bacteriophage fd, pfd plasmids and their host strains. Microbiological Research 15:337-346.

Geier G. and Geider K. (1993) Characterization and influence on virulence of the levansucrase gene from fireblight pathogen *Erwinia amylovora.* Physiol. Mol. Plant Pathol. 42:387-404.

Gouk S.C., Bedford R.J. and Hutchins S.O. (1996) Effect of apple flower phenology on growth of *Erwinia amylovora*. Phytopathology 86, S42.

Green J. and Paget M.S. (2004) Bacterial redox sensors. Nature reviews 2:954-966.

Greenberg J. T. and Yao N. (2004) The role and regulation of programmed cell death in plant–pathogen interactions. Cell. Microbiol. 6:201–211.

Gross M., Geier G., Rudolph K. and Geider K. (1992) Levan and levansucrase synthesized by the fire blight pathogen *Erwinia amylovora.* Physiol. Mol. Plant Pathol. 40:371-381.

Hacker J. and Kaper J.B. (2000) Pathogenicity islands and the revolution of microbes. Annu. Rev. Microbiol. 54:641-679.

Heil M. and Ton J. (2008) Long-distance signalling in plant defence. Trends in plant science 13:264-272.

Heimans E., Heinsius H.W. and Thijsse J.P. (1998) Geïllustreerde flora van Nederland België en Luxemburg en aangrenzend Duitsland en Frankrijk. J. Mennema. Uitgeverij Den Gulden Engel, Antwerpen.

Heyens K. (2004) Fire blight: study of host defense mechanisms and bacterial migration in host plant tissue. Phd thesis. Limburgs universitair centrum.

Hildebrand E.M. (1937) The blossom-blght phase of fire blight and methods of control. Cornell University Agriculture Experiment Station Memoirs 207, Ithaca, New York, 40 pp.

Hildebrand M., Aldridge P. and Geider K. (2006) Characterization of *hns* genes from *Erwinia amylovora*. Mol. Gen. Genomics 275:310-319.

Hoang T.T., Sullivan S.A., Cusickç J.K. and Schweizer H.P. (2002) *b*-Ketoacyl acyl carrier protein reductase (FabG) activity of the fatty acid biosynthetic pathway is a determining factor of 3-oxo-homoserine lactone acyl chain lengths. Microbiology 148, 3849–3856

Holub O., Seufferheld C., Gohlke C., Govindjee, Heiss G.J. and Cleg R.M. (2006) Fluorescence lifetime imaging microscopy of *Chlamydomonas reinhardtii*: non-photochemical quenching mutants and the effect of photosynthetic inhibitors on the slow chlorophyll fluorescence transient. Journal of microscopy 226:90-120.

Holt J.G., Krieg N.R., Sneath P.H.A., Staley J.T. and Williams S.T. (1994) Bergey's Manual of Determinative Bacteriology, 9th ed. Williams and Wilkins, Baltimore, Maryland, USA, 787 pp.

Ishimaru C.A., Klos E.J. and Burbaker R.R. (1988) Multiple antibiotic production by *Erwinia herbicola*. Phytopathology 78:746–750.

Johnson K.B., Stockwell V.O., McLaughlin R.J., Sugar D., Loper J.E. and Roberts R.G. (1993) Effect of antagonistic bacteria on establishment of honey bee-dispersed *Erwinia amylovora* in pear blossoms and on fire blight control. Phytopathology 83:995–1002.

Johnson K.B. and Stockwell V.O. (1998) Management of fire blight: A case study in microbial ecology. Annual Review of Phytopathology 36:227-248.

Johnson K.B. and Stockwell V.O. (2000) Biological control of fire blight. In: Fire Blight: The Disease and its Causative Agent, *Erwinia amylovora* Vanneste J.L., (ed), CABI Publishing, Oxon pp. 319–337.

Jones A.M.E., Thomas V., Truman B., Lilly K., Mansfield J. and Grant. M. (2004) Specific changes in the Arabidopsis proteome in response to bacterial challenge: differentiating basal and R-gene mediated resistance. Phytochemistry 65:1805-1816.

Jones J.D.G. and Dangl J.L. (2006) The plant immune system. Nature 444:323-329.

Jones M.B. and Blaser M.J. (2003) Detection of a luxS-signaling molecule in Bacillus anthracis. Infect. Immun. 71:3914–3919.

Kim J.F. (1997) Molecular characterization of anovel harpin and two *hrp* secretory operons of *Erwinia amylovora*, and a *hrp* operon of *E. chrysanthemi.* Ph.D. Cornell University, Ithica, NY.

Kim J.F. and Beer S.V. (1998) HrpW of *Erwinia amylovora*, a new harpin that contains a domain homologous to pectate lyases of a distinct class. J. Bacteriol. 180:5203-5210.

Kim J.F. and Beer S.V. (2000) *hrp* genes and harpins of *Erwinia amylovora*: a decade of discovery. . In Fire Blight. The disease and its causative agent, *Erwinia amylovora*. Vanneste J.L. (ed), CABI Publishing, Oxon, pp 141-161.

Kiraly Z., El-Zahaby H.M. and Klement Z. (1997) Role of extracellular polysaccharide (EPS) slime of plant pathogenic bacteria in protecting cells to reactive oxygen species. J. Phytopathology 145:59-68.

Kitagawa M., Matsumura Y. and Tsuchido T. (2000) Small heat shock proteins, IbpA and IbpB, are involved in resistances to heat and superoxide stresses in *Escherichia coli*. FEMS Microbiology Letters 184:165-171.

Kunze G., Zipfel C, Robatzek S., Niehaus K., Boller T. and Felix G. (2004) The N Terminus of Bacterial Elongation Factor Tu Elicits Innate Immunity in Arabidopsis Plants. Plant Cell 16:3496-3507.

Lamb C. and Dixon R.A. (1997) The oxidative burst in plant disease resistance. Annu. Rev. Plant Physiol. Plant Mol. Biol. 48:251-275.

Lam E., Kato N. and Lawton M. (2001) Programmed cell death, mitochondria and the plant hypersensitive response. Nature 411:848-853.

Langlotz C., Ullrich H., Geider K., Nimtz M., Huber A. and Coplin D.L. (1999) Biosynthesis and characterization of capsular exopolysaccharides from *Erwinia amylovora* and *Erwinia stewartii.* Acta Horticulturae 489:307-313.

Lesniak J., Barton W.A. and Nikolov D.B. (2008) Structural and functional features of *Escherichia coli* hydroperoxide resistance protein OsmC. Protein Science 12:2838-2843.

Leung D.W., Otomo C., Chory J. and Rosen M.K. (2008) Genetically encoded photoswitching of actin assembly through the Cdc42-WASP-Arp2/3 complex pathway. PNAS 105:12797-12802.

Leveau J.H.J. and Lindow S.E. (2001) Predictive and interpretive simulation of green fluorescent protein expression in reporter bacteria. J. Bacteriol. 183:6752-6762.

Lewis D.H., Smith D.C. (1967) Sugar alcohols (polyols in fungi and green plants. I. Distribution, physiology and metabolism. New Phytology 66:143-184.

Loescher W.H. (1987) Physiology and metabolism of sugar alcohols in higher plants. Physiology of Plantarum 70:553-557.

Lushchak V.I. (2001) Oxidative stress and mechanisms of protection against it in bacteria. Biochemistry (Moscow) 66:476-489.

Madger S. (2006) Reactive oxygen species: toxic molecules or spark of life? Crit. Care 10:208.

Maes M., Orye K., Bovev S., DevreeseB., Van Beeumen J., De Bruyn A., Busson R., Herdewijn P., Morreel K. and Messens E. (2001) Influence of amylovoran production on virulence of *Erwinia amylovora* and a different amylovoran structure in *E. amylovora* isolates from *rubus.* European journal of plant pathology 107:839-844.

Martinez A. and Kolter R. (1997) Protection of DNA during oxidative stress by the nonspecific DNA-binding protein Dps. J. Bacteriol. 179:5188-5194.

Mehta A., Brasileiro A.C.M., Souze D.S.L., Romano E., Camos M.A., Grossi-de-Sá M.F., Silva M.S., Franco O.L., Fragoso R.R., Betivori R. and Rocha T.L. (2008) Plant-pathogen interactions: what is proteomics telling us? FEBS Journal. 275:3731-3746.

Meiring H.D. van der Heeft E., ten Hove G.J. and de Jong A.P.J.M. (2002) Nanoscale LC-MS(n): technical design and applications to peptide and protein analysis. Journal of Separation Science 25:557-568.

Michel A., Agerer F., Hauck C.R., Herrmann M., Ullrich J., Hacker J. and Ohlsen K. (2006) Global regulatory impact of ClpP protease of *Staphylococcus aureus* on regulons involved in virulence, oxidative stress response, autolysis, and DNA repair. J. Bacteriol. 188: 5783–5796.

Miller H.J. (1984) *Erwinia amylovora* detection and its significance in survival studies. Acta Horticulturae 151:63-68.

Mojica F.J. and Higgins C.F. (1997) In vivo supercoiling of plasmid and chromosomal DNA in an *Escherichia coli hns* mutant. J. Bacteriol. 179:3528-3533.

Mulvey M.R., Switala J., Borys A. and Loewen P.C. (1990) Regulation of *katE* and *katF* in *Escherichia coli.* J. Bacteriol. 172:6713-6720.

Nimtz M., Mort A., Domke T., Wray V., Zhang Y., Qiu F., Coplin D. and Geider K. (1996) Structure of amylovoran, the capsular exopolysaccharide from the fire blight pathogen *Erwinia amylovora.* Carbohydrate Research 287(1):59-76.

Nissinen R.M., Ytterberg A.J., Bogdanove A.J. Van Wijk K.J. and Beer S.V. (2007) Analyses of the secretomes of *Erwinia amylovora* and selected *hrp* mutants reveal novel type III secreted proteins and an effect of HrpJ on extracellular harpin levels. Mol. Plant Pathol. 8:55-67.

Norelli J.L., Jones A.L., Aldwinckle H.S. (2003) Fire blight management in the twenty-first century. Using new technologies that enhance host resistance in apple. Plant Disease 87(7):756-765.

Nosarszewski M., Clements A.M., Downie A.B., Archbold D. (2004) Sorbitol dehydrogenase expression and activity during apple fruit set and early development. Physiology of Plantarum 121:391-398.

Oh C.S. and Beer S.V. (2005) Molecular genetics of *Erwinia amylovora* involved in the development f fire blight. FEMS Microbiol. Lett. 253:185-192.

Oh C.S., Kim J.F. and Beer S.V. (2005) The Hrp pathogenicity island of *Erwinia amylovora* and the identification of three novel genes required for systemic infection. Mol. Plant Pathol. 6:125-138.

Oshima T., Ishikawa S., Kurokawa K., Aiba H. and Ogasawara N. (2006) *Escherichia coli* histone-like protein H-NS preferentially binds to horizontally acquired DNA in association with RNA polymerase. DNA Research 13, 141–153.

Park S.W., Kaimoyo E., Kumar D., Mosher S. and Klessig D.F. (2007) Methyl salicylate is a critical mobile signal for plant systemic acquired resistance. Science 318,113-116.

Paulin J.-P. (2000). *Erwinia amylovora*: general characteristics, biochemistry and serology. In: Fire Blight. The disease and its causative agent, *Erwinia amylovora*. Vanneste J.L. (ed), CABI Publishing, Oxon, pp 87-115.

Peng J.L., Dong H.S., Dog H.P., Delaney T.P., Bonasera J.M. and Beer S.V. (2003) Harpin-elicted hypersensitive cell deaeth and pathogen resistance requires the *NDR1* and *EDS1* genes. Physiol. Mol. Plant Pathol. 62:317-326.

Pusey P.L. (1997) Crab apple blossoms as a model for research on biological control of fire blight. Phytopathology 87:1096–1102.

Rademacker W. (2000) Growth retardants: Effects on gibberellin biosynthesis and other metabolic pathways. Annu. Rev. Plant Physiol. Plant Mol. Biol. 51:501-531.

Raivio T.L. and Silhavy T.J. (2001) Periplasmic stress and ECF sigma factors. Annu. Rev. Microbiol. 55:591-624.

Reading N.C. and Sperandio V. (2006) Quorum sensing: the many languages of bacteria. FEMS Microbiol. Lett. 254:1-11.

Ros Barceló A. (1997) Lignification in plant cell walls. Int. Rev. Citol. 176:87-132.

Roshchina V.V., Melnikova E.V. and Kovaleva L.V. (1997) Changes in fluorescence during development of the male gametophyte. Russ. J. Plant Physiol. 44:36-44.

Rosen H.R. (1935) The mode of penetration of pear and apple blossoms by the fire-blight pathogen. Science 81, 26.

Rosen H.R. (1936) Mode of penetration and of progressive invasion of fire-blight bacteria into apple and pear blossoms. Arkansas Agricultural Experiment Station Bulletin 331, Fayetteville, Arkansas.

Rosen H.R. (1938) Life span and morphology of fire blight bacteria as influenced by relative humidity, temperature, and nutrition. Journal of Agricultural Research 56, 239-258.

Seaver C.L. and Imlay J.A. (2001) Alkyl hydroperoxide reductase is the primary scavenger of endogenous hydrogen peroxide in *Escherichia coli*. Journal of bacteriology. 183:7173-7181.

Seet B.T., Didic I., Zhou M.M. and Pawson T. (2006) Reading protein modifications with interaction domains. Nature Rev. Mol. Cell Biol. 7:473-483.

Seibold A., Viehrig M., Jelkmann W. (2006) Yeast as antagonists against *Erwinia amylovora*. Acta Horticult. (ISHS) 704: 367-369.

Seganov A., Polonskaia A., Tuân Phan A., Braeker R.R. and Patel D.J. (2006) structural basis for gene regulation by a thiamine pyrophosphate-sensing riboswitch. Nature 441:1167-1171.

Shevchenko A., Wilm M., Vorm O. and Mann M. (1996) Mass spectrometric sequencing of proteins from silver-stained polyacrylamide gels. Analytical Chemistry 68:850-858.

Smith T.J. (1996) A risk assessment model for fire blight of apple and pear. Acta Horticult. (ISHS) 411:97-104.

Soballe B. and Poole R.K. (2000) Ubiquinone limits oxidative stress in *Escherichia coli*. Microbiology 146:787-796.

Spinelli F., Ciampolini F., Cresti M., Geider K. and Costa G. (2005) Influence of stigmatic morphology on flower colonization by *Erwinia amylovora* and *Pantoea agglomerans*. European journal of plant pathology 113:395-405.

Stebbins C.E. and Galán J.E. (2003) Priming virulence factors for delivery into the host. Nat. Rev. Mol. Cell Biol. 4:738-743.

Steiner P.W. (1990) Predicting apple blossom infections by *Erwinia amylovora* using the MARYBLYT model. Acta Horticult. (ISHS) 273:139-148.

Steiner P.W. (2000) Integrated orchard and nursery management for the control of fire blight. In Fire Blight. The disease and its causative agent, *Erwinia amylovora*. Vanneste J.L. (ed), CABI Publishing, Oxon, pp 339-358.

Stockwell V.O., Johnson K.B. and Loper J.E. (2002) Biological control of fire blight: understanding interactions among introduced and indigenous microbial communities. In: Phyllosphere Microbiology Lindow S.E., Hecht-Poinar E.I. and Elliot V.J. (eds), APS, St Paul, Minn., pp. 225–239.

Sukchawalit R., Loprasert S., Atichartpongkul S. and Mongkolsuk S. (2001) Complex regulation of the organic hydroperoxide resistance gene (*ohr*) from *Xanthomonas* involves OhrR, a novel organic peroxide-inducible negative regulator, and posttranscriptional modifications. J. Bacteriol. 183:4405-4412.

Tang Y., Quail M.A., Artymiuk P.J., Guest J.R. and Green J. (2002) *Escherichia coli* aconitases and oxidative stress: post-transcriptional regulation of *sodA* expression. Microbiology 148:1027-1037.

Thomson S.V. (1986) The role of the stigma in fire blight infection. Phytopathology 76:476-482.

Thomson S.V., Wgner A.C. and Gouk S.C. (1999) Rapid colonization of apple flowers and the role of insects and rain. Acta Horticultrae 489:459-464.

Thomson S.V. (2000) Epidemiology of fire blight. In Fire Blight. The disease and its causative agent, *Erwinia amylovora*. Vanneste J.L. (ed), CABI Publishing, Oxon, pp 9-36.

Touati D. (2000) Iron and oxidative stress in bacteria. Archives of Biochemistry and Biophysics. 373:1-6.

Truman W., de Zabala M. T. and Grant M. (2006) Type III effectors orchestrate a complex interplay between transcriptional networks to modify basal defence responses during pathogenesis and resistance. Plant J. 46:14–33.

Van der Zwet T., Beer S.V. (1995) Fire blight – its nature, prevention and control; a practical guide to integrated disease management. U.S.Dep.Agric., Inform. Bull. #631.

Van der Zwet T., Keil H.L. (1979) Fireblight: a bacterial disease of rosaceous plants. USDA Agriculture Handbook No.510.

Vanneste J.L. and Eden-Green S. (2000) Migration of *Erwinia amylovora* in Host Plant Tissues. In: Fire Blight. The disease and its causative agent, *Erwinia amylovora*. Vanneste J.L. (ed), CABI Publishing, Oxon, pp 73-83.

Vanneste J.L., Cornish D.A., Yu J. and Voyle M.D. (2002) P10c: a new biological control agent for control of fire blight which can be sprayed or distributed using honey bees. Acta Hortic 590:231–236.

Venisse, J. S., Barny, M. A., Paulin, J. P., and Brisset, M. N. (2003) Involvement of three pathogenicity factors of Erwinia amylovora in the oxidative stress associated with compatible interaction in pear. Febs Letters 537: 198-202.

Venisse J.S., Gullner G., and Brisset M.N. (2001) Evidence for the involvement of an oxidative stress in the initiation of infection of pear by *Erwinia amylovora*. Plant Physiol. 125:2164-2172.

Vorob'eva L.I. (2004) Stressors, stress reactions, and survival of bacteria: A review. Applied biochemistry and microbiology. 40:217-224.

Vuilleumier S. (1997) Bacterial glutathione S-transferases: what are they good for? J. Bacteriol. 179:1431-1441.

Wehland M., Kiecker C., Coplin D.L., Kelm O., Saenger W. and Bernhard F. (1999) Identification of an RcsA/Rcsb recognition motif in the promoters of exopolysaccharide biosynthetic operons from *Erwinia amylovora* and *Pantoea stewartii.* J. Biol. Chem. 274:3300-3307.

Wei Z., Kim J.F. and Beer S.V. (2000) Regulation of *hrp* genes and type III protein in *Erwinia amylovora* by HrpX/HrpY, anovel two-component system, and HrpS. Mol. Plant-Microbe Interact. 13,1251-1262.

Wei Z.M. and Beer S.V. (1995) *hrpL* activates *Erwinia amylovora hrp* gene transcription and is a member of the ECF subfamily of s factors. J. Bacteriol. 177,6201-6210.

Wei Z.M., Laby R.J., Zumoff C.H., Bauer D.W., He S.Y., Collmer A. and Beer S.V. (1992) Harpin, elictor of the hypersensitive response produced by the plant pathogen *Erwinia amylovora*. Science 257:85-88.

Wilson M., Sigee D.C. and Epton H.A.S. (1989) *Erwinia amylovora* infection of hawthorn blossom. I. The anther. Journal of Phytopathology 127:1-14.

Wilson M., Epton H.A.S. and Sigee D.C. (1992) Interactions between *Erwinia herbicola* and *E. amylovora* on the stigma of hawthorn blossoms. Phytopathology 82:914–918.

Wilson M. and Lindow S.E. (1993) Interactions between the biological control agent Pseudomonas fluorescens strain A506 and *Erwinia amylovora* in pear blossoms. Phytopathology 83:117–123.

Wilson M., Sigee D.C. and Epton H.A.S. (1990) *Erwinia amylovora* infection of hawthorn blossom. III. The nectary. Journal of Phytopathology 128:62-74.

Wilson M., Epton H.A.S. and Sigee D.C. (1989) *Erwinia amylovora* infection of hawthorn blossom. II. The stigma. Journal of Phytopathology 127:15-28.

Withers H., Swift S. and Williams P. (2001) Quorum sensing as an integral component of gene regulatory networks in Gram-negative bacteria. Curr. Opin. Microbiol. 4:186–193.

Yoder K.S., Miller S.S. and Byers R.E. (1999) Suppression of fire blight in apple shoots by prohexadione-calcium following experimental and natural inoculation. HortScience 34:1202-1204.

Zhang Y. and Geider K. (1999) Molecular analysis of the *rlsA* gene regulating levan production by the fireblight pathogen *Erwinia amylovora*. Physiol. Mol. Plant Pathol. 54:187-201.

Zhao Y., Blumer S.E. and Sundin G.W. (2005) Identification of *Erwinia amylovora* genes induced during infection of immature pear tissue. J. Becteriol. 187:8088-8103.

Zheng M., Wang X., Templeton L.J., Smulski D.R, La Rossa R.A. and Storz G. (2001) DNA microarray-mediated transcriptional profiling of the *Escherichia coli* response to hydrogen peroxide. Journal of bacteriology. 183:4562-4570.

Zipfel C. and Felix G. (2005) Plants and animals: a different taste for microbes? Curr. Opin. Plant Biol. 8:353-360.

Dankwoord

Nu we aan de laatste pagina's aanbeland zijn wordt het tijd om een aantal mensen te bedanken. Dit werk is niet enkel mijn verdienste en ik heb dit ook nooit kunnen verwezenlijken zonder de hulp en inspiratie van heel wat personen.

Eerst en vooral wil ik mijn promotor bedanken. Roland, bedankt dat je mij alle vrijheid hebt gegeven om mijn onderzoek te voeren. Maar ook dat ik steeds bij je kon aankloppen voor tips en suggesties.

De jury wil ik bedanken voor hun kritische evaluatie. Dankzij hun opmerkingen en raadgevingen is mijn werk er alleen maar beter van geworden.

Voor het praktische werk zijn er heel wat mensen die ik speciaal zou willen danken. Greet, dank je wel voor al je hulp in het labo, je goede ideeën, de toffe babbels en je luisterend oor. Jan, bedankt voor al je goede zorgen voor de planten. Natascha voor het prepareren van de elektronenmicroscopische coupes. Erik en Jean-Paul voor de hulp bij de massaspectrometrische analysen.

Dan zijn we aanbeland bij de rest van de collega's. Anne, Kristof, Sofie en Lieve, bedankt voor de toffe sfeer en de interessante discussies (al dan niet over het werk). Merci voor deze leuke tijden. Anne, Kristof en Sofie; jullie wil ik nog veel succes wensen met het geëxperimenteer en het schrijfwerk. Kristin, Kelly en Tony; het was me aangenaam met jullie de bureau te delen. Verder wil ik ook iedereen van milieu- en dierkunde bedanken voor alle leuke momenten.

Sandy, jij mag zeker niet ontbreken in dit dankwoordje. Samen in Diepenbeek, daarna samen naar Gent en dan weer terug samen in Diepenbeek. De vele uren die we al samen hebben doorgebracht, de vele momenten op de agora, de discussies over de leerstof, je raadgevingen en goede tips (zeker de laatste maanden), het vele gezaag en gezever, de pruttelmomentjes,... Voor al deze dingen een dank je wel.

Aan de collega's van school wil ik een woordje van dank richten voor de fijne werksfeer. De studenten mag ik dan natuurlijk ook niet vergeten. Jullie zijn een toffe bende om les aan te geven. Dank jullie wel daarvoor.

Elke, mijn kleine zus. Voor al die dwaze discussies die zussen horen te voeren over vanalles en nog wat. Gewoon om mijn zus te zijn. Dank je wel. Nu ook jij je eerste stappen gezet hebt aan de unief wil ik je heel veel succes en doorzettingsvermogen toewensen met je verdere studies.

Oma, dank je wel voor je steun en je interesse in mijn studies gedurende al die jaren. Tante Sylvia ook jou wil ik bedanken voor de leuke momenten, de babbels, de wandelingen,...

Gust, Marie-Jeanne en Ruben. Bedankt om mee steeds een welkom gevoel te geven en voor de vele gezellige etentjes. Merci.

Mama en papa. Jullie wil ik vandaag speciaal bedanken. Gewoon voor alles. Omdat jullie steeds in mij geloven en mij steunen in alles wat ik doe. Mama, papa, dank jullie wel! Mama, jou wil ik ook bedanken voor de mooie tekeningen in dit boekje.

Manu, tot slot wil ik ook jou bedanken. Dank je voor alle momenten samen, dat ik bij jou gewoon mezelf kan zijn. Het is gewoon heerlijk om te weten dat jij er steeds voor mij bent.
Zeker voor de laatste maanden wil ik je speciaal bedanken. Dank je dat steeds voor me klaar stond, om mijn persoonlijke helpdesk te zijn, om me te steunen tijdens die moeilijke momenten...
Voor alles, dank je wel!

Addendum I

Table 4.1:
Identification results of the selected spots, those differ in expression in *E. amylovora* grown *in vitro* versus *in planta*. Spot numbers are indicated in figure 4.1.
Average fold change of spot expression, either upregulated (+) or downregulated (-) in *E. amylovora* grown *in planta*, compared with *E. amylovora* grown *in vitro*. The left part of the table shows the proteins, differentially more expressed *in vitro* versus *in planta*. The right part of the table shows the proteins, differentially more expressed *in planta* versus *in vitro*. The numbering in the first column refers to the functional annotation of proteins.

A: Aminoacid transport and metabolism
B: Carbohydrate transport and metabolism
C: Oxidative stress related proteins
D: Energy production and conversion
E: Nucleotide transport and metabolism
F: Translation, ribosomal structure and biogenesis
G: Coenzyme metabolism
H: Lipid metabolism
I: Cell enveloppe biogenesis, outer membrane
J: Inorganic ion transport and metabolism
K: Signal transduction mechanisms
L: Cell division and chromosome partitioning
M: Cell motility and secretion
N: Others
O: Unknown function

	in vitro > in planta			in planta > in vitro		
	Spot ID	Fold change	Protein name	Spot ID	Fold change	Protein name
A	15	-4.27	Serine hydroxymethyltransferase (GlyA)	81	2.82	1-(5-phosphoribosyl)-5-[(5-phosphoribosylamino)methylideneamino]imidazole-4-carboxamide isomerase (HisA)
	59	-3.7	2,3,4,5-tetrahydropyridine-2-carboxylate N-succinyltransferase (DabD)	6	2.21	periplasmic dipeptide transport protein (DppA)
	25	-2.93	Acetylornithine aminotransferase (ArgD)	63	2.1	N-succinyl-diaminopimelate deacylase (DabE)
	22	-2.87	Phosphoserine aminotransferase (SerC)	54	1.9	N-acetyl-gamma-glutamyl-phosphate reductase (ArgC)
	60	-2.68	5,10 methylenetetrahydrofolate reductase (MetF)	54	1.9	Glycine betaine-binding periplasmic protein (ProX)
	30	-2.53	branched-chain amino acid-binding protein (LivK)	78	1.87	Glutamine high-affinity transporter (GlnH)
	72	-2.3	High-affinity branched-chain amino acid transport ATP-binding protein (LivG)	42	1.79	3-dehydroquinate synthase (AroB)
	93	-2.17	Gamma-glutamyltranspeptidase (Ggt)	23	1.67	Peptidase M20
	67	-2.14	pyrroline-5-carboxylate reductase (ProC)	82	1.52	Glutamine high-affinity transporter (GlnH)
	32	-1.99	N-succinyl-diaminopimelate deacylase (DabE)	5	1.22	Acetolactate synthase, catabolic (BudB)
	38	-1.77	Cystathionine gamma-synthase (MetB)			
	39	-1.62	Aspartate-semialdehyde dehydrogenase (Asd)			
	58	-1.54	Agmatinase (Agmatine ureohydrolase) (SpeB)			
	84	-1.37	Arginine-binding periplasmic protein 1 (ArtI)			
	1	-1.36	Peptidyl-dipeptidase (Dcp)			
B	76	-4.22	Glyceraldehyde 3-phosphate dehydrogenase A (GapA)	49	7.33	Glyceraldehyde 3-phosphate dehydrogenase A (GapA)
	71	-3.62	2,3-bisphosphoglycerate-dependent phosphoglycerate mutase(GpmA)	45	6.69	Transaldolase A (TalA)
	3	-3.15	transketolase (TktA)	85	3.34	Ribulose-phosphate 3-epimerase (Pentose-5-phosphate 3-epimerase) (Rpe)
	36	-2.14	Phosphoglycerate kinase (Pgk)	46	2.49	Phosphoglycerate kinase (Pgk)
	48	-2.1	Transaldolase B (TalB)	42	1.79	6-phosphofructokinase isozyme I (PfkA)

	in vitro > in planta			in planta > in vitro		
	Spot ID	Fold change	Protein name	Spot ID	Fold change	Protein name
B	12	-2.01	Gluconate-6-phosphate dehydrogenase (Gnd)	18	1.71	Enolase (2-phospho-D-glycerate hydrolyase) (Eno)
	68	-1.96	Glyceraldehyde 3-phosphate dehydrogenase A (GapA)	103	1.39	Triosephosphate isomerase (TpiA)
	50	-1.71	Glyceraldehyde 3-phosphate dehydrogenase A (GapA)	19	1.33	Enolase (2-phospho-D-glycerate hydrolyase) (Eno)
	75	-1.68	Triose-phosphate isomerase (TpiA)	47	1.33	Glyceraldehyde 3-phosphate dehydrogenase A (GapA)
	90	-1.22	Phosphoheptose isomerase (Sedoheptulose 7-phosphate isomerase) (GmhA)	13	1.21	Gluconate-6-phosphate dehydrogenase (Gnd)
C	38	-1.77	Xenobiotic reductase A (XenA)	96	11.78	DNA protecting during starvation protein (Dps)
				95	7.89	DNA protecting during starvation protein (Dps)
				85	3.34	Manganese superoxide dismutase (SodA)
				81	2.82	Putative ATP-dependent Clp protease proteolytic subunit (ClpP1)
				81	2.82	Putative alkyl hydroperoxide reductase subunit C (AhpC)
				86	2.37	Putative alkyl hydroperoxide reductase subunit C (AhpC)
				89	2.04	glutatione-S-transferase (Gst)
				88	1.61	Putative alkyl hydroperoxide reductase subunit C (AhpC)
				21	1.48	Recombinase A (RecA)
D	33	-1.56	Succinyl-CoA synthetase beta chain (SucC)	63	2.1	Succinyl-CoA synthetase, alpha subunit (SucD)
	52	-1.55	Malate dehydrogenase (Mdh)	7	2.03	ATP synthase, F1 complex, alpha subunit
	17	-1.52	isocitrate dehydrogenase (Icd)	9	1.48	ATP synthase, F1 complex, alpha subunit
	87	-1.27	inorganic pyrophosphatase (Ppi - Pi + Pi) (Ppa)	9	1.48	pyruvate dehydrogenase multienzyme complex, Dihydrolipoamide dehydrogenase component (IpdA)
E	56	-3.37	Cytidine deaminase (Cdd)	69	2.41	deoxyribose-phosphate aldolase 2 (DeoC2)
	72	-2.3	Uridylate kinase (PyrH)	78	1.87	Purine nucleoside phosphorylase deoD-type (DeoD)
	21	-1.73	Putative GTP-binding protein (EngD)	80	1.82	Purine nucleoside phosphorylase deoD-type (DeoD)
	77	-1.66	adenylate kinase (Adk)			

	in vitro > in planta			in planta > in vitro		
	Spot ID	Fold change	Protein name	Spot ID	Fold change	Protein name
E	102	-1.03	Nucleoside diphosphate kinase (Ndk)			
F	20	-1.87	Elongation factor Tu-A (TufA)	101	5.2	Elongation factor Tu-A (TufA)
				51	1.79	Elongation factor Ts
				18	1.71	Elongation factor Tu-A (TufA)
G	55	-1.8	NH(3)-dependent NAD(+) synthetase (NadE)	46	2.49	Thiamine-binding periplasmic protein (TbpA)
	50	-1.71	Ferrochelatase (HemH)	54	1.9	Coproporphyrinogen III oxidase (HemF)
				78	1.87	Probable dethiobiotin synthetase 2
H	61	-2.96	Malonyl CoA-acyl carrier protein transacylase (FabD)	85	3.34	3-oxoacyl-[acyl-carrier-protein] reductase (FabG)
	58	-1.54	Malonyl CoA-acyl carrier protein transacylase (FabD)			
	73	-1.26	arylesterase (alpfa/beta hydrolase fold)			
	11	-1.25	Acetyl CoA carboxylase, biotin carboxylase subunit			
I	65	-3.62	outer membrane protein A (OmpA)	43	1.76	Glucose-1-phosphate uridylyltransferase (GalU)
	27	-1.78	Penicillin-binding protein 5 (D-alanyl-D-alanine carboxypeptidase fraction A) (DacA)			
J	62	-6.62	Iron transport protein, periplasmic-binding protein (PsaA)	53	3.26	ABC superfamily high affinity Zn transport protein (ZnuA)
	32	-1.99	ABC transporter, substrate binding protein			
K	91	-1.62	LuxS-Like protein (LuxS)			
	40	-1.53	PhoH-like protein			
	4	-1.39	PrkA serine kinase			
L	64	-1.86	Septum site-determining protein (MinD)			
	16	-1.76	Cell division protein FtsA			
M	66	-17.26	FliC (flagellin)			
	72	-2.3	FliC (flagellin)			
	58	-1.54	FliC (flagellin)			
N	79	-13.17	YcfA protein (involved in yellow colour of colonies)	46	2.49	Putrescine-binding periplasmic protein (PotF)
	2	-2.16	ferrioxamine receptor (FoxR)	78	1.87	YcfA protein (involved in yellow colour of colonies)
				80	1.82	YcfA protein (involved in yellow colour of colonies)

	in vitro > in planta			in planta > in vitro		
	Spot ID	Fold change	Protein name	Spot ID	Fold change	Protein name
N				92	1.86	YcfA protein (involved in yellow colour of colonies)
				54	1.9	Putative carboxymethylenebutenolidase
				100	1.4	heat-stable nucleoid-structuring protein (Hns)
O	29	-2.29	Alcohol dehydrogenase (AdhP)	92	1.86	hypothetical protein ETA_10300
	98	-1.86	hypothetical protein ETA_06200	49	7.33	Putative oxidoreductase YghA
	8	-1.77	Conserved hypothetical protein (DUF945 Superfamily)	94	3.87	Protein YceI
	38	-1.77	hypothetical protein plu1873	63	2.1	2,5-diketo-D-gluconic acid reductase A (DkgA)
	38	-1.77	Zinc-containing alcohol dehydrogenase superfamily	97	1.61	hypothetical protein ETA_06200
	50	-1.71	Conserved hypothetical protein (DUF1471)			
	58	-1.54	Putative haloacid dehalogenase-like hydrolase			
	40	-1.53	hypothetical protein plu1873			
	99	-1.49	no homologs found; conserved cupin domain			
	74	-1.32	putative hydrolase, alpha/beta fold family			
	10	-1.32	Conserved hypothetical protein YjgR			

Addendum II

Figure 4.3:
Overview of expression patterns of the proteins that may be correlated with the virulence degree of the strains. The points on the graphs represent the different samples of each strain grown *in vitro* or *in planta*. Each line links the means of the repetitions of the different strains grown or *in planta* or *in vitro* to each other. The X-axis represents the different strains and the Y-axis the expression level.
The following colour codes are used:

- LMG2024 *in vitro*
- PD437 *in vitro*
- PFB5 *in vitro*
- BG16 *in vitro*
- LMG2024 *in planta*
- PD437 *in planta*
- PFB5 *in planta*
- BG16 *in planta*

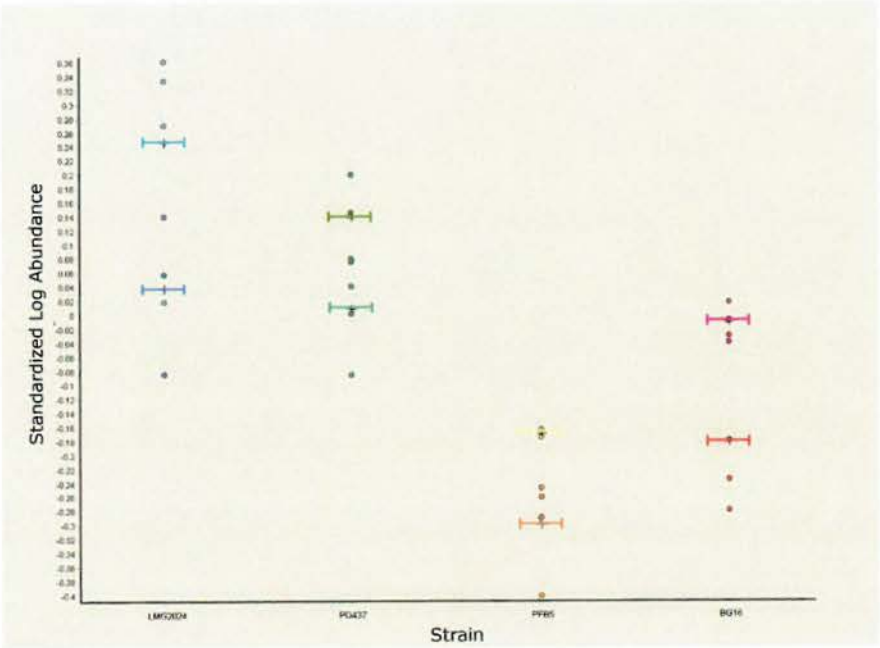

Spot nr. 14

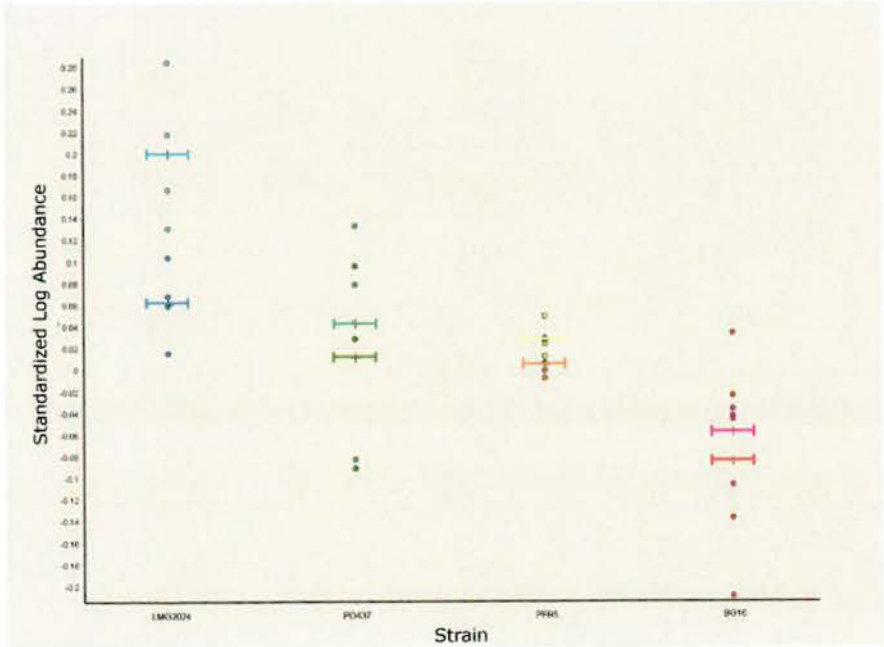

Spot nr. 26

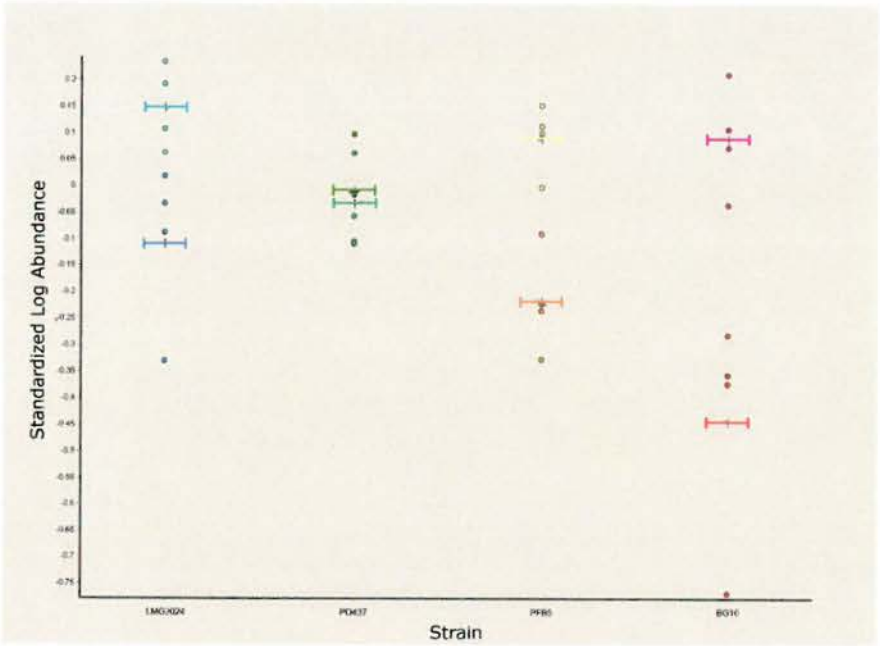

Spot nr. 28

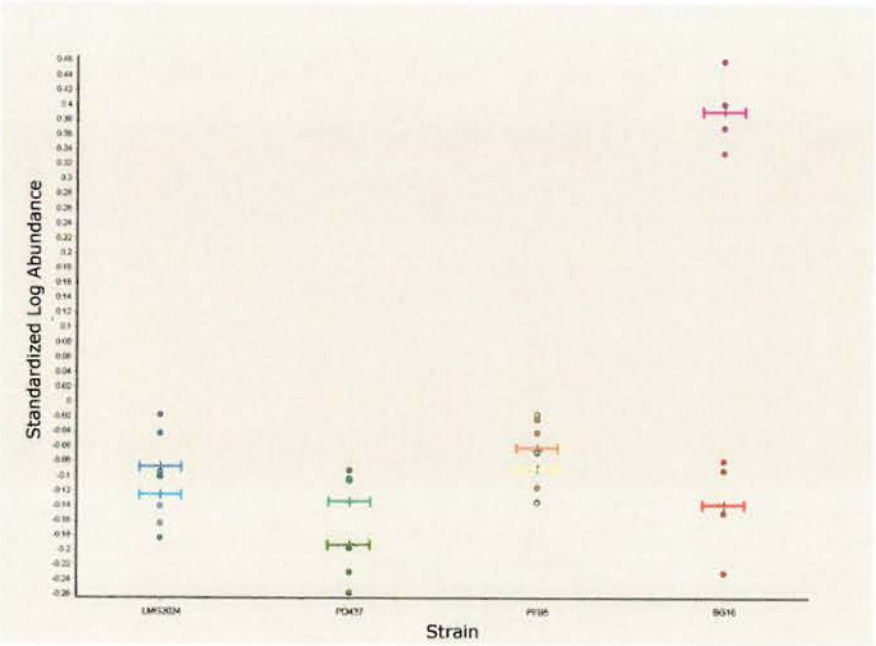

Spot nr. 31

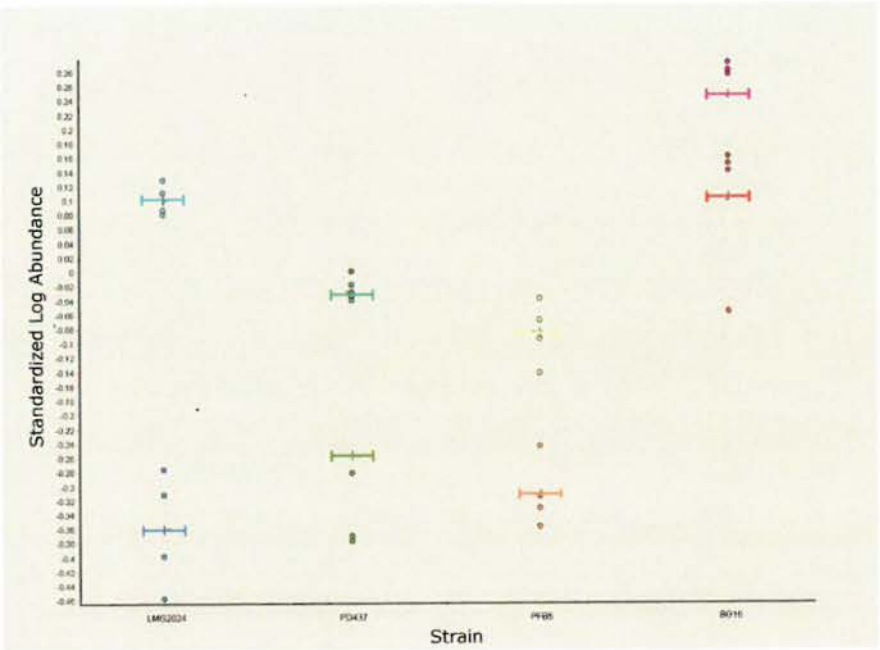

Spot nr. 35

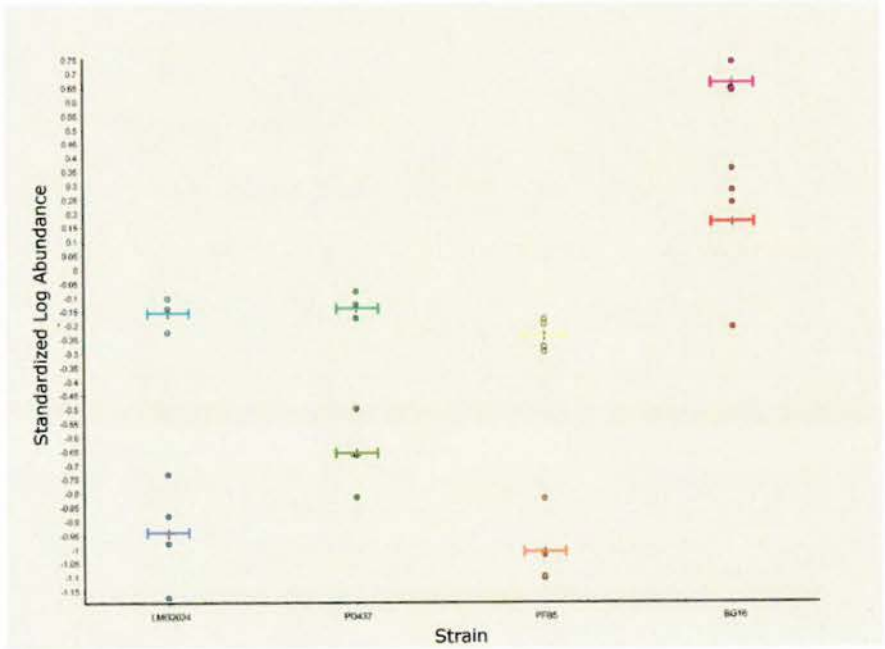

Spot nr. 37

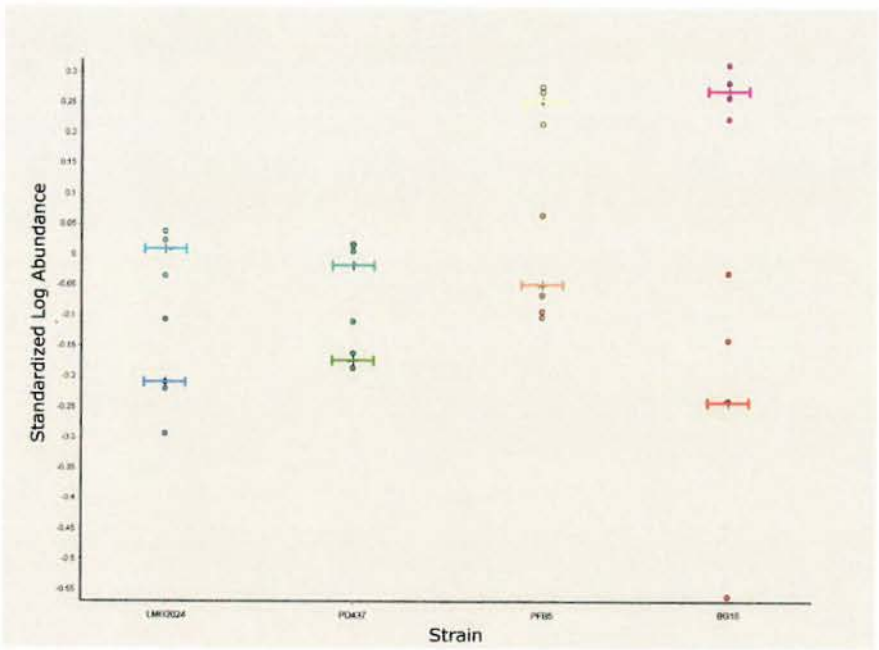

Spot nr. 40

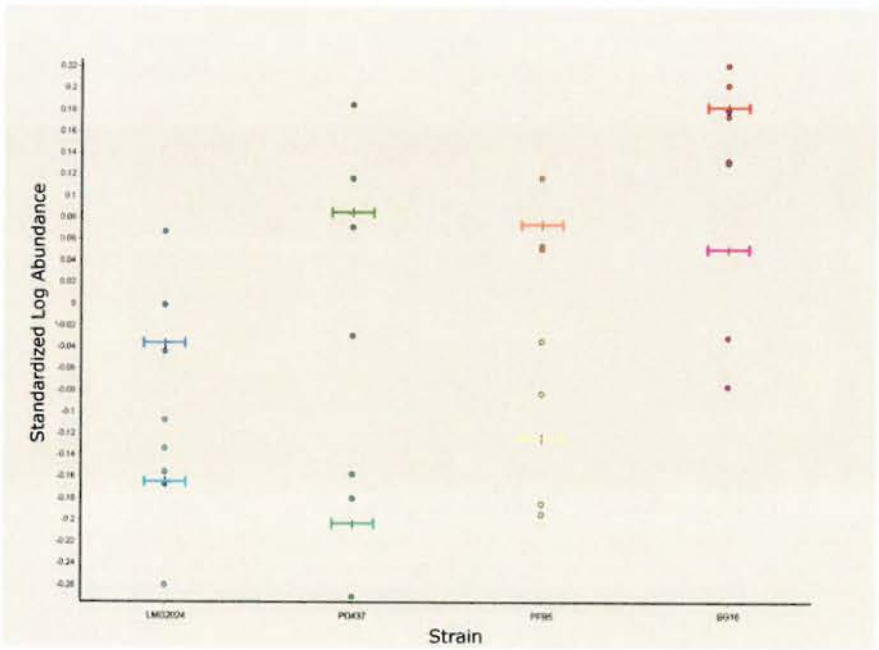

Spot nr. 51

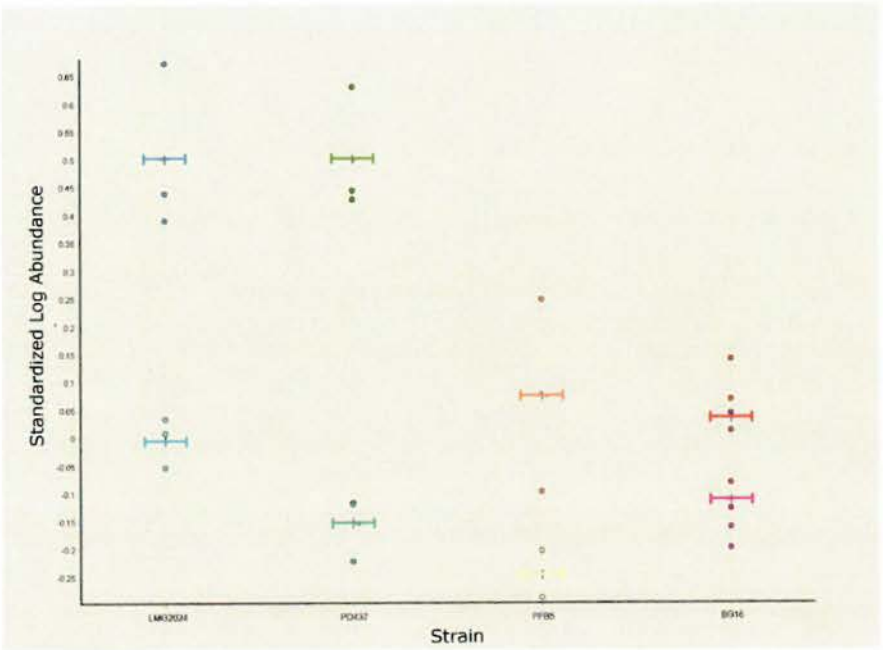

Spot nr. 53

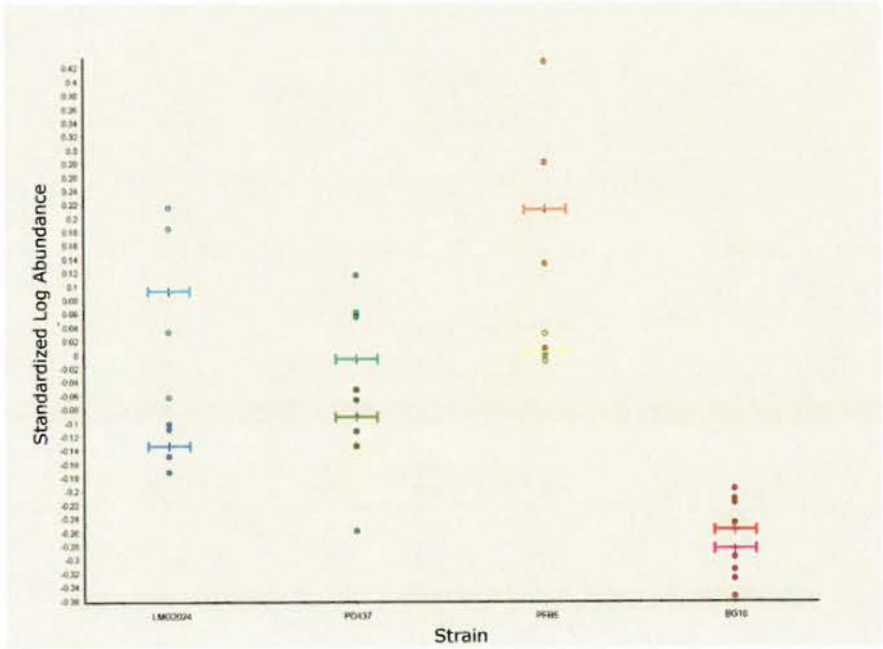

Spot nr. 70

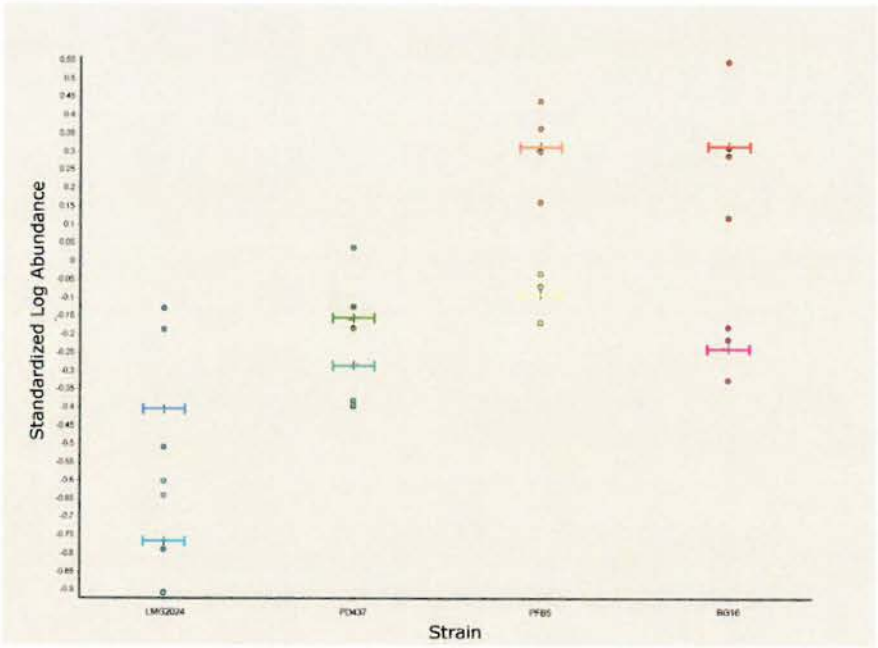

Spot nr. 94

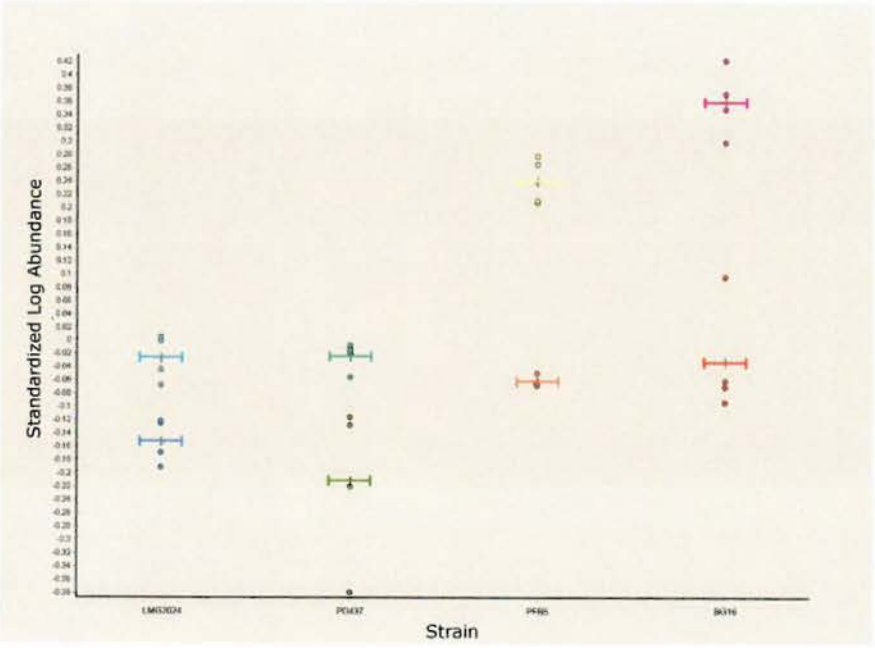

Spot nr. 99

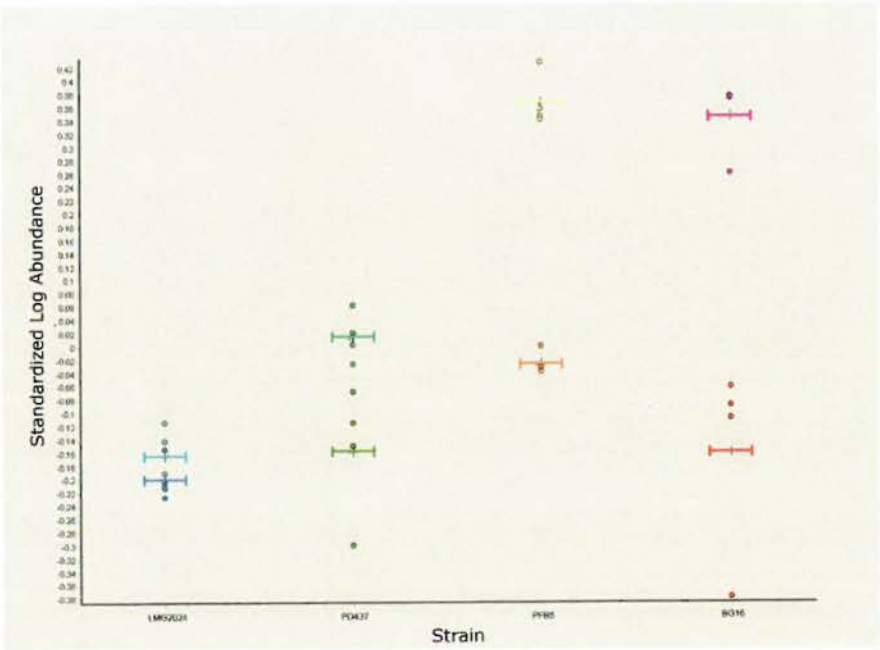

Spot nr. 102